549

Lightning Parameters for Engineering Applications

Working Group C4.407

August 2013

LIGHTNING PARAMETERS FOR ENGINEERING APPLICATIONS

WG C4.407

Members

V.A. Rakov, **Convenor** (US), A. Borghetti, **Secretary** (IT),

C. Bouquegneau (BE), W.A. Chisholm (CA), V. Cooray (SE), K. Cummins (US),

G. Diendorfer (AT), F. Heidler (DE), A. Hussein (CA), M. Ishii (JP), C.A. Nucci (IT), A. Piantini (BR),

O. Pinto, Jr. (BR), X. Qie (CN), F. Rachidi (CH), M.M.F. Saba (BR), T. Shindo (JP), W. Schulz (AT),

R. Thottappillil (SE), S. Visacro (BR), W. Zischank, Corresponding Member (DE)

IISBN: 978-2-85873-244-9

Lightning Parameters for Engineering Applications

No Extra Cover page or "blank pages"
Use CIGRE abbreviations insofar as possible: Study Committee – SC, Technical Brochure – TB, Working Group – WG
Joint Working Group – JWG, Technical Committee – TC
Photos: must be of reasonable definition (preferably 300 dpi); all figures and tables must be titled, legible and numbered with legends provided.
No Company logos…

Table of Contents

Appendix 1. List of Acronyms

Appendix 2. Term of Reference (TOR) for CIGRE WG C4.407, Lightning Parameters for Engineering Applications

EXECUTIVE SUMMARY

This document is an update on previous CIGRE documents on the subject published in Electra more than three decades ago: Berger, K., Anderson, R.B., and Kroninger, H. 1975. Parameters of lightning flashes. Electra, No. 41, pp. 23-37 and Anderson, R.B., and Eriksson, A.J. 1980. Lightning parameters for engineering application. Electra, No. 69, pp. 65-102.

About 80% or more of negative cloud-to-ground lightning flashes are composed of two or more strokes. This percentage is appreciably higher than 55% previously estimated by Anderson and Eriksson (1980), based on a variety of less accurate records. The average number of strokes per flash is typically 3 to 5, with the geometric mean interstroke interval being about 60 ms. Roughly one-third to one-half of lightning flashes create two or more terminations on ground separated by up to several kilometers. When only one location per flash is recorded, the correction factor for measured values of ground flash density to account for multiple channel terminations on ground is about 1.5-1.7, which is considerably larger than 1.1 previously estimated by Anderson and Eriksson (1980). First-stroke current peaks are typically a factor of 2 to 3 larger than subsequent-stroke current peaks. However, about one third of cloud-to-ground flashes contain at least one subsequent stroke with electric field peak, and, by theory, current peak, greater than the first-stroke peak.

From direct current measurements, the median return-stroke peak current is about 30 kA for negative first strokes in Switzerland, Italy, South Africa, and Japan, and typically 10-15 kA for subsequent strokes in Switzerland and for triggered and upward (object-initiated) lightning. Corresponding values from measurements in Brazil are 45 kA and 18 kA. Additional measurements are needed. The “global” distributions of lightning peak currents for negative first strokes currently recommended by CIGRE and IEEE (see Fig. 3.2) are each based on a mix of direct current measurements and less accurate indirect measurements, some of which are of questionable quality. However, since the “global” distributions have been widely used in lightning protection studies and are not much different from that based on direct measurements only (median = 30 kA, $\sigma_{lg}I$ = 0.265 for Berger et al.’s distribution), continued use of these “global” distributions for representing negative first strokes is recommended. For negative subsequent strokes, distribution 4 (median = 12 kA, $\sigma_{lg}I$ = 0.265) in Fig. 3.1 should be used. For positive lightning strokes, distribution 2 (median = 35 kA, $\sigma_{lg}I$ = 0.544) in Fig. 3.1 is recommended, although the data are very limited and may be influenced by the presence of strike object located on the mountain top. Direct lightning current measurements on instrumented towers should be continued. Currently, direct current measurements are performed on instrumented towers in Austria, Brazil, Canada, Germany, and Switzerland, although the overwhelming majority of flashes observed on those towers (except for Brazil) are of upward type.

Recommended lightning current waveshape parameters are still based on Berger et al.’s (1975) data (see Table 3.6), although the current rate-of-rise parameters estimated by Anderson and Eriksson (1980) from Berger et al.'s oscillograms are likely to be significantly underestimated, due to limitations of the instrumentation used by Berger et al. Triggered-lightning data for current rates of rise (see Table 3.7) can be applied to subsequent strokes in natural lightning. Relatively strong correlation is observed between the lightning peak current and impulse charge transfer and between the current rate-of-rise characteristics and current peak, and relatively weak or no correlation between the peak and risetime.

The field-to-current conversion procedure employed by the U.S. National Lightning Detection Network (NLDN) and other similar lightning locating systems has been calibrated only for negative subsequent strokes, with the median absolute error being 10 to 20%. Peak current estimation errors for negative first strokes and for positive lightning are presently unknown. Besides systems of NLDN type (such as the European systems participating in EUCLID or nationwide and regional systems in Japan), there are other lightning locating systems that are also reporting lightning peak currents inferred from measured fields, including LINET (mostly in Europe), USPLN (in the U.S., but similar systems operate in other countries), WTLN (in the U.S. and other countries), WWLLN (global), and GLD360 (global). Peak current estimation errors for the latter systems are presently unknown.

The percentage of positive flashes or strokes containing continuing currents (CC) is much higher than those of negative flashes or strokes. Positive strokes tend to be followed by longer and more intense CC than negative strokes. In contrast with negative strokes, positive strokes can produce both a high peak current and a long CC. Waveshapes of CC in natural cloud-to-ground flashes may be grouped into six categories. The average number of

M components (surges superimposed on continuing currents) per CC appears to depend on polarity: while an average of 5.5 M components per CC were observed for negative flashes, an average of 9.0 M components per CC were observed for positive flashes. It has been inferred that strokes initiating long CC in negative flashes tend to have a lower peak current and are preceded by higher-peak-current strokes and by relatively short interstroke intervals.

The lightning return-stroke speed is needed in computing lightning electromagnetic fields that cause induced overvoltages in power distribution lines. It is also explicitly or implicitly assumed in procedures to infer lightning currents from measured fields. The average propagation speed of a negative return stroke (first or subsequent) below the lower cloud boundary is typically between one-third and one-half of the speed of light. It appears that the return-stroke speed for first strokes is lower than that for subsequent strokes, although the difference is not very large (9.6×10^7 vs. 1.2×10^8 m/s). For positive return strokes, the speed is of the order of 10^8 m/s, although data are very limited. The negative return-stroke speed within the bottom 100 m or so (corresponding to current and field peaks) is expected to be between one-third and two-thirds of the speed of light. The negative return stroke speed usually decreases with height for both first and subsequent strokes. There exists some experimental evidence that the negative return stroke speed may vary non-monotonically along the lightning channel, initially increasing and then decreasing with increasing height. There are contradicting data regarding the variation of positive return stroke speed with height. The often assumed relationship between the return-stroke speed and peak current is generally not supported by experimental data.

The equivalent impedance of the lightning channel is needed for specifying the source in studies of either direct-strike or induced lightning effects. The estimates of this impedance from limited experimental data suggest values ranging from several hundred ohm to a few kiloohm. In many practical situations the impedance “seen” by lightning at the strike point is some tens of ohm or less, which allows one to assume infinitely large equivalent impedance of the lightning channel. In other words, lightning in these situations can be viewed as an ideal current source. In case of direct lightning strike to an overhead conductor of a power line with 400 ohm surge impedance (effective impedance 200 ohm, since 400 ohm is “seen” in either direction), the ideal current source approximation may still be suitable. Representation of lightning by a current source with internal impedance of 400 ohm, similar to that of an overhead wire, is probably not justified.

Although positive lightning discharges account for 10% or less of global cloud-to-ground lightning activity, there are several situations, including, for example, winter storms, that appear to be conducive to the more frequent occurrence of positive lightning. The highest directly measured lightning currents (near 300 kA vs. a maximum of about 200 kA or less for negative lightning) and the largest charge transfers (hundreds of coulombs or more) are associated with positive lightning. Positive flashes are usually composed of a single stroke, although up to four strokes per flash have been observed. Subsequent strokes in positive flashes can occur either in a new (a more common situation) or in the previously-formed channel. In spite of recent progress, our knowledge of the physics of positive lightning remains considerably poorer than that of negative lightning. Because of the absence of other direct current measurements for positive lightning return strokes, it is still recommended to use the peak current distribution based on the 26 events recorded by K. Berger (see Fig. 3.1 and Table 7.3), even though some of those 26 events are likely to be not of return-stroke type. However, caution is to be excersized, particularly for the waveshape parameters listed in Table 7.3, for which sample sizes are smaller than for peak currents. Clearly, additional measurements for positive lightning return strokes are needed to establish reliable distributions of peak current and other parameters for this type of lightning. Bipolar lightning discharges are usually initiated by upward leaders from tall objects. However, natural downward flashes also can be bipolar.

Tall objects (higher than 100 m or so) located on flat terrain and objects of moderate height (some tens of meters) located on mountain tops experience primarily upward lightning discharges that are initiated by upward-propagating leaders. The percentage of upward flashes increases with increasing object height. Upward (object-initiated) lightning discharges always involve an initial stage that may or may not be followed by downward-leader/upward-return-stroke sequences. The percentage of upward flashes with return strokes varies from 20 to 50%. The initial-stage steady current typically has a magnitude of some hundreds of amperes and often exhibits superimposed pulses whose peaks range from tens of amperes to several kiloamperes (occasionally a few tens of kiloamperes). Object-initiated lightning events may occur relatively independently from downward lightning during the non-convective season, and it has been observed that in many cases several flashes were initiated from a tall object

within a period of some hours. At tall objects, the probability of occurrence of bipolar lightning is about the same as for positive lightning. Possible reasons for the observed differences between the downward lightning and the high-complexity upward lightning are the multiple upward branches of the leader initiated from the tower and the relative proximity of the cloud charge regions to the object tip.

From the information available in the literature at the present time, there is no evidence of a dependence of negative cloud-to-ground lightning parameters on geographical location, except maybe for first and subsequent return-stroke peak currents, for which relatively insignificant (less than 50%), from the engineering point of view, variations may exist. It is important to note, however, that it cannot be ruled out that the observed differences in current measurements are due to reasons other than "geographical location", with limited sample size for some observations being of particular concern. Similarly, no reliable information on seasonal dependence is available. In summary, at the present time, the available information is not sufficient to confirm or refute a hypothesis on dependence of negative CG lightning parameters on geographical location or season. On the other hand, some local conditions may exist (for example, winter storms in Japan) that give rise to more frequent occurrence of unusual types of lightning, primarily of upward type, whose parameters may differ significantly from those of “ordinary” lightning. Further studies are necessary to clarify those conditions and their possible dependence on geographical location.

Lightning parameters needed for specific engineering applications are summarized. The emphasis is placed on the parameters that have an influence in the electric power engineering calculations, although lightning parameters needed for designing lightning protection of ordinary ground-based structures are also discussed.

1. Introduction

This document summarizes the work done from April 2008 to April 2013 by CIGRE WG C4.407, Lightning Parameters for Engineering Applications. The Term of Reference (TOR) for this Working Group is found in Appendix 1. The document can be viewed as an update on previous CIGRE documents on the subject published in 1975 and 1980:

Berger, K., Anderson, R.B., and Kroninger, H. 1975. Parameters of lightning flashes. Electra, No. 41, pp. 23-37.

Anderson, R.B., and Eriksson, A.J. 1980. Lightning parameters for engineering application. Electra, No. 69, pp. 65-102.

Anderson, R.B., and Eriksson, A.J. 1980. A summary of lightning parameters for engineering application, CIGRE 1980 Session, paper 33-06, 12 p.

It is also related to the following CIGRE reports:

CIGRE WG 33.01, Report 63. Guide to Procedures for Estimating the Lightning Performance of Transmission Lines, October 1991, 61 p.

CIGRE TF 33.01.02, Report 94, Lightning characteristics relevant for electrical engineering: Assesment of sensing, recording and mapping requirements in the light of present technological advancements, 1995, 37 p.

CIGRE TF 33.01.03, Report 118, Lightning exposure of structures and interception efficiency of air terminals, October 1997, 86 p.

CIGRE TF 33.01.02, Report 172, Characterization of lightning for applications in electric power systems, December 2000, 35 p.

CIGRE TF C4.404, Report 376, Cloud-to-ground lightning parameters derived from lightning location systems: The effects of system performance, April 2009, 117 p.

Traditional lightning parameters needed in engineering applications include lightning peak current, maximum current derivative, average current rate of rise, current risetime, current duration, charge transfer, and specific energy (action integral), all derivable from direct current measurements. Distributions of these parameters presently adopted by CIGRE are based on direct measurements by K. Berger and co-workers in Switzerland, supplemented by less accurate magnetic link measurements to increase the sample size. There also exist more recent direct current measurements obtained using instrumented towers in Austria, Brazil, Canada, Germany, Japan, Russia, and Switzerland, as well as those obtained in several countries using rocket-triggered lightning. Further, modern lightning locating systems report peak currents estimated from measured magnetic or electric field peaks. One of the objectives of present document is to evaluate these new experimental data, along with the old data, to determine their applicability to various engineering calculations. Evaluation includes both instrumental and methodological aspects. Possible geographical, seasonal and other variations in lightning parameters are examined. Additional lightning parameters such as the number of strokes per flash (multiplicity), interstroke interval, number of channels per flash, relative intensity of strokes within a flash, return-stroke speed, and equivalent impedance of the lightning channel, as well as characteristics of continuing currents and M-components are included. More detailed information than before is given about less frequent, but potentially more destructive, positive and bipolar lightning flashes.

2. General Characterization of Lightning

In this section, we introduce the basic lightning terminology, describe different types of lightning and three basic modes of charge transfer to ground. We also briefly discuss the ground flash density, which is the primary descriptor of lightning incidence. Then, for the most common negative cloud-to-ground lightning, we will consider the number of strokes per flash, interstroke intervals and flash duration, multiple channel terminations on ground, and relative stroke intensity within the flash.

2.1. Definitions and Terminology

Lightning can be defined as a transient, high-current (typically tens of kiloamperes) electric discharge in air whose length is measured in kilometers. The lightning discharge in its entirety, whether it strikes ground or not, is usually termed a "lightning flash" or just a "flash." A lightning discharge that involves an object on ground or in the atmosphere is sometimes referred to as a "lightning strike." A commonly used non-technical term for a lightning discharge is a "lightning bolt." The terms "stroke" or "component stroke" apply only to components of cloud-to-ground discharges. Most lightning flashes are composed of multiple strokes. All strokes other than the “first” are referred to as “subsequent” strokes.

Each lightning stroke is composed of a downward-moving process, termed a “leader”, and an upward-moving process, termed a “return stroke”. The leader creates a conducting path between the cloud charge source region and ground and distributes electric charge from the cloud source along this path, and the return stroke traverses that path moving from ground toward the cloud charge source and neutralizes the leader charge. Thus, both leader and return stroke processes serve to effectively transport electric charge of the same polarity (positive or negative) from the cloud to ground. The first-stroke leader in negative flashes appears optically to be an intermittent process, hence the term “stepped leader”, while the tip of a subsequent-stroke leader in negative flashes appears to move continuously. The continuously moving subsequent-stroke leader tip appears on time-resolved photographs as a downward-moving “dart”, hence the term “dart leader”. The apparent difference between the two types of leaders is related to the fact that the stepped leader develops in virgin air, while the dart leader follows the “pre-conditioned” path of the preceding stroke or strokes. Sometimes continuously moving dart leader becomes stepped, in which case it is called “dart-stepped leader”. Interestingly, all three types of leaders produce bursts of x-ray emission with energies typically up to about 250 keV (twice the energy of a typical chest x-ray) (Dwyer et al., 2005).

The electric potential difference between a downward-moving stepped-leader tip and ground is probably some tens of megavolts, comparable to or a considerable fraction of that between the cloud charge source and ground (50 to 500 MV). When the descending leader attaches to the ground, the return stroke begins. The high-current return-stroke wave rapidly heats the channel to a peak temperature near or above $30{,}000^{o}$ K and creates a channel pressure of 10 atm (1 megapascal) or more, resulting in channel expansion, intense optical radiation, and an outward propagating shock wave that eventually becomes the thunder (sound wave) we hear at a distance. Each cloud-to-ground lightning flash involves an energy of the order of 10^{9} J. Lightning energy is approximately equal to the energy required to operate five 100-W light bulbs continuously for one month. Note that not all the lightning energy is available at the strike point, only 10^{-2}-10^{-3} of the total energy, since most of the energy is spent for producing thunder, hot air, light, and radio waves.

The kiloamperes-scale impulsive component of the current in a return stroke is often followed by a “continuing current” which has a magnitude of tens to hundreds of amperes and a duration up to hundreds of milliseconds. Continuing currents with a duration in excess of 40 ms are traditionally termed “long continuing currents”. These usually occur in subsequent strokes. Between 30% and 50% of all negative cloud-to-ground flashes contain long continuing currents. Transient processes occurring in a lightning channel while it carries continuing current are termed “M components”.

According to Rakov and Uman (2003), any self-propagating electrical discharge creating a channel with electrical conductivity of the order 10^{4} S/m (comparable to that of carbon) is called a “leader”. “Streamers”, on the other hand, are characterized by much lower electrical conductivity; the air behind the streamer tip remains essentially an

insulator (e.g., Bazelyan et al., 1978). Corona or point discharge can consist of numerous individual streamers. Corona is confined to the immediate vicinity of an "electrode" such as a grounded object, a leader tip, the lateral surface of the leader channel, or a hydrometeor, that is, it is not a self-propagating discharge. It is worth noting that the terms leader and streamer in the lightning literature are sometimes used interchangeably, in most cases the term streamer being used to denote a low-luminosity leader, particularly the “upward connecting leader”.

2.2. Types of Lightning Discharges

The global lightning flash rate is some tens to a hundred flashes per second or so. The majority of lightning flashes, about three-quarters, do not involve ground. These are termed cloud flashes (discharges) and sometimes are referred to as ICs. Cloud discharges include intracloud, intercloud, and cloud-to-air discharges. Lightning discharges between cloud and Earth are termed cloud-to-ground discharges and sometimes referred to as CGs. The latter constitute about 25% of global lightning activity.

From the observed polarity of the charge "effectively" lowered to ground and the direction of propagation of the initial leader, four different types of lightning discharges between cloud and Earth have been identified. The term "effectively" is used to indicate that individual charges are not transported all the way from the cloud to ground during the lightning processes. Rather the flow of electrons (the primary charge carriers) in one part of the lightning channel results in the flow of other electrons in other parts of the channel, as discussed by Uman (1987, 2001). For example, individual electrons in the lightning channel move only a few meters during a return stroke which transfers a coulomb or more of charge to ground. The four types of lightning, illustrated in Fig. 2.1, are (a) downward negative lightning (b) upward negative lightning (c) downward positive lightning, and (d) upward positive lightning. Downward flashes exhibit downward branching, while upward flashes are branched upward. It is believed that downward negative lightning flashes (type a) account for about 90% or more of global cloud-to-ground lightning, and that 10% or less of cloud-to-ground discharges are downward positive lightning flashes (type c). Upward lightning discharges (types b and d) are thought to occur only from tall objects (higher than 100 m or so) or from objects of moderate height located on mountain tops.

Lightning can be artificially initiated (triggered) by launching a small rocket trailing a thin grounded or ungrounded wire toward a charged cloud overhead (the so-called rocket-and-wire triggering technique). To date, approximately 1,000 lightning flashes were triggered worldwide using this technique. Leader/return stroke sequences in rocket-triggered lightning are similar in most (if not all) respects to subsequent leader/return stroke sequences in natural downward lightning and to all such sequences in object-initiated (upward) lightning. The results of triggered-lightning experiments have provided considerable insight into natural lightning processes that would not have been possible from studies of natural lightning due to its random occurrence in space and time (e.g., Rakov, 2009).

As noted above, positive lightning discharges are relatively rare (less than 10% of global cloud-to-ground lightning activity), but there are five situations that appear to be conducive to the more frequent occurrence of positive lightning. These situations include (1) the dissipating stage of an individual thunderstorm, (2) winter (cold-season) thunderstorms, (3) trailing stratiform regions of mesoscale convective systems, (4) some severe storms, and (5) thunderclouds formed over forest fires or contaminated by smoke. Positive lightning is typically more energetic and potentially more destructive than negative lightning.

Sometimes both positive and negative charges are transferred to ground during the same flash. Such flashes (not represented in Fig. 2.1) are referred to as bipolar. Bipolar lightning discharges are usually initiated from tall objects (are of upward type). It appears that positive and negative charge sources in the cloud are tapped by different upward branches of the lightning channel. Downward bipolar lightning discharges do exist, but appear to be rare.

Positive and bipolar discharges are primarily discussed in Chapter 7. Upward discharges are characterized in Chapter 8.

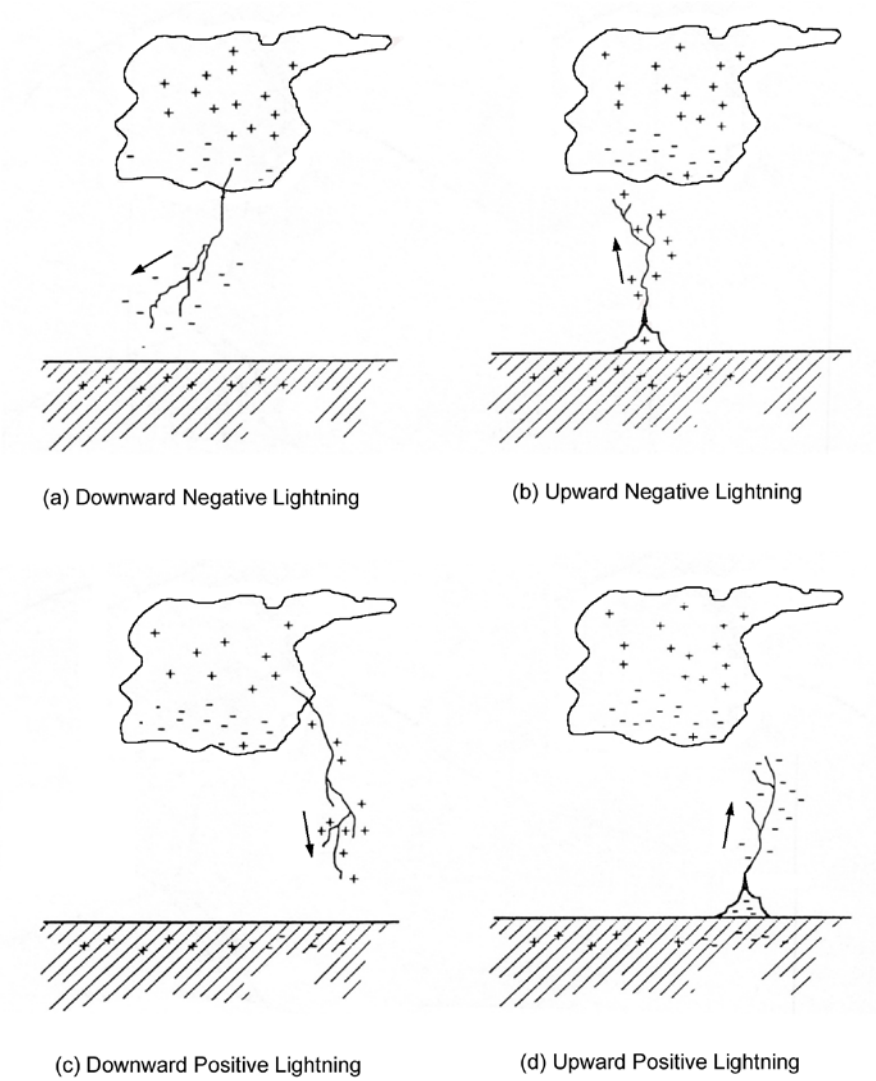

Fig. 2.1 Four types of lightning effectively lowering cloud charge to ground. Only the initial leader is shown for each type. For each lightning-type name given below the sketch, direction indicates the direction of propagation of the initial leader and polarity refers to the polarity of the cloud charge effectively lowered to ground. In (a) and (c), the polarity of charge lowered to ground is the same as the leader polarity, while in (b) and (d) those polarities are opposite. Not shown in this Figure are upward (object-initiated) and downward bipolar lightning flashes. Adapted from Rakov and Uman (2003).

2.3. Three Modes of Charge Transfer to Ground

There are three possible modes of charge transfer to ground in lightning discharges that are convenient to illustrate for the case of negative subsequent strokes. In negative subsequent strokes these three modes are represented by (a) dart leader/return stroke sequences, (b) continuing currents, and (c) M-components. Fig. 2.2 schematically shows current profiles corresponding to these three modes.

(a) In a negative leader/return stroke sequence, the descending leader creates a conductive path between the cloud charge source region and ground and deposits negative charge along this path. The following return stroke traverses that path, moving from ground toward the cloud charge source region, and neutralizes the negative leader charge. Thus, both leader and return stroke processes serve to transport effectively negative charge from the cloud to ground.

(b) The lightning continuing current can be viewed as a quasi-stationary arc between the cloud charge source region and ground. The typical arc current is tens to hundreds of amperes, and the duration is up to some hundreds of milliseconds.

(c) Lightning M-components can be viewed as perturbations (or surges) in the continuing current and in the associated channel luminosity. It appears that an M-component involves the superposition of two waves propagating in opposite directions (see Fig. 2.2).

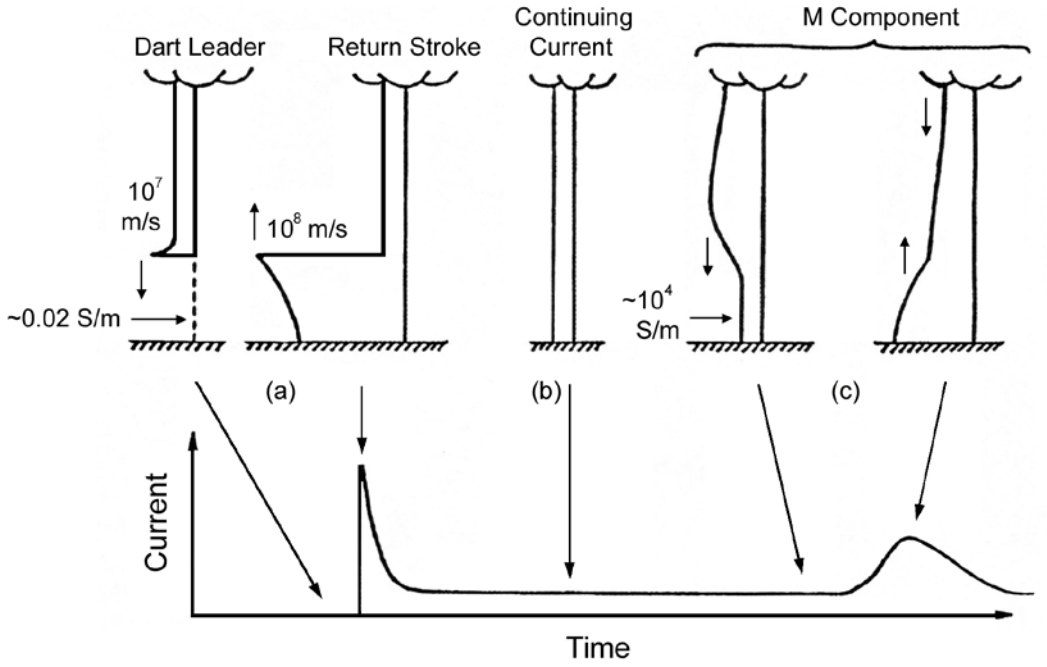

Fig. 2.2 Schematic representation of current versus height profiles for three modes of charge transfer to ground in negative lightning subsequent strokes: (a) dart leader/return stroke sequence, (b) continuing current, and (c) M-component. The corresponding current versus time waveform represents current at the ground. Adapted from Rakov et al. (2001).

The spatial front length for M-component waves is of the order of a kilometer (shown shorter in Fig. 2.2 for illustrative purposes), while for dart-leader and return-stroke waves the spatial front lengths are of the order of 10 and 100 m, respectively. The M-component mode of charge transfer to ground requires the existence of a grounded channel carrying a continuing current which acts as a wave-guiding structure. In contrast, the leader/return stroke mode of charge transfer to ground occurs only in the absence of such a conducting path to ground. In this latter mode, the wave-guiding structure is not available and is created by the leader. For all the processes shown in Fig. 2.2, the channel conductivity is of the order of 10^4 S/m, except for the channel section between the dart-leader tip and ground shown by a dashed line. For this latter channel section, the conductivity is about 0.02 S/m (Rakov, 1998). Thus, the primary distinction between the leader/return stroke and M-component modes is the availability of a conducting path to ground. It is possible that, as the conductivity of the path to ground decreases, the downward M-component wave can transform to a dart leader.

M components are more numerous than leader/return stroke sequences (Thottappillil et al., 1995) and can represent a threat to various objects and systems. Specifically, M-components may impart electrodynamic stresses on metallic structural elements already weakened due to thermal effects of the background continuing current. Further, Uman et al. (1997), who studied the responses of a test power distribution system to lightning strikes, reported that, in the transformer secondary, current pulses due to return strokes and those due to M-components

had peaks of the same order of magnitude, while the corresponding currents at the lightning channel base differed by 1 to 2 orders of magnitude (were much lower for M-components). Finally, positive current waveforms that have very large peaks (many in excess of 100 kA) and risetimes up to hundreds of microseconds (Berger et al. 1975) are likely to be a result of the M-component mode of charge transfer to ground, as discussed in Section 7.4.

2.4. Ground Flash Density

The ground flash density N_g is often viewed as the primary descriptor of lightning incidence, at least in lightning protection studies. Ground flash density has been estimated from records of (1) lightning flash counters (LFCs) and (2) lightning locating systems (LLSs) and can potentially be estimated from records of satellite-based optical or radio-frequency radiation detectors. It is worth noting that satellite detectors cannot distinguish between cloud and ground discharges and, hence, in order to obtain N_g maps from satellite observations, a spatial distribution of the fraction of discharges to ground relative to the total number of lightning discharges is needed. IEEE Std 1410-2010 recommends, in the absence of ground-based measurements of N_g, to assume that N_g is equal to one-third of the total flash density (including both cloud and ground discharges) based on satellite observations.

Lightning Locating Systems. Locating lightning discharges with reasonable accuracy requires the use of multiple-station systems. The principles of operation of multiple-station lightning locating systems (LLS) are described, for example, in CIGRE TF C4.404, Report 376 (2009). Such systems are presently used in many countries to acquire lightning data that can be used for mapping N_g. Any LLS fails to detect relatively small cloud-to-ground flashes (particularly near the periphery of the network) and fails to discriminate against some cloud flashes, unwanted in determining N_g. The corresponding system characteristics, the detection efficiency and the selectivity with respect to ground flashes, are influenced by network configuration, position of the lightning relative to the network, system's sensor gain and trigger threshold, sensor waveform selection criteria, lightning parameters, and field propagation conditions. The interpretation of system output in terms of N_g is subject to a number of uncertainties (e.g., Lopez et al. 1992), but multiple-station lightning locating networks are by far the best available tool for mapping N_g. More detailed information about LLSs is found in CIGRE TF C4.404, Report 376 (2009).

It is important to note that LLSs record strokes, not flashes, and therefore estimation of N_g from LLS data depends on the method to group strokes into flashes. Further, many lightning flashes produce multiple terminations on ground, so that the number of ground strike points is larger than the number of flashes (see Section 2.7). This should be taken into account in estimating lightning incidence to areas when, for example, performing risk calculations. Finally, the accuracy of N_g mapping depends on the number of events per grid cell, which in turn depends on the grid cell size and period of observations (Diendorfer, 2008). It is recommended that the number of events per grid cell be at least 80 (Diendorfer, 2008) or 400 (IEEE Std 1410-2010).

Lightning Flash Counters. The lightning flash counter (LFC) is an antenna-based instrument that produces a registration if the electric (or magnetic) field generated by lightning, after being appropriately filtered (the center frequency is typically in the range from hundreds of hertz to tens of kilohertz), exceeds a fixed threshold level. The output of an LFC is the number of lightning events and/or time sequence of lightning events recorded at a given location. If the fraction of ground flashes in the total number of lightning flash counter registrations Y_g and its effective range R_g are known, LFCs can provide reasonably accurate data on ground flash density. However, estimation of Y_g and R_g is not a trivial task (Rakov and Uman, 2003, Chapter 2).

If no measurements of the ground flash density N_g for the area in question are available, this parameter can be roughly estimated from the annual number of thunderstorm days T_D, also called the keraunic level. Apparently the most reliable expression relating N_g and T_D is the one proposed by Anderson et al. (1984a):

$$N_g = 0.04\ T_D^{\ 1.25} \tag{2.1}$$

This expression is based on the regression equation relating the logarithm of the five-year-average value of N_g measured with CIGRE 10 kHz lightning flash counters at 62 locations in South Africa and the logarithm of the value of T_D as reported by the corresponding weather stations. The range for T_D was from 4 to 80, the range for N_g was from about 0.2 to about 13 flashes/km^2 /yr, and the correlation coefficient between the logarithms of N_g and T_D was 0.85. Another characteristic of lightning activity that can be used for the estimation of N_g is the annual number of thunderstorm hours T_H. The relation between N_g and T_H proposed by MacGorman et al. (1984) is

$$N_g = 0.054\ T_H^{\ 1.1} \quad (2.2)$$

Although T_H is a parameter potentially more closely related to N_g than T_D, the long-term annual number of lightning-caused outages of power lines that have similar geometrical and electrical characteristics and are located in areas with different long-term values of T_D and T_H do not show a better correlation with T_H than with T_D (Dulzon and Rakov, 1991). Both T_D and T_H are generally based on human observations at weather stations.

Variation in ground flash density from one region to another can be very large. For example, in the contiguous United States it is more than two orders of magnitude.

2.5. Number of Strokes in a Downward Negative Cloud-to-Ground Flash

A typical negative cloud-to-ground flash is composed of 3 to 5 strokes (leader/return stroke sequences), with typical interstroke intervals of some tens of milliseconds. The largest number of strokes per flash, observed in New Mexico (Kitagawa et al, 1962), is 26. Note that the stroke count includes both strokes developing in pre-existing channels (channel established by the first stroke in a flash) and those creating new terminations on ground (ground contact points). Parameters of new-ground-termination strokes are intermediate between first strokes and subsequent strokes developing in pre-existing channels.

The average numbers of strokes per flash and percentages of single-stroke flashes observed in different locations, using accurate stroke count methods, are summarized in Table 2.1. It follows from Table 2.1 that the percentage of single-stroke flashes previously recommended by CIGRE, 45% (Anderson and Eriksson, 1980), is an overestimate by a factor of two or so. Note that the percentage of single-stroke flashes in the tropics (Sri Lanka and Malaysia) is about the same as that in the temperate regions.

Table 2.1: Number of strokes per negative flash and percentage of single-stroke flashes.

Location (Reference)	Average Number of Strokes per Flash	Percentage of Single-Stroke Flashes	Sample Size
New Mexico (Kitagawa et al., 1962)	6.4	13%	83
Florida (Rakov and Uman, 1990b)	4.6	17%	76
Sweden (Cooray and Perez, 1994)	3.4	18%	137
Sri Lanka (Cooray and Jayaratne, 1994)	4.5	21%	81
Brazil (Ballarotti et al., 2012)	4.6	17%	883
Arizona (Saraiva et al., 2010)	3.9	19%	209
Malaysia (Baharudin et al., 2012)	4.0	16%	100

Qie et al. (2002), from their observations of 83 negative flashes in the Chinese inland plateau (Gansu province), reported the average number of strokes per flash and percentage of single-stroke flashes to be about 3.8 and 40%, respectively. It is presently unknown why the latter figure (40%) differs significantly from its counterparts in Table 2.1. Additional data for China are needed.

2.6. Interstroke Intervals and Flash Duration

Interstroke intervals are usually measured between the peaks of current or electromagnetic field pulses. Some interstroke intervals contain continuing currents (see Chapter 4) of appreciable duration. However, these currents always vanish before the next stroke (McCann, 1944; Berger, 1967; Fisher et al., 1993). The time interval between the end of continuing current and the beginning of the next stroke is referred to as the no-current interstroke interval. Less accurate estimates of interstroke intervals can be obtained from high-speed (interframe intervals of 1 ms or less) video observation.

From accurate-stroke-count studies of negative flashes in Florida and New Mexico, the geometric mean interstroke interval is about 60 ms (Rakov and Uman, 2003, Fig. 4.4). When long continuing currents (see Chapter 4) are involved, interstroke intervals can be as large as several hundreds of milliseconds. Occasionally, two leader/return stroke sequences occur in the same lightning channel with a time interval between them as short as 1 ms or less (Rakov and Uman, 1994; Ballarotti et al., 2005). Interstroke intervals preceding strokes initiating long continuing currents show a clear tendency to be shorter than regular interstroke intervals (Shindo and Uman, 1989; Rakov and Uman, 1990a; Saba et al., 2006a). Table 2.2 gives a summary of geometric mean interstroke intervals observed for negative lightning in different geographical locations. Additionally given are multiple-stroke flash durations.

Table 2.2: Interstroke interval and flash duration (sample sizes are given in the parentheses).

Location (Reference)	Geometric Mean Interstroke Interval, ms	Geometric Mean Flash Duration*, ms
Florida and New Mexico (Rakov and Uman, 1990a)	60 (516)	-
Brazil (Saraiva et al., 2010)	62 (624)	229 (179)
Arizona (Saraiva et al., 2010)	61 (598)	216 (169)
Malaysia (Baharudin et al., 2012)	67(305)	-

*Multiple-stroke flashes only.

Qie et al. (2002) reported the geometric mean interstroke interval of 47 ms (sample size = 238) for 50 negative flashes in Gansu province, China.

2.7. Multiple Channel Terminations on Ground

One-third to one-half of all lightning discharges to earth, both single- and multiple-stroke flashes, strike ground at more than one point with the spatial separation between the channel terminations being up to many kilometres. Most measurements of lightning flash density do not account for multiple channel terminations on ground. When only one location per flash is recorded, while all strike points separated by distances of some hundreds of meters or more are of interest, as is the case where lightning damage is concerned, measured values of ground flash density should, in general, be increased. According to Table 2.3, the correction factor of about 1.5 to 1.7 is needed for measured values of ground flash density to account for multiple channel terminations on ground, which is considerably larger than 1.1 previously estimated by Anderson and Eriksson (1980).

In most cases, multiple ground terminations within a given flash are associated not with an individual multi-grounded leader but rather with the deflection of a subsequent leader from the previously formed channel. According to Thottappillil et al. (1992), the distances between separate channel terminations in a given flash, located via TV direction finding and thunder ranging for 22 flashes in Florida, vary from 0.3 to 7.3 km with a

geometric mean of 1.7 km (see Fig. 2.3). The geometric mean separation between two channel terminations created by the same leader (in 7 or 32% of the 22 flashes) was also 1.7 km. The NLDN-based distances between the first stroke and 59 new-ground-termination strokes in southern Arizona had a median of 2.1 km (Stall et al., 2009).

According to Rakov and Uman (1990b), the percentage of subsequent leaders that create a path to ground different from that of the previous stroke path decreases rapidly with stroke order: 37% of all second leaders, 27% of all third leaders, 2% of all fourth leaders, and none of the leaders of the order of 5 and higher. Interestingly, if only those third leaders which followed the formation of a new second-stroke path to ground (19 total) are considered, the percentage of the new terminations is 37%, the same as for second leaders, all of which are preceded by the formation of a new channel, the first-stroke channel. Rakov and Uman (1990b) interpreted these results as indicating that the first stroke (or even a sequence of the first two strokes) of the flash often does not create a properly conditioned channel capable of supporting the propagation of the following leader all the way to ground. An unalterable path to ground in a given flash is apparently established only after at least four (possibly more) consecutive strokes have participated in channel conditioning. Note that the behavior described above cannot be explained in terms of relatively long preceding interstroke intervals (and hence more aged channels) for strokes of the order of 2 through 4. In fact, the fraction of interstroke intervals lasting longer than 100 ms and not containing long continuing current for strokes from 2 to 4 is about the same as for the higher-order strokes. Further, the geometric mean preceding interstroke interval for second strokes is similar to that for strokes of the order of 5 and higher. According to Ferro et al. (2012), the preceding interstroke interval becomes a factor after two or more strokes have used the previously-created channel, with new ground terminations being more likely produced following longer interstroke intervals.

Table. 2.3: Number of channel terminations per flash

Location (Reference)	Average Number of Channels per Flash	Percentage of Multi-grounded Flashes	Sample Size
New Mexico (Kitagawa et al., 1962)	1.7 1.6	49% 42%	72* 83**
Florida (Rakov and Uman, 1990b)	1.7	50%	76
France (Berger et al., 1996; Hermant, 2000)	1.5	34%	2995
Arizona (Valine and Krider, 2002)	1.4	35%	386
US Central Great Plains Fleenor et al. (2009)	1.6	33%	103
Brazil (Saraiva et al., 2010)	1.7	51%	138
Arizona (Saraiva et al., 2010)	1.7	48%	206

* multiple-stroke flashes only

** including 11 single-stroke flashes assumed to each have a single channel per flash

In southern Arizona, Stall et al. (2009) observed that 59% of the time it was the second stroke that produced a new ground termination, and 27% of the time it was the third stroke (the sample size was 59). In three cases they observed new ground terminations created by the fifth stroke and in one case by the seventh stroke. Ferro et al. (2012) reported two cases of new ground terminations created by nineth strokes (but none by eighth strokes).

The percentage of multi-grounded flashes exhibits significant storm-to-storm variation. Rakov and Uman (1990b) reported a range of 29% to 69% for three individual thunderstorm days, with a mean of 50%. Thottappillil et al. (1992) observed up to four different strike points per flash in Florida, as did Fleenor et al. (2009) in the U.S. Central Great Plains. Saraiva et al. (2010) reported up to five strike points in Arizona and up to four in Brazil. Berger et al. (1996) and Hermant (2000) observed up to six strike points in France. The largest reported number of ground terminations in a single flash is seven (Rakov and Uman, 2003, Fig. 4.1).

Kong et al. (2009) studied multiple channel terminations created by the same negative leader in China. The percentage of flashes showing this feature varied from 11% to 20% with a mean of 15% (9 out of a total of 59 flashes). It is of interest to compare this result with observations in Florida. As noted earlier, Rakov and Uman (1990a) reported that 50% of 76 negative flashes in Florida created multiple channel terminations on ground. Individual channel terminations were located for 22 of their multigrounded flashes (Thottappillil et al., 1992). Of these 22, 7 (32%) flashes contained double-grounded leaders, which translates to 16% of all flashes, if we assume that the 22 multi-grounded flashes constitute 50% of all flashes, which is similar to the mean percentage reported by Kong et al. (2009).

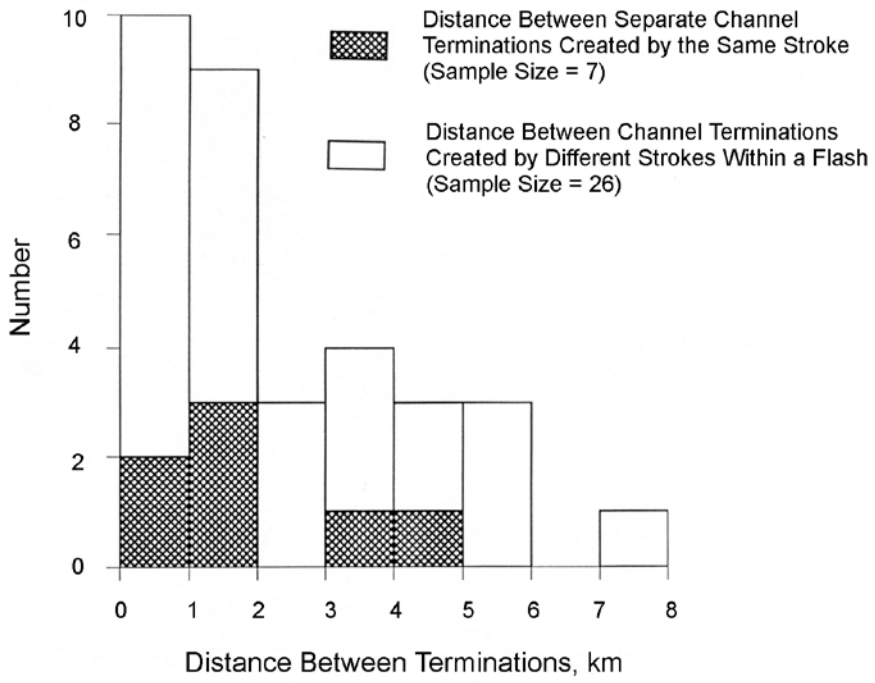

Fig. 2.3. Histogram of the distance between the multiple terminations of 22 individual ground flashes in Florida. Adapted from Thottappillil et al. (1992).

2.8. Relative Stroke Intensity Within the Flash

Relative magnitudes of electric field peaks of first and subsequent return strokes in negative cloud-to-ground lightning flashes recorded in Florida, Austria, Brazil, and Sweden were analyzed by Nag et al. (2008). On average, the electric field peak of the first stroke is appreciably, 1.7 to 2.4 times, larger than the field peak of the subsequent stroke (except for studies in Austria where the ratio varies from 1.0 to 2.3, depending on methodology and instrumentation). Similar results were previously reported from electric field studies in Florida, Sweden, and Sri Lanka by Rakov et al. (1994), Cooray and Perez (1994), and Cooray and Jayaratne (1994), respectively. Directly

measured peak currents for first strokes are, on average, a factor of 2.3 to 2.5 larger than those for subsequent strokes (Berger et al., 1975; Anderson and Eriksson, 1980; Visacro et al., 2004). The generally larger ratio for currents than for fields possibly implies a lower average return-stroke speed for first strokes than for subsequent strokes. There appear to be some differences between first versus subsequent stroke intensities reported from different studies based on data reported by lightning locating systems (LLSs). The ratio of LLS-reported peak currents for first and subsequent strokes confirmed by video records is 1.7 to 2.1 in Brazil (for strokes followed by continuing currents with durations ranging from 4 to 350 ms), while in the U.S. (Arizona, Texas, Oklahoma, and the Great Plains) it varies from 1.1 to 1.6, depending on methodology used. Ratios involving arithmetic means are generally larger than those involving geometric means. The smaller ratios derived from the LLS studies are likely to be due to poor detection of relatively small subsequent strokes. The smaller values in Austria are possibly related (at least in part) to the higher percentage (about 50% versus 24% to 38% in other studies) of flashes with at least one subsequent stroke greater than the first. The effects on the ratio of excluding single-stroke flashes or subsequent strokes in newly formed channels appear to be relatively small. Additional data are needed to further clarify the issue of relative intensity of first and subsequent strokes in different geographical locations, as well as possible instrumental and methodological biases involved.

Results of Nag et al. (2008) are summarized in Fig. 2.4 and Table 2.4. Also, Qie et al. (2002) found the geometric mean of first to subsequent stroke peak ratio to be 2.2 for 83 negative flashes in Gansu province, China.

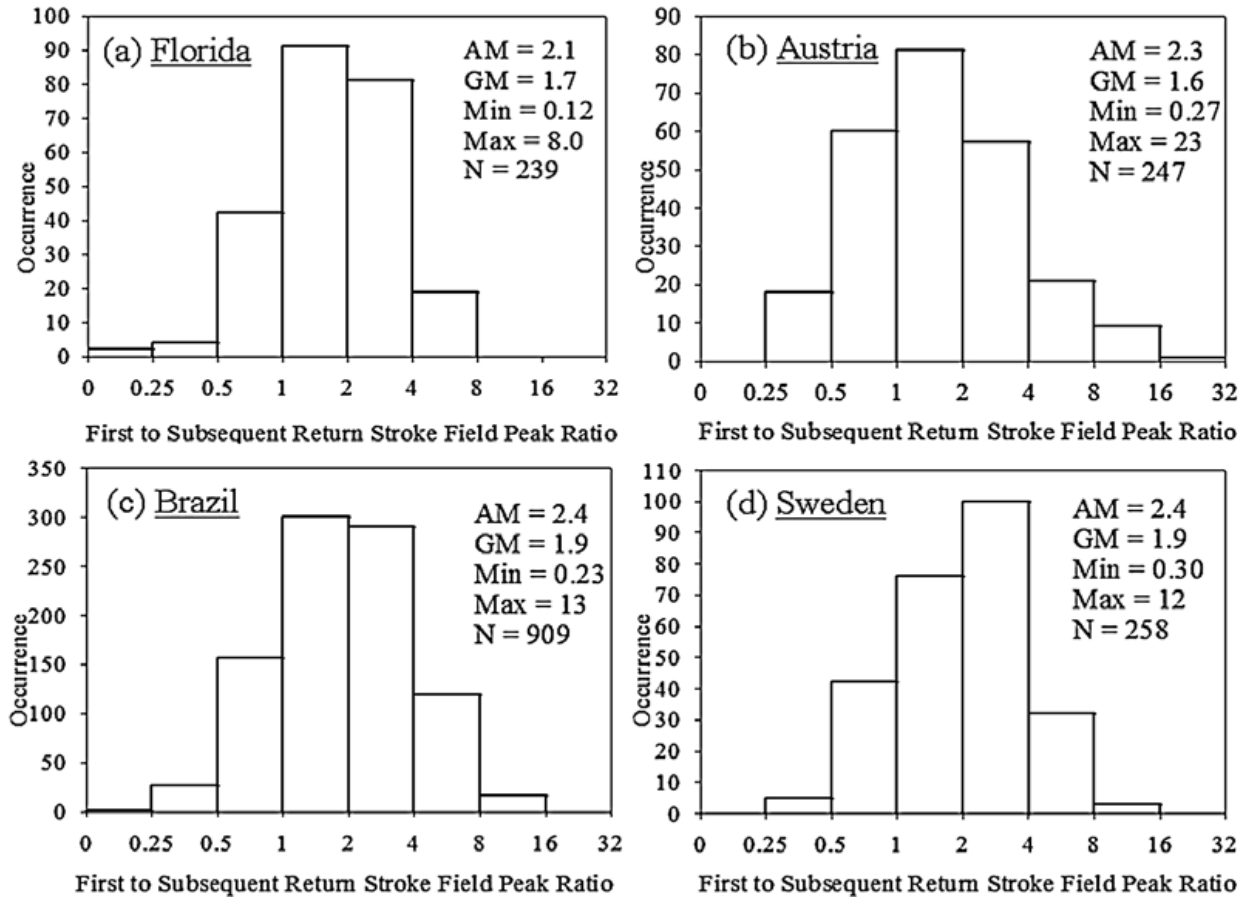

Fig. 2.4. Histograms of the ratio of the first-to-subsequent-return-stroke electric field peak for multiple-stroke negative cloud-to-ground lightning flashes in (a) Florida, (b) Austria, (c) Brazil, and (d) Sweden. Adapted from Nag et al. (2008).

Table 2.4: Summary of first to subsequent stroke electric field or current peak ratios estimated from different studies. Adapted from Nag et al. (2008).

Reference(s) and location	AM of first to subsequent stroke peak ratio	Ratio of AM first to AM subsequent stroke peak	GM of first to subsequent stroke peak ratio	Ratio of GM first to GM subsequent stroke peak	Ratio of median first to median subsequent stroke peak	Number of subsequent strokes	Number of first strokes	Number of single-stroke flashes	Stroke identification method
Electric Field									
Rakov and Uman (1990a, b), Florida	-	1.9	-	2.0[a]	-	270	76	13	Electric field and TV records
Diendorfer et al. (1998), Austria	-	-	-	1.0	1.0	53443	43133	24120	LLS reports
Schulz and Diendorfer (2006), Austria	2.3	1.4	1.6	1.3	1.1	247	81	0	Electric field records
Oliveira et al. (2007), Brazil	2.4	1.7	1.9	1.7	1.8	909	259	0	Electric field records
Schulz et al. (2008), Sweden	2.4	2.0	1.9	1.8	2.0	258	93	0	Electric field records
Nag et al. (2008), Florida	2.1	-	1.7	-	1.7[b]	239	176	0	Electric field records
Current									
Berger et al. (1975), Switzerland	-	-	-	-	2.5	135	101	~50	Direct current measurements
Anderson and Eriksson (1980), Switzerland	-	-	-	2.3	2.3	114	75	-	Direct current measurements
Visacro et al. (2004), Brazil	-	-	-	2.5	2.5	59	31	15	Direct current measurements
Saba et al. (2006b), Brazil	-	2.1[c]	-	1.7[c]	1.6[c]	193	55	16	LLS reports confirmed by video records
Biagi et al. (2007), Arizona	-	1.5	-	1.3	1.2	1602	953	388	LLS reports confirmed by video record
Biagi et al. (2007), Texas-Oklahoma	-	1.6	-	1.2	1.1	371	273	131	LLS reports confirmed by video record
Krider et al. (2007), Great Plains	-	1.3	-	1.3	1.2	150	90	40	LLS reports confirmed by video record

[a] For all subsequent strokes combined. For subsequent strokes following a previously-formed channel, Rakov et al. (1994) reported the ratio to be 2.2.

[b] The median of the ratio of first to corresponding subsequent stroke peak (in multiple stroke flashes), not the ratio of the medians of the first and subsequent stroke peaks, as for other studies in this column.

[c] For strokes followed by continuing currents with durations ranging from 4 to 350 ms.

Although first-stroke current peaks are typically a factor of 2 to 3 larger than subsequent-stroke current peaks, about one third of cloud-to-ground flashes contain at least one subsequent stroke with electric field peak, and, by theory, current peak, greater than the first-stroke peak. This relatively high percentage suggests that such flashes are not unusual, contrary to the implication of most lightning protection and lightning test standards (e.g., Anderson, 1982; Military Standard, 1983). Thottappillil et al. (1992) observed subsequent strokes with larger field peaks both in the first-stroke channel (13 strokes) and in a different channel (12 strokes). Of the latter 12 strokes, 6 strokes created new channels to ground and the remaining 6 strokes followed a previously formed channel. Parameters of subsequent strokes with larger field peaks which followed the same channel as the first stroke are summarized in Table 2.5. Note that larger subsequent strokes are associated with relatively short leader duration (and, by inference, higher leader speed) and relatively long preceding interstroke interval. Larger subsequent strokes never followed interstroke intervals shorter than 35 ms, whereas many regular subsequent strokes did (Thottappillil et al., 1992, Fig. 1c).

Table 2.5: Geometric mean values for various parameters of larger subsequent strokes in the same channel as the first stroke versus those for all subsequent strokes in the first-stroke channel. Adapted from Thottappillil et al. (1992).

Parameter	Larger Strokes	All Strokes
Return-stroke field peak (at 100 km), V/m	7.7 (13)	2.6 (176)
Return-stroke current peak*, kA	-27	-8.1
Preceding interstroke interval, ms	98 (13)	53 (176)
Leader duration, ms	0.55 (8)	1.8 (117)
Ratio of subsequent to first stroke field peak	1.2 (13)	0.39 (176)

The numbers in the parentheses are the sample sizes.

* Inferred from formula $I_p = 1.5 – 3.7*E_p$ where E_p is return-stroke initial electric field peak normalized to 100 km taken as positive and in V/m and I_p is return-stroke current peak, negative, and in kA (Rakov et al., 1992).

Larger-than-first subsequent strokes were also observed in direct current measurements. Five (15%) of the 33 negative downward multiple-stroke flashes striking instrumented towers in Switzerland, from the Atlas of lightning currents offered by Berger (1972), contained one or two subsequent strokes with initial return-stroke peak currents greater than their respective first-stroke peak currents. There were eight subsequent strokes with greater current peaks than the first-stroke peak (7% of all 115 subsequent strokes in the 33 flashes mentioned above), all of them necessarily following the same channel to the instrumented tower as the first stroke, The subsequent current peaks, greater than the first had a GM of 26 kA, which is about 1.2 times the GM of the first-stroke current peaks of those flashes and about 2.2 times the GM for all the 115 subsequent-stroke current peaks. The GM of the immediately preceding interstroke interval for the subsequent strokes with greater peaks was 69 ms, about 1.6 times the 43 ms GM for all the interstroke intervals.

The relative return-stroke peak and preceding interstroke interval statistics for larger subsequent strokes in the first-stroke channel derived from Florida electric field data are similar to those from direct channel-base current measurements in Switzerland.

Larger-than-first subsequent strokes may represent an additional threat to power transmission lines, as discussed in Section 10.3.

2.9. Summary

A typical negative cloud-to-ground flash is composed of 3 to 5 strokes (leader/return stroke sequences), with the geometric mean interstroke interval being about 60 ms. Occasionally, two leader/return stroke sequences occur in

the same lightning channel with a time interval between them as short as 1 ms or less. The observed percentage of single-stroke flashes, based on accurate-stroke-count studies in New Mexico, Florida, Sri Lanka, Sweden, Arizona, Brazil, and Malaysia, is about 20% or less, which is considerably lower than 45% presently recommended by CIGRE (Anderson and Eriksson, 1980). Roughly one-third to one-half of all lightning discharges to earth, both single- and multiple-stroke flashes, strike ground at more than one point with the spatial separation between the channel terminations being up to many kilometers. The correction factor of 1.5 to 1.7 is needed for measured values of ground flash density to account for multiple channel terminations on ground. This is considerably larger than 1.1 presently recommended by CIGRE (Anderson and Eriksson, 1980). First-stroke current peaks are typically a factor of 2 to 3 larger than subsequent-stroke current peaks. However, about one third of cloud-to-ground flashes contain at least one subsequent stroke with electric field peak, and, by theory, current peak, greater than the first-stroke peak.

3. Return-Stroke Parameters Derived from Current Measurements

Traditional lightning parameters needed in engineering applications include lightning peak current, maximum current derivative, average current rate of rise, current risetime, current duration, charge transfer, and action integral (specific energy), all derivable from direct current measurements. Distributions of these parameters presently adopted by most lightning protection standards are largely based on measurements by K. Berger and coworkers in Switzerland. More recently, additional direct current measurements on instrumented towers were made. Further, currents were measured for triggered-lightning strokes that are thought to be similar to subsequent strokes in natural lightning. Presented below is information on lightning peak currents, followed by that on other parameters derived from current measurements and on correlations between the parameters. Estimation of lightning peak currents from measured electric and magnetic fields, including the field-to-current procedures implemented in lightning locating systems, is also discussed. Additionally, the channel-base current equations found in the literature are reviewed.

3.1. Peak current – "Classical" Distributions

Essentially all national and international lightning protection standards (e.g., IEEE Std 1410-2010; IEEE Std 1243-1997; IEC 62305-1) include a statistical distribution of peak currents for first strokes in negative lightning flashes (including single-stroke flashes). This distribution, which is one of the cornerstones of most lightning protection studies, is largely based on direct lightning current measurements conducted in Switzerland from 1963 to 1971 (e.g., Berger, 1972; Berger et al., 1975). The cumulative statistical distributions of lightning peak currents for (1) negative first strokes, (2) positive first strokes, (3) negative and positive first strokes, and (4) negative subsequent strokes are presented in Fig. 3.1. The distributions are assumed to be log-normal (because they are positively skewed; that is, exhibit long "tails" extending toward higher values) and give percent of cases exceeding abscissa value.

It is worth noting that directly measured current waveforms of either polarity found in the literature do not exhibit peaks exceeding 300 kA or so, although inferences from remotely measured electric and magnetic fields suggest the existence of currents up to 500 kA and even higher. It is important to note that peak current estimates reported by the U.S. National Lightning Detection Network (NLDN) and by other similar systems are based on an empirical formula the validity of which has been tested, using triggered lightning in Florida and instrumented tower in Austria, only for negative subsequent strokes (Jerauld et al., 2005; Nag et al., 2011; Diendorfer et al., 2008). Remote measurements of lightning peak currents are discussed in Section 3.5.

The log-normal probability density function for peak current I is given by

$$f(I) = \frac{1}{\sqrt{2\pi}\beta I}\exp(-z^2/2) \tag{3.1}$$

where

$$z = \frac{\ln I - \text{Mean}(\ln I)}{\beta} \tag{3.2}$$

In (3.2), ln I is the natural (base e) logarithm of I, Mean (ln I) is the mean value of ln I, and $\beta=\sigma_{\ln}I$ is the standard deviation of ln I.

For a log-normal distribution, Mean (ln I) is equal to both the logarithm of geometric mean (GM) and logarithm of median (M) of I. It follows that the antilog of Mean (ln I) is the median (50% value) of I. Thus, a log-normal distribution is completely described by two parameters, the median and logarithmic standard deviation of the variable. Logarithmic standard deviations of lightning peak currents are often given for base 10 (base 10 logarithms are often denoted lg); those should be multiplied by ln 10 = 2.3026 in order to obtain $\beta=\sigma_{\ln}I$.

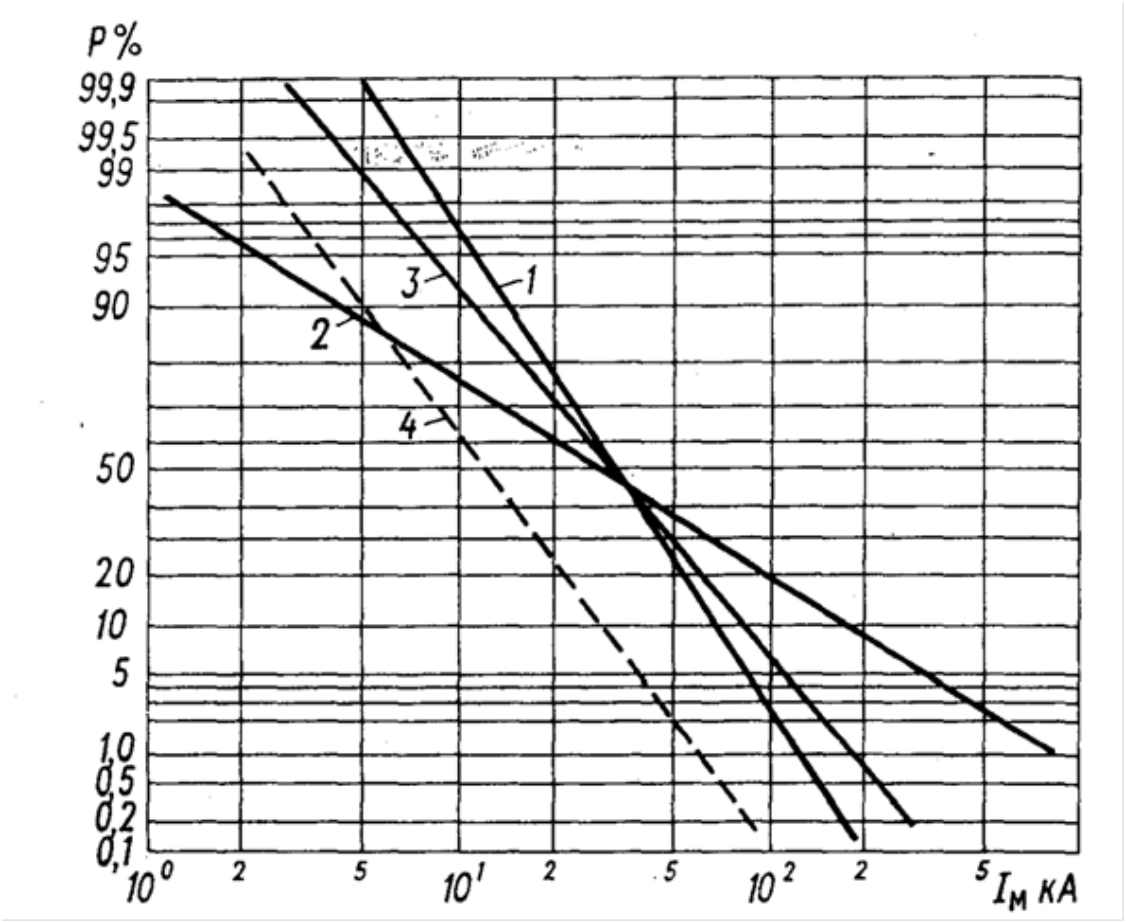

Fig. 3.1. Cumulative statistical distributions of lightning peak currents, giving percent of cases exceeding abscissa value, from direct measurements in Switzerland (Berger, 1972; Berger et al. 1975). The distributions are assumed to be log-normal and given for (1) negative first strokes (median = 30 kA, $\sigma_{lg}I$ = 0.265), (2) positive first strokes (median = 35 kA, $\sigma_{lg}I$ = 0.544), (3) negative and positive first strokes, and (4) negative subsequent strokes (median = 12 kA, $\sigma_{lg}I$ = 0.265). Note that no first strokes (of either polarity) with peak currents below 5 kA were observed. Adapted from Bazelyan et al. (1978).

The probability for peak current to exceed a specified value I is given by

$$P(I) = \int_{I}^{\infty} \frac{1}{\sqrt{2\pi}\beta I} \exp(-z^2/2)\, dI \tag{3.3}$$

P(I) can be evaluated as follows

$$P(I) = 1 - \Phi(z) = \frac{1}{2}\mathrm{erfc}\left(\frac{z}{\sqrt{2}}\right) \tag{3.4}$$

where Φ is the cumulative distribution function of the standard normal distribution and erfc is the complementary error function.

Only a few percent of negative first strokes exceed 100 kA, while about 20% of positive strokes have been observed to do so. On the other hand, it is thought that less than 10% of global cloud-to-ground lightning is positive. About 95% of negative first strokes are expected to exceed 14 kA, 50% exceed 30 kA, and 5% exceed 80

kA. The corresponding values for negative subsequent strokes are 4.6, 12, and 30 kA, and 4.6, 35, and 250 kA for positive strokes. Subsequent strokes are typically less severe in terms of peak current and therefore often neglected in lightning protection studies (see Chapter 10). According to Fig. 3.1 (line 3), slightly more than 5% of lightning peak currents exceed 100 kA, when positive and negative first strokes are combined. Additional information on positive lightning is found in Chapter 7.

Berger's peak current distribution for negative first strokes shown in Fig. 3.1 is based on about 100 direct current measurements accompanied by detailed optical observations and, as of today, is thought to be the most accurate one. The minimum peak current value included in Berger's distributions is 2 kA (note that no first strokes with peak currents below 5 kA were observed). Clearly, the parameters of statistical distributions can be affected by the lower and upper measurement limits. Rakov (1985) showed that, for a log-normal distribution, the parameters of a measured, "truncated" distribution and knowledge of the lower measurement limit can be used to recover the parameters of the actual, "untruncated" distribution. He applied the recovery procedure to the various lightning peak current distributions found in the literature and concluded that the peak current distributions published by Berger et al. (1975) can be viewed as practically unaffected by the effective lower measurement limit of 2 kA. Further it has been shown by Rakov (2003b) that Berger's peak currents for first strokes, based on measurements at the top of 70-m towers, are not influenced by the transient process (reflections) excited in the tower. For subsequent strokes, reflections are expected to increase the tower-top current by 10% or so. The distribution of peak currents based on measurements on tall instrumented towers may be biased (relative to the ground-surface peak-current distribution) toward higher values due to the peak-current-dependent attractive effect of the tower (Sargent, 1972; Borghetti et al., 2004). Borghetti et al. (2004), using the electrogeometric model, showed that median values of peak current based on measurements at instrumented towers should be reduced by 20% to 40% (depending on the attractive radius expression) to obtain the corresponding values for flat ground (in the absence of the tower). Interestingly, the electrogeometric model predicts that even the presence of a 5-m tall strike object appreciably alters the flat-ground peak current distribution (Mata and Rakov, 2008), although in practice this is unlikely because of the influence of neighboring objects such as buildings and trees. As of today, there is no experimental evidence that peak current distributions for downward lightning are materially affected by the presence of the tower (CIGRE TF 33.01.03 Report 118, 1997). In fact, Popolansky (1990) reported that the median negative peak currents for strike objects with heights 15-55 m (n = 64) and 56–65 m (n = 81) were 30 and 27 kA, respectively, not in support of the expected object-height dependence. For these height ranges, influence of upward lightning is usually neglected. To summarize, it appears that Berger's distributions of peak currents for first and subsequent negative strokes are not materially affected by either lower measurement limit or the presence of the tower.

In lightning protection standards, in order to increase the sample size, Berger's data are often supplemented by limited direct current measurements in South Africa and by less accurate indirect lightning current measurements obtained (in different countries) using magnetic links (se Table 3.1 and additional discussion below). There are two main distributions of lightning peak currents for negative first strokes adopted by lightning protection standards: the IEEE distribution (e.g., IEEE Std 1410–2010; IEEE Std 1243–1997; Anderson, 1982) and CIGRE distribution (e.g., Anderson and Eriksson, 1980). Both these "global distributions" are presented in Fig. 3.2 (taken from CIGRE Document 63 (1991)).

In the coordinates of Fig. 3.2 (also Fig. 3.1), a cumulative log-normal distribution appears as a slanted straight line. Anderson and Eriksson (1980) arbitrarily introduced two slanted lines having different slopes and intersecting at 20 kA to approximate their peak current distribution based on data listed in table 3.1. The same approach was adopted in the CIGRE Document 63 (1991). Note that IEEE Std 1243–1997 makes reference to the two-slope CIGRE distribution as well.

For the CIGRE distribution, 98% of peak currents exceed 4 kA, 80% exceed 20 kA, and 5% exceed 90 kA.

For the IEEE distribution, the "probability to exceed" values are given by the following equation

$$P(I) = \frac{1}{1+\left(I/31\right)^{2.6}} \tag{3.5}$$

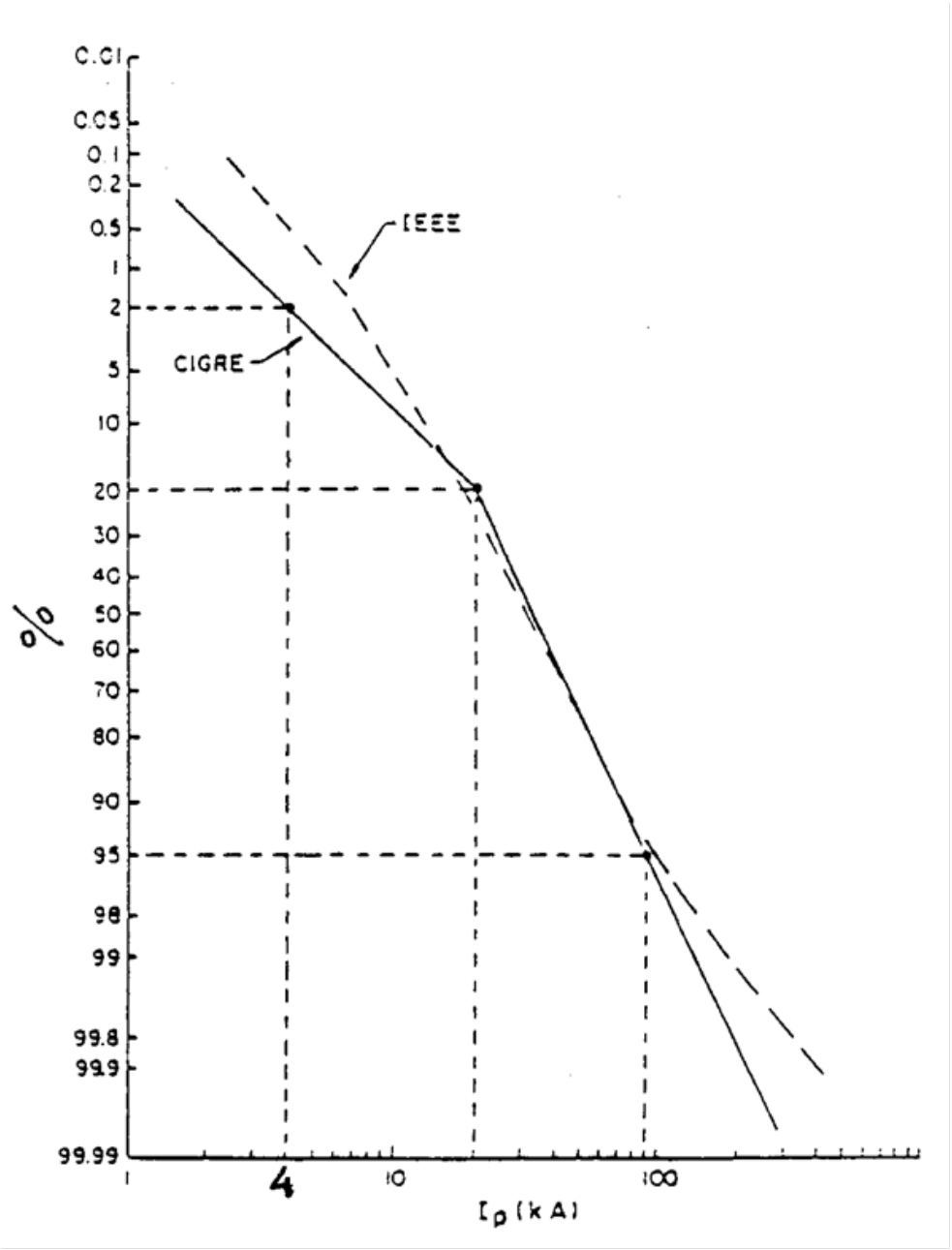

Fig. 3.2. Cumulative statistical distributions of peak currents (percent values on the vertical axis should be subtracted from 100% to obtain the probability to exceed, as in Fig. 3.1, the peak current value on the horizontal axis) for negative first strokes adopted by IEEE and CIGRE and used in various lightning protection standards. Taken from CIGRE Document 63 (1991).

where P(I) is in per unit and I is in kA. According to Hileman (1999), this equation, usually assumed to be applicable to negative first strokes, is based on data for 624 strokes analyzed by Poplansky (1972), whose sample included both positive and negative strokes, as well as strokes in upward lightning (see Table 3.1 and additional discussion below). Equation (3.5) applies to values of I up to 200 kA. For higher peak currents, IEEE Std 1243–1997 recommends the use of the two-slope CIGRE distribution, while IEEE Std 1410–2010 apparently relies on the log-normal approximation of Berger's distribution for the global current peak (I_F) found in Table 3.6. Values of P_I for I varying from 5 to 200 kA, computed using equation (3.5), are given in Table 3.2. The median (50%) peak current value is equal to 31 kA.

In the range of 10 to 100 kA that is well supported by experimental data, the IEEE and CIGRE distributions are very close to each other. Outside that range, the uncertainty, due to relative paucity of data, is apparently too large to allow one to favor either of the two distributions.

The peak-current distribution for subsequent strokes adopted by the IEEE (IEEE Std 1243-1997; IEEE Std 1410-2010) is given by

$$P(I) = \frac{1}{1+\left(I/12\right)^{2.7}} \tag{3.6}$$

which is compared with equation (3.5) in Table 3.2. CIGRE recommends for negative subsequent stroke peak currents a log-normal distribution with the median of 12.3 kA and β = 0.53 (CIGRE Document 63 (1991)), which is also included in IEEE Std 1410–2010 (see Table 3.6).

Table 3.1. Sample sizes for "global" peak current distributions for negative first strokes.

Country	Popolansky (1972)	Anderson and Eriksson (1980)	CIGRE Document 63 (1991)	Remarks
Switzerland	192 (positive and negative)	125 (negative only)	125 (negative only)	Direct measurements on towers
Czechoslovakia	208	123	123	Magnetic links on chimneys
Poland	122	3	3	Magnetic links on chimneys
Sweden	28	14	14	Magnetic links on chimneys
Norway	3	0	0	Magnetic links on chimneys
Great Britain	8	0	0	Magnetic links on chimneys
Australia	19	18	18	Magnetic links on power lines
USA	44	44	44	Magnetic links on power lines
South Africa	0	11 (negative only)	81*	Direct and magnetic link measurements on mast and power line
Total	624	338	408	

*Apparently, 29 values were current measurements on the 160-m mast and 52 were indirect (magnetic link) measurements on the test power distribution line.

We now further discuss the “global“ distributions found in most lightning protection standards. They are not much different from the distributions based on direct current measurements by Berger et al. (1975), which are still considered to be the most reliable ones (e.g., Gamerota et al., 2012). However, the extremely low and particularly extremely high (greater than 100 kA or so) peak current tails require much larger sample sizes (probably of the order of thousands or more) than presently available (or to be available in the foreseeable future) to bring the uncertainties within an engineering accuracy range.

In this regard, it is natural to attempt to combine as many measurements as possible to increase the sample size and, hence, reduce statistical uncertainties. One such attempt was made by Popolansky (1972) who combined direct and indirect (magnetic link) current measurements made on tall objects and on power lines in eight countries (see Table 3.1). The overall sample size was 624. Later it was realized (Anderson and Eriksson, 1980) that some of the indirect measurements on taller objects could be associated with strokes in upward lightning. Since upward lightning is unlikely to occur at objects less than 60 m in height, only measurements on shorter than 60 m objects were retained for compiling the next edition of the “global” peak current distribution. Additionally, all positive current measurements were excluded and 11 current measurements from South Africa were added (Anderson and Eriksson, 1980). The overall sample size became 338. Finally, in CIGRE Document 63 (1991), 70 more measurements (both direct and indirect) from South Africa were added bringing the overall sample size to 408. The majority of the additional 70 currents were obtained by adding typically 4 to 5 partial currents measured with magnetic links installed on wooden poles of the test power distribution line (Eriksson and Meal, 1984).

One concern about the “global” lightning peak current distributions is the inclusion of less accurate indirect (magnetic link) measurements. Even in the case of measurements on simple lightning down-conductors or measurements at vertical strike rods mounted on the top of transmission-line towers, very significant errors are likely. Specifically, magnetic links can be saturated or demagnetized by shaking during their transportation or by incomplete discharges from the strike object top occurring in response to nearby lightning flashes. Bazelyan et al. (2006), via modeling, showed that the collapse of charge accumulated at the tip of object (or on the unconnected upward leader) in response to a nearby downward leader can involve kiloampere-scale currents in the object at the time of return stroke initiated by that downward leader. Such induced currents, usually have polarity opposite to those of direct negative strikes. Taller objects were found to experience higher induced currents. This effect might be responsible for the observed decrease in median peak current measured using magnetic links with strike-object height, even when objects with heights greater than 65 m (for which upward flashes could be a factor) were excluded (Popolansky, 1990). In summary, it is probably best not to “compromise” direct current measurements by adding indirect measurements that may contain significant errors.

Additional concern about the “global” lightning peak current distributions is related to homogeneity of data coming from different sources and being lumped in a single sample. Popolansky (1972) noted that out of seven distributions based on indirect current measurements only two (from Czechoslovakia and Poland) were in “very good” agreement with the Swiss distribution based on direct current measurements. For one of the distributions (from the U.S.), the lowest measured value was 7 kA, which suggests that it might be significantly truncated (Rakov, 1985). Nevertheless, the U.S. distribution was included in the later editions of the “global” distributions (Anderson and Eriksson, 1980; CIGRE Document 63, 1991). Further, 11 peak current values from South Africa were added by Anderson and Eriksson (1980), although they suggested a quite different distribution (median = 41 kA, min = 10 kA). Out of the 11 values, only 8 were positively identified as corresponding to downward flashes, and 2 other values were measured with magnetic links. There has been a concern that the South African measurements, made at the bottom of the tower, might have been significantly affected by the transient process in the tower (e.g. Melander, 1984). Finally, 70 more values (including both direct and indirect measurements) from South Africa were added in CIGRE Document 63 (1991), with most of the values being obtained by summing partial currents measured at multiple poles of a test distribution line. The latter data were acquired during several years for different line configurations (presence or absence of arresters, transformers, and power follow current)(Eriksson et al., 1984), which could have introduced additional uncertainties.

As noted earlier, the latest version of the CIGRE “global” distribution was approximated by two straight lines having different slopes and intersecting at 20 kA (see Fig. 3.2). The change in slope at 20 kA might be due to combining data sets that do not represent the same general population. It is not clear if mixing direct current measurements

with less accurate indirect ones served to build a more statistically reliable distribution; it could have actually amounted to contamination of the relatively high quality data with more numerous data of questionable quality.

Table 3.2. The IEEE peak current distributions given by equations (3.5) and (3.6).

Peak current, I, kA		5	10	20	40	60	80	100	200
Percentage exceeding tabulated value, P(I) · 100%	First strokes	99	95	76	34	15	7.8	4.5	0.78
	Subsequent strokes	91	62	20	3.7	1.3	0.59	0.33	0.050

3.2. Peak Current – Recent Direct Measurements

More recently direct current measurements on instrumented towers were made in Russia, South Africa, Canada, Germany, Brazil, Japan, Austria, and again in Switzerland (on a different tower). Important results from the Brazilian, Japanese, and Austrian studies are reviewed and compared with Berger's data below. Recent direct current measurements for rocket-triggered lightning are also considered. Additional information on currents in upward lightning is found in Chapter 8.

Brazil. Visacro et al. (2004) presented a statistical analysis of parameters derived from lightning current measurements performed in 1985-1998 on the 60-m Morro do Cachimbo tower near Belo Horizonte, Brazil. Current sensors were installed at the tower base. In 1985-1998, two Pearson coils with a frequency bandwidth of 100 Hz to 10 MHz were connected to two oscilloscopes recording with a sampling interval of 50 ns. One coil was used for measuring currents above 20 kA and the other below 20 kA. A calibrated spark gap was used to bypass the latter coil when the current attained 20 kA. Up to 16 current pulses per flash could be recorded, with the individual pulse record length being 400 μs. The trigger threshold was 800 A. The dead time between two consecutive triggers was less than 12 ms. Apparently, there were no reliable current measurements in 1999-2007. By 2008, the measuring system was upgraded. Two new Pearson coils with bandwidths of 0.25 Hz to 4 MHz and 3 Hz to 1.5 MHz were installed, one of them for measuring currents from 20 A to 9 kA and the other from 20 A to 200 kA, respectively. Now currents are recorded using a multiple-channel, 12-bit data acquisition system capable of sampling at up to 60 MHz (17-ns sampling interval). No spark gap is used. The trigger threshold is 60 A. The record length is either 1 s with 30-ms pre-trigger (33-ns sampling interval) or 0.5 s with 15-ms pre-trigger (17-ns sampling interval). Thus, the entire flash current can be recorded. Current measurements were resumed in 2008.

A total of 31 negative downward flashes containing 80 strokes were recorded in 1985-1998 (during a period of 13 years). Median peak currents for first and subsequent strokes were found to be 45 and 16 kA, respectively, higher than the corresponding values 30 and 12 kA, reported for 101 flashes containing 236 strokes by Berger et al. (1975). Possible reasons for the discrepancy include: 1) a relatively small sample size in Brazil; 2) dependence of lightning parameters on geographical location (Brazil versus Switzerland) (see also Chapter 9); and 3) different positions of current sensors on the tower at the two locations (bottom of 60-m tower in Brazil versus top of 70-m tower in Switzerland). For typical first strokes (longer rise times), the towers in question are expected to behave as electrically short objects, so that the position of current sensor should not influence measurements. On the other hand, for subsequent strokes (shorter rise times), the towers may exhibit a distributed-circuit behavior, in which case the peak current measured at the bottom of tower is expected to be more strongly influenced by the transient process in the tower compared to the peak current at the top (Melander, 1984; Rakov, 2001). Visacro and Silveira (2005), using a hybrid electromagnetic (HEM) model and assuming a 100-m long upward connecting leader, showed that, for typical subsequent-stroke current rise times, peak currents at the top and bottom of the Morro do Cachimbo tower should be essentially the same. Visacro et al. (2012) increased the sample sizes for first and subsequent strokes by 7 and 12, respectively, by including additional measurements from 2008-2010. The overall ranges of variation are 14 to 153 kA for first strokes and 4.7 to 65 kA for subsequent ones. The new median values for first and subsequent strokes are 45 kA (n = 38) and 18 kA (n = 71), respectively. Additional measurements are needed. Note that the median peak current in Japan changed from 39 kA to 29 kA as the sample size increased

from 35 to 120 (see below). Similarly, the median peak current in South Africa (from measurements on the research mast) changed from 41 kA to 33 kA as the sample size increased from 11 to 29.

Another peculiarity of Brazilian measurements is virtual absence of upward flashes (only five were reported to date; Visacro, personal communication, 2012) that are expected for a 60-m tower on the top of 200-m hill. Zhou et al. (2010) estimated the effective height for this tower to be 145 m. It is conceivable that an unusual proportion of different types of lightning (due to some specific meteorological and topographic conditions) could lead to a bias toward higher peak currents.

Japan. Takami and Okabe (2007) presented lightning return-stroke currents directly measured on 60 transmission-line towers (at the top) whose heights ranged from 40 to 140 m (90 m on average). Most of the towers were located on the mountain ridges, at altitudes ranging from 100 m to 1.5 km. Currents were measured at 2.5-m strike rods installed on tower tops using Rogowski coils with RC external integrators, connected, via short shielded cables, to 10-bit memory cards. Each memory card was connected, via a fiber optic cable, to the communication terminal at the base of the tower (data could be read out remotely). The measuring system had a frequency bandwidth of 10 Hz to 1 MHz and recorded currents on two amplitude scales, ±10 kA and ±300 kA. The record length was 3.2 ms, and the sampling interval was 100 ns. The trigger threshold was relatively high, 9 kA. The maximum number of waveforms that could be recorded was 40 (J. Takami, personal communication, 2012).

A total of 120 current waveforms for negative first strokes were obtained from 1994 to 2004. This is the largest sample size for negative first strokes as of today. The median peak current was 29 kA, which is similar to that reported by Berger et al. (1975), although the trigger threshold in Japan (9 kA) was higher than in Switzerland. After compensation for the lower measurement limit (Rakov, 1987), the median peak current in Japan decreases from 29 kA to 26 kA. The largest measured peak current was 130 kA. Interestingly, initial data from this Japanese study (for 35 negative first strokes recorded in 1994–1997) yielded the median peak current of 39 kA (Narita et al., 2000).

Austria. Diendorfer et al. (2009) analyzed parameters of 457 upward negative flashes initiated from the 100-m Gaisberg Tower in 2000–2007. The overall current waveforms are measured at the base of the air terminal installed on the top of the tower with a current-viewing resistor (shunt) of 0.25 mΩ having a bandwidth of 0 Hz to 3.2 MHz. Fiber optic links (frequency bandwidth from dc to 15 MHz) were used for transmission of the shunt output signal to a digital recorder installed in the building next to the tower. Two separate channels of different sensitivity with current scales of ±2 kA and ±40 kA were used. The signals were recorded at a sampling rate of 20 MHz (50-ns sampling interval) by an 8-bit digitizing board installed in a personal computer. The trigger threshold of the recording system was set to ±200 A. The record length was 800 ms with a pre-trigger recording time of 15 ms. A digital low-pass filter with a cut-off frequency of 250 kHz and appropriate offset correction had been applied to the current records before the lightning peak currents were determined.

Upward flashes contain only strokes that are similar to subsequent strokes in natural downward flashes, i.e., they do not contain first strokes initiated by downward stepped leaders. Many upward flashes contain no strokes at all, only the so-called initial-stage current (see Chapter 8). The median return-stroke peak current in Austria was 9.2 kA (n = 615).

Triggered Lightning. Direct current measurements for return strokes in rocket-triggered lightning were performed in France, the United States, China, and Brazil. Representative measurements in Florida are discussed below.

Schoene et al. (2009) presented a statistical analysis of the salient characteristics of current waveforms for 206 return strokes in 46 rocket-triggered lightning flashes. The flashes were triggered during a variety of experiments related to the interaction of lightning with power lines that were conducted from 1999 through 2004 at Camp Blanding, Florida. Lightning channel-base currents were measured using non-inductive shunts mounted at the bottom of the launcher. Different shunts were used at different launchers, but in all cases the upper frequency response of the shunt exceeded 5 MHz. Shunt output signals were transmitted via fiber optic links (frequency bandwidth from dc to 15 MHz) to different digitizing oscilloscopes. The latter recorded either continuously for 1 or 2 s (at a sampling rate of 1 MHz or 2 MHz) or in a few millisecond long segments (at a sampling rate between 10 MHz and 50 MHz). The data were appropriately low-pass filtered to avoid aliasing. The lowest measured current peak was 2.8 kA, and the highest one was 42 kA.

The return-stroke current was injected into either one of two test power lines or into the earth near a power line via a grounding system of the rocket launcher. The geometric mean return-stroke peak current was found to be 12 kA, which is consistent with those reported from other triggered lightning studies (see Schoene et al. (2003, Table I)). Further, this parameter was found not to be much influenced by either strike-object geometry or level of man-made grounding, as previously reported by Rakov et al. (1998). Specifically, the peak current was about the same for the cases of current injection into an overhead power line conductor (impedance initially "seen" by lightning at its attachment point of about 200 Ω) and into a concentrated grounding system via a short down conductor. On the other hand, the means of the 10%-to-90% current risetimes were significantly different, as discussed in Section 3.3. Cooray et al. (2011) theoretically showed that the peak current decrease is negligible as the ground conductivity decreases from infinity to 10^{-3} S/m and is about 20% lower (compared to the perfectly conducting ground case) for ground conductivity of 10^{-4} S/m. The effect of ground conductivity on the maximum rate-of-rise was much more significant (see Section 3.3).

Fisher et al. (1993) compared return-stroke current parameters for classical triggered-lightning strokes with their counterparts for natural lightning reported by Berger et al. (1975) and Anderson and Eriksson (1980). Note that triggered-lightning strokes are considered to be similar to subsequent strokes in natural lightning; there is no stepped leader/first return stroke sequence in classical triggered lightning. Therefore, the comparison presented by Fisher et al. (1993) applies only to subsequent strokes that are initiated by continuously-moving dart leaders or by dart-stepped leaders.

Summarizing Tables. Distributions of lightning peak currents from individual studies (direct measurements only) and those synthesized by combining different measurements are compared for first and subsequent strokes in Tables 3.3 and 3.4, respectively. There may be a tendency for median return-stroke peak current in upward flashes initiated from tall towers to be somewhat lower than in downward or rocket-triggered flashes. This is probably because the lower-charge-density downward leaders that are not capable of making their way to flat ground or a small strike object may be able to make connection to a tall tower. Note that in rocket-triggered lightning the triggering wire is destroyed during the initial stage and downward leaders have to propagate all the way to the relatively small rocket launcher. An additional factor in lowering return-stroke peak currents in upward flashes is the lower cloud charge region, since upward flashes often occur in cold season (at least in Austria and Germany).

Table 3.3. Comparison of return-stroke peak currents (the largest peak, in kA) for first strokes in negative downward lightning

References	Location	Sample size	Percent exceeding tabulated value			$\sigma_{lg}I$	Remarks
			95%	50%	5%		
Berger et al. (1975)	Switzerland	101	14	30 (~30)	80	0.265	Direct measurements on 70-m towers
Anderson and Eriksson (1980)	Switzerland	80	14	31	69	0.21	Direct measurements on 70-m towers
Dellera et al. (1985)	Italy	42	-	33	-	0.25	Direct measurements on 40-m towers
Geldenhuys et al. (1989)	South Africa	29	7*	33 (43)	162*	0.42	Direct measurements on a 60-m mast
Takami and Okabe (2007)	Japan	120	10	29**	85	0.28**	Direct measurements on 40- to 140-m transmission-line towers
Visacro et al. (2012)	Brazil	38	21	45	94	0.20	Direct measurements on a 60-m mast
Anderson and Eriksson (1980)	Switzerland (N=125), Australia (N=18), Czechoslovakia (N=123), Poland (N=3), South Africa (N=11), Sweden (N=14), and USA (N=44)	338	9*	30 (34)	101*	0.32	Combined direct and indirect (magnetic link) measurements
CIGRE Report 63 (1991)	Switzerland (N=125), Australia (N=18), Czechoslovakia (N=123), Poland (N=3), South Africa (N=81), Sweden (N=14), and USA (N=44)	408	-	31 (33)	-	0.21	Same as Anderson and Eriksson's (1980) sample plus 70 additional measurements from South Africa

The 95%, 50%, and 5% values are determined using the lognormal approximation to the actual data, with 50% values in the parentheses being based on the actual data.

$\sigma_{lg}I$ is the standard deviation of the logarithm (base 10) of peak current in kA; $\beta = 2.3026\ \sigma_{lg}I$.

* As reported by Takami and Okabe (2007).

**26 kA and 0.32 after compensation for the 9-kA lower measurement limit.

Table 3.4. Comparison of return-stroke peak currents (in kA) for subsequent strokes in negative lightning

References	Location	Sample size	Percent exceeding tabulated value			$\sigma_{lg}I$	Remarks
			95%	50%	5%		
Berger et al. (1975)	Switzerland	135	4.6	12	30	0.265	Direct measurements on 70-m towers
Anderson and Eriksson (1980)	Switzerland	114	4.9	12	29	0.23	Direct measurements on 70-m towers
Dellera et al. (1985)	Italy	33	-	18	-	0.22	Direct measurements on 40-m towers
Geldenhuys et al. (1989)	South Africa	?	-	7- 8	-	-	Direct measurements on a 60-m mast
Visacro et al. (2012)	Brazil	71	7.5	18	41	0.23	Direct measurements on a 60-m mast
Diendorfer et al. (2009)	Austria	615	3.5	9.2	21	0.25	Direct measurements on a 100-m tower; upward lightning
Schoene et al. (2009)	Florida	165	5.2	12	29	0.22	Direct measurements; rocket-triggered lightning

The 95%, 50%, and 5% values are determined using the lognormal approximation to the actual data.
$\sigma_{lg}I$ is the standard deviation of the logarithm (base 10) of peak current in kA; $\beta = 2.3026\ \sigma_{lg}I$. Data for strokes in upward and rocket-triggered flashes are included because those strokes are similar to subsequent strokes in natural downward flashes.

3.3. Other Parameters Derived from Current Measurements

Lightning parameters, other than lightning peak current, derivable from direct current measurements include maximum current derivative, average current rate of rise, current rise time, current duration, charge transfer, and action integral (specific energy). Similar to the peak current, the most reliable and complete information on the other parameters is based on the direct current measurements of K. Berger and co-workers in Switzerland. Berger et al. (1975) summarized the lightning current parameters for 101 downward negative and 26 positive cloud-to-ground lightning flashes, the types that normally strike flat terrain and structures of moderate height. This summary, which is used to a large extent as a primary reference in the literature on both lightning protection and lightning research, is reproduced in Table 3.5. The Table gives the percentages (95%, 50%, and 5%) of cases exceeding the tabulated values, based on the log-normal approximations to the respective statistical distributions. The action integral represents the energy that would be dissipated in a 1 Ω resistor if the lightning current were to flow through it. All the parameters presented in Table 3.5 are estimated from current oscillograms with the shortest measurable time being 0.5 μs (Berger and Garbagnati, 1984). It is thought that in Table 3.5 the distribution of front durations might be biased toward larger values and the distribution of maximum current derivative (di/dt) toward smaller values. Anderson and Eriksson (1980) digitized the return-stroke current oscillograms of Berger et al. (1975) and determined additional wavefront parameters. Most of the current waveform parameters are illustrated

in Fig. 3.3. Parameters of log-normal distributions of current waveform parameters (for both first and subsequent strokes) are summarized in Table 3.6, adapted from CIGRE Document 63 (1991) and IEEE Std 1410-2010.

Table 3.5. Lightning Current Parameters for Negative Flashes (Berger et al., 1975)

Parameters	Units	Sample Size	Percent Exceeding Tabulated Value		
			95%	50%	5%
Peak current (minimum 2 kA)	kA	101	14	30	80
First strokes		135	4.6	12	30
Subsequent strokes					
Charge (total charge)	C				
First strokes		93	1.1	5.2	24
Subsequent strokes		122	0.2	1.4	11
Complete flash		94	1.3	7.5	40
Impulse charge (excluding continuing current)	C				
First strokes		90	1.1	4.5	20
Subsequent strokes		117	.22	0.95	4
Front duration (2 kA to peak)	μs				
First strokes		89	1.8	5.5	18
Subsequent strokes		118	.22	1.1	4.5
Maximum di/dt	kA/μs				
First strokes		92	5.5	12	32
Subsequent strokes		122	12	40	120
Stroke duration (2 kA to half peak value on the tail)	μs				
First strokes		90	30	75	200
Subsequent strokes		115	6.5	32	140
Action integral ($\int i^2 dt$)	A^2s				
First strokes		91	6.0×10^3	5.5×10^4	5.5×10^5
Subsequent strokes		88	5.5×10^2	6.0×10^3	5.2×10^4
Time interval between strokes	ms	133	7	33	150
Flash duration	ms				
All flashes		94	0.15	13	1100
Excluding single-stroke flashes		39	31	180	900

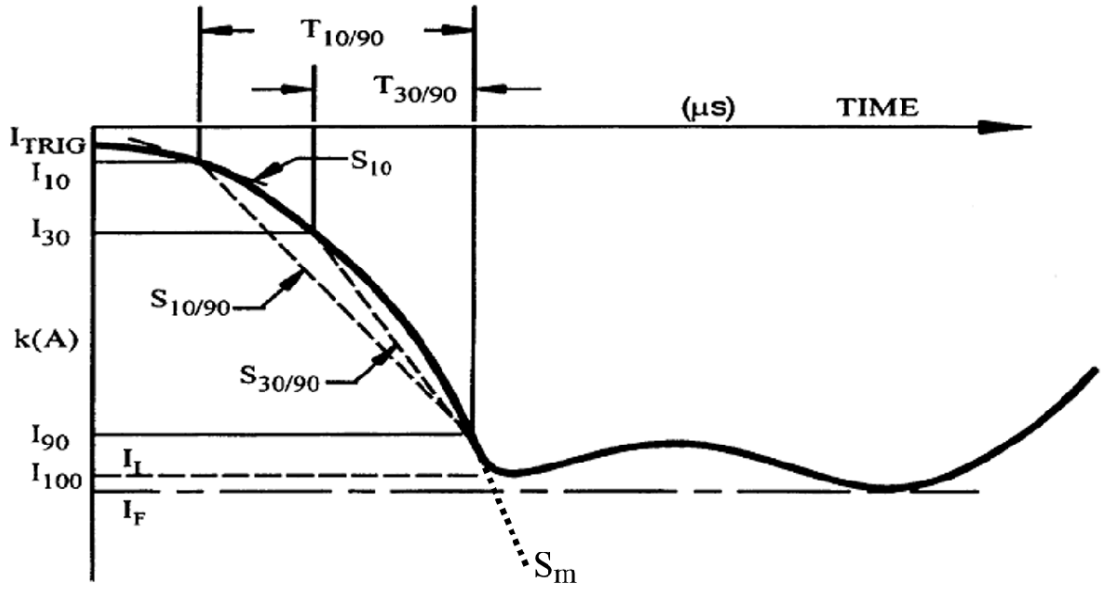

Parameter in Fig. 3.3	Description
I_{10}	10% intercept along the stroke current waveshape
I_{30}	30% intercept along the stroke current waveshape
I_{90}	90% intercept along the stroke current waveshape
$I_{100} = I_I$	Initial peak of current
I_F	Final (global) peak of current (same as peak current without an adjective)
$T_{10/90}$	Time between I_{10} and I_{90} intercepts on the wavefront
$T_{30/90}$	Time between I_{30} and I_{90} intercepts on the wavefront
S_{10}	Instantaneous rate-of-rise of current at I_{10}
$S_{10/90}$	Average steepness (through I_{10} and I_{90} intercepts)
$S_{30/90}$	Average steepness (through I_{30} and I_{90} intercepts)
S_m	Maximum rate-of-rise of current along wavefront, typically at I_{90}
$t_{d\ 10/90}$	Equivalent linear wavefront duration derived from $I_F / S_{10/90}$
$t_{d\ 30/90}$	Equivalent linear wavefront duration derived from $I_F / S_{30/90}$
t_m	Equivalent linear waveform duration derived from I_F / S_m
Q_I	Impulse charge (time integral of current)

Fig. 3.3. Description of lightning current waveform parameters. The waveform corresponds to the typical negative first return stroke. Adapted from CIGRE Document 63 (1991) and IEEE Std 1410-2010.

Table 3.6. Lightning current parameters (based on Berger's data) recommend by CIGRÉ Document 63 (1991) and IEEE Std 1410-2010.

Parameters of log-normal distribution for negative downward flashes				
Parameter	**First stroke**		**Subsequent stroke**	
	***M*, Median**	**β, logarithmic (base e) standard deviation**	***M*, Median**	**β, logarithmic base standard deviation**
FRONT TIME (μs)				
$t_{d10/90} = T_{10/90}/0.8$	5.63	0.576	0.75	0.921
$t_{d30/90} = T_{30/90}/0.6$	3.83	0.553	0.67	1.013
$t_m = I_F / S_m$	1.28	0.611	0.308	0.708
STEEPNESS (kA/μs)				
S_m, Maximum	24.3	0.599	39.9	0.852
S_{10}, at 10%	2.6	0.921	18.9	1.404
$S_{10/90}$, 10-90%	5.0	0.645	15.4	0.944
$S_{30/90}$, 30-90%	7.2	0.622	20.1	0.967
PEAK (CREST) CURRENT (kA)				
I_I, initial	27.7	0.461	11.8	0.530
I_F, final	31.1	0.484	12.3	0.530
Ratio, I_I/I_F	0.9	0.230	0.9	0.207
OTHER RELEVANT PARAMETERS				
Tail Time to Half Value t_h (μs)	77.5	0.577	30.2	0.933
Number of strokes per flash	1	0	2.4	0.96 based on median N_{total}=3.4
Stroke Charge, Q_I (Coulomb)	4.65	0.882	0.938	0.882
$\int I^2 dt$ ($(kA)^2 s$)	0.057	1.373	0.0055	1.366
Interstroke interval (ms)	—	—	35	1.066

For $T_{10/90}$, the median and logarithmic (base e) standard deviation are 4.5 μs and 0.576, respectively, and the corresponding values for $T_{30/90}$ are 2.3 μs and 0.553.

The median 10-to-90% risetime estimated for subsequent strokes by Anderson and Eriksson (1980) from Berger et al.'s (1975) oscillograms is 0.6 μs, comparable to the median values ranging from 0.3 to 0.6 μs for triggered lightning strokes (Leteinturier et al., 1991; Fisher et al., 1993). The median 10-to-90% current rate of rise reported for natural subsequent strokes by Anderson and Eriksson (1980) is 15 kA/μs, almost three times lower than the corresponding value of 44 kA/μs in data of Leteinturier et al. (1991) and more than twice lower than the value of 34

kA/μs found by Fisher et al. (1993). The largest value of maximum rate of rise of 411 kA/μs (see Fig. 3.4) was measured by Leteinturier et al. (1991, Fig. 4) for a triggered lightning stroke terminating on a launcher grounded to salt water. The corresponding directly measured current was greater than 60 kA, the largest value reported for summer triggered lightning. The mean value of current derivative peak reported by Leteinturier et al. (1991) is 110 kA/μs. The higher observed values of current rate of rise for triggered-lightning return strokes than for natural return strokes are likely due to the use of better instrumentation (digital oscilloscopes with better upper frequency response).

Note from Table 3.5 that the median return-stroke current peak for first strokes is 2 to 3 times higher than that for subsequent strokes. Also, negative first strokes transfer about a factor of 4 larger total charge than do negative subsequent strokes. On the other hand, subsequent return strokes are characterized by 3 to 4 times higher maximum steepness (the current maximum rate of rise).

Current waveform parameters for negative strokes in rocket-triggered lightning are summarized in Table 3.7.

Table 3.7. Current waveform parameters for negative strokes in rocket-triggered lightning flashes.

Experimental site	Sample size	Minimum	Maximum	Arithmetic Mean	Standard deviation	Geometric Mean	Standard deviation ($\log_{10}$ (x))	References
Peak current (kA)								
Camp Blanding, Florida, 1999-2004	165	2.8	42.3	13.9	6.9	12.2	0.22	*Schoene et al.* (2009)
Camp Blanding, Florida, 1998	25	5.9	33.2	14.8	7.0	13.5	0.19	*Uman et al.* (2000)
Camp Blanding, Florida, 1997	11	5.3	22.6	12.8	5.6	11.7	0.20	*Crawford* (1998)
Camp Blanding, Florida,1993	37	5.3	44.4	15.1	-	13.3	0.23	*Rakov et al.* (1998)
KSC, Florida, 1990; Alabama, 1991	45	-	-	-	-	12.0	0.28	*Fisher et al.* (1993)
France, Saint-Privat d'Allier, 1986, 1990-1991	54	4.5	49.9	11.0	5.6	-	-	*Depasse* (1994)
KSC, Florida, 1985-1991	305	2.5	60.0	14.3	9.0	-	-	*Depasse* (1994)
SHATLE, China, 2005-2011	36	4.4	41.6	14.3	9.2	12.1	0.23	Qie et al. (2013)
Current 10-90% risetime (μs)								
Camp	81	0.2	5.7	1.2	0.8	0.9	0.32	*Schoene*

Blanding, Florida, 1999-2004								*et al.* (2009)
KSC, Florida, 1990; Alabama 1991	43	-	2.9	-	-	0.37	0.29	*Fisher et al.* (1993)
France, Saint-Privat d'Allier, 1990-1991	37	0.25	4.9	1.14	1.1	-	-	*Depasse* (1994)
Camp Blanding, Florida,1997	11	0.3	4.0	0.9	1.2	0.6	0.39	*Crawford* (1998)
SHATLE, China, 2005-2011	36	0.2	8.4	2.0	2.1	1.9	0.47	Qie et al. (2013)
Current half-peak width (μs)								
Camp Blanding, Florida, 1999-2004	142	4	93	23	17	19	0.30	*Schoene et al.* (2009)
France, Saint-Privat d'Allier, 1990-1991	24	14.7	103.2	49.8	22.4	-	-	*Depasse* (1994)
KSC, Florida, 1990; Alabama 1991	41	-	-	-	-	18	0.30	*Fisher et al.* (1993)
Camp Blanding, Florida, 1997	11	6.5	100	35.7	24.6	29.4	0.29	*Crawford* (1998)
SHATLE, China, 2005-2011	36	1	68	23.7	17.1	14.8	0.52	Qie et al. (2013)
Return-stroke charge transfer within 1 ms (C)								
Camp Blanding, Florida, 1999-2004	151	0.3	8.3	1.4	1.4	1.0	0.35	*Schoene et al.* (2009)
SHATLE, China, 2005-2011	36	0.18	4.2	1.1	0.76	0.86	0.31	Qie et al. (2013)

Schoene et al. (2009), who presented a statistical analysis of the salient characteristics of current waveforms for 206 return strokes in 46 rocket-triggered lightning flashes, found that the means of the 10-to-90% current risetimes for strikes to the power line (geometric mean 1.2 μs) and for strikes to the ground nearby (geometric mean 0.4 μs) were significantly different. This indicates that the electrical properties of the strike object affect the risetime. This effect is likely related to the impedance seen by lightning at the strike point and/or to reflections at impedance discontinuities within the strike object, larger effective impedances apparently resulting in larger risetimes. A

dependence of the return-stroke current half-peak width on the electrical properties of the strike object was not observed. Cooray et al. (2011) theoretically showed that the peak value of current rate-of-rise is influenced by ground conductivity: it decreases by about 40% as the ground conductivity decreases from infinity to 10^{-3} S/m and by 83% when the conductivity becomes 10^{-4} S/m.

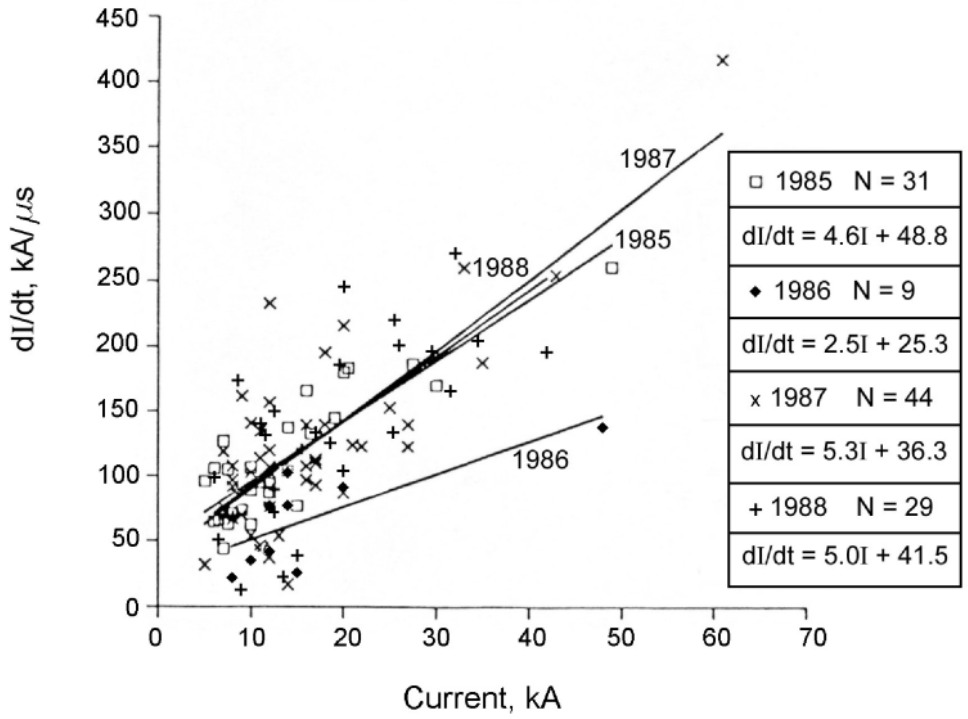

Fig. 3.4. Relation between the peak value of current rate of rise and peak current from triggered-lightning experiments conducted at the NASA Kennedy Space Center, Florida, in 1985, 1987, and 1988 and in France in 1986. The regression line for each year is shown, and the sample size and the regression equation are given. Adapted from Leteinturier et al. (1991).

3.4. Correlations Between the Parameters

Correlation coefficients for the current waveshape parameters defined in Fig. 3.3 are summarized in Table 3.8.

Table 3.8. Correlation coefficients between current waveshape parameters defined in Fig. 3.3. Adapted from Anderson and Eriksson (1980).

	$T_{10/90}$	$T_{30/90}$	S_{10}	$S_{10/90}$	$S_{30/90}$	S_m
I_I (first strokes)	0.40	0.47	(0.12)	0.30	(0.19)	0.43
I_F (first strokes)	0.33	0.45	(0.06)	(0.20)	(0.17)	0.38
I_F (subsequent strokes)	(0.15)	(0.00)	(0.05)	0.31	0.23	0.56

Values in the parentheses are not statistically significant at the 5% level.

As noted above, the current rate-of-rise parameters estimated by Anderson and Eriksson (1980) from Berger et al.'s (1975) oscillograms are likely to be significantly underestimated due to limitations of the instrumentation used by Berger et al. Therefore, not much significance should be attached to the last three columns of Table 3.8.

Anderson and Eriksson (1980) gave the following relationships between S_m and $S_{30/90}$ and peak currents (I in kA and S in kA/μs) for natural lightning:

First strokes: $S_m = 3.9\ I^{0.55}$ $S_{30/90} = 3.2\ I^{0.25}$ (3.7)

Subsequent strokes: $S_m = 3.8\ I^{0.93}$ $S_{30/90} = 6.9\ I^{4.2}$ (3.8)

Positive correlation between the peak value of current rate-of-rise and peak current for triggered lightning is illustrated in Fig. 3.4. Fisher et al. (1993), also for triggered lightning, found a relatively strong positive correlation between the 10-to-90% average steepness ($S_{10/90}$) and current peak (correlation coefficient = 0.71) and between the 30-to-90% average steepness ($S_{30/90}$) and current peak (correlation coefficient = 0.74). Essentially no linear correlation was found between the current peak and 10-to-90% risetime (this was also reported for triggered lightning in China; Yang et al., 2010) and between the current peak and current half-peak width. Similarly, but for first strokes in natural lightning, Takami and Okabe (2007) observed strong positive correlation between the current steepness characteristics and peak current and weak correlation between the peak current and front duration. Opposite trends for first strokes were reported by Visacro et al. (2004). Reasons for the latter peculiarity are not clear.

According to Berger et al. (1975), for first and subsequent negative strokes, correlation coefficients between the current peak and stroke duration (the time interval between the 2-kA point on the front and the point on the tail where the current has fallen to 50% of its peak value) are 0.56 and 0.25, respectively. Both values should be considered low, since even in the former case the determination coefficient (the square of the correlation coefficient) is as low as 0.31, which means that only 31% of the variation of one of the parameters is due to variation in the other one, while 69% is due to variation in other (unknown) factors.

All published experimental data regarding the relation between the return stroke peak current I and charge transfer Q (we consider only the so-called impulse charge transfer here) in natural lightning are derived from the data of K. Berger and coworkers (e.g., Berger, 1972; Berger et al., 1975; Berger and Garabagnati, 1984), for lightning striking two towers in Switzerland and two towers in Italy, and have been analyzed by them and by Cooray et al. (2007). According to Cooray et al. (2007), for natural negative first strokes, there is a linear regression $Q = 0.061\ I$ (R^2 = 0.88) for charge transfer to 100 μs, and for natural subsequent strokes, $Q = 0.028\ I$ (R^2 not stated) for charge transfer to 50 μs. In the above equations, charge transfer Q is in coulombs and peak current I is in kiloamperes. Additionally, Schoene et al. (2009) have shown that for triggered-lightning strokes (which as noted above are similar to natural-lightning subsequent strokes) the scatter-plot of return stroke peak current versus charge transfer to 1 ms is surprisingly similar to the 1 ms natural-lightning first stroke data of Berger (1972). The regression equation for 143 triggered-lightning strokes as given by Schoene et al. (2009) is $I = 12.3\ Q^{0.54}$ (R^2 = 0.76) and the regression equation for Berger's 89 natural-lightning first strokes is $I = 10.6\ Q^{0.7}$ (R^2 = 0.59). Qie et al. (2007) reported that $I = 18.5\ Q^{0.65}$ for ten triggered-lightning strokes in China.

Schoene et al. (2010) examined data on 117 return strokes in 31 rocket-and-wire-triggered lightning flashes acquired during experiments conducted from 1999 through 2004 at Camp Blanding, Florida, in order to compare the peak currents of the lightning return strokes with the corresponding charges transferred during various time intervals within 1 ms after return stroke initiation. They found that the determination coefficient (R^2) for lightning return stroke peak current versus the corresponding charge transfer decreases with increasing the duration of the charge transfer starting from return stroke onset. For example, R^2 = 0.91 for a charge transfer duration of 50 μs after return stroke onset, R^2 = 0.83 for a charge transfer duration of 400 μs, and R^2 = 0.77 for a charge transfer duration of 1 ms. Their results support the view that (1) the charge deposited on the lower portion of the leader channel determines the current peak and that (2) the charge transferred at later times is increasingly unrelated to both the current peak and the charge deposited on the lower channel section. Additionally, they found that the

relation between the return-stroke peak current and charge transfer to 50 μs for triggered lightning in Florida is essentially the same as that for subsequent strokes in natural lightning in Switzerland, further confirming the view that triggered-lightning strokes are very similar to subsequent strokes in natural lightning.

3.5. Peak Current Inferred from Measured Electromagnetic Field

Estimation of lightning peak currents from measured electric or magnetic fields requires a field-to-current conversion procedure. Lightning locating systems, such as the U.S. National Lightning Detection Network (NLDN), implement one such procedure. The NLDN uses an empirical formula, based on triggered-lightning data, to estimate the return-stroke peak current from the measured magnetic field peaks and distances to the strike point reported by multiple sensors. The conversion procedure includes compensation for the field attenuation due to its propagation over lossy ground (Cummins and Murphy, 2009).

Rakov et al. (1992) proposed the following empirical formula (EF) (linear regression equation) to estimate negative return-stroke peak current, I_{EF}, from the initial (essentially radiation) electric field peak, E, and distance, r, to the lightning channel:

$$I_{EF} = 1.5 - 0.037rE \tag{3.9}$$

where I_{EF} is in kA and taken as negative, E is positive and in V/m, and *r* is in km. Equation (3.9) was derived using data for 28 triggered-lightning strokes acquired by Willett et al. (1989) at the Kennedy Space Center (KSC), Florida. The fields were measured at about 5 km and their initial peaks were assumed to be pure radiation. The currents were directly measured at the lightning channel base.

Lightning peak currents can also be estimated using the radiation-field-to-current conversion equation based on the transmission line (TL) model (Uman and McLain, 1969), which is given by:

$$I_{TL} = \frac{2\pi\varepsilon_0 c^2 r}{v} E \tag{3.10}$$

where ε_0 is the permittivity of free space, c is the speed of light, and v is the return-stroke speed (assumed to be constant). The return-stroke speed is generally unknown and its range of variation is from one-third to two-thirds of the speed of light (Rakov, 2007) (see also Chapter 5). Both I_{TL} and E in equation (3.10) are absolute values.

Mallick et al. (2013b) compared peak currents obtained using the three methods outlined above with directly measured peak currents for 91 negative strokes in 24 lightning flashes triggered using the rocket-and-wire technique at Camp Blanding (CB), Florida, in 2008-2010. The empirical formula, based on data from the Kennedy Space Center (KSC), tended to overestimate peak currents, whereas the NLDN-reported peak currents were on average underestimates. The field-to-current conversion equation based on the transmission line model gave the best match with directly measured peak currents for return-stroke speeds between c/2 and 2c/3 (1.5 and 2×10^8 m/s, respectively). Possible reasons for the discrepancy between the peak current estimated from the empirical formula and the directly measured current, including an error in the field calibration factor, difference in the typical return-stroke speeds at CB and KSC, and limited sample sizes, were discussed. A new empirical formula, $I = -0.74 - 0.028rE$, based on data for 91 strokes in lightning flashes triggered at CB, was derived. Note that the electric fields used in deriving this formula were measured about 45 km from the lightning channel.

NLDN-reported peak currents vs. directly-measured currents for negative strokes in rocket-triggered lightning are shown in Fig. 3.5. Median absolute current estimation errors in two studies were 20% and 13%. As noted above, strokes in triggered lightning are similar to subsequent strokes in natural lightning and, hence, these results are applicable only to subsequent strokes. Unfortunately, no similar peak current error estimates are available for negative first strokes or for positive strokes. Preliminary results of comparison of peak currents obtained by summing directly measured currents in nine downleads (at ground level) of lightning protection system of one of the launch pads (LC39B) at the Kennedy Space Center, Florida, with NLDN-reported peak currents suggest that NLDN current estimation errors for negative first strokes do not exceed 40% (Mata et al. 2012; Mata and Mata 2012). The

LC39B lightning protection system includes three 183-m tall towers separated by 189, 270, and 276 m that support a catenary-wire system grounded at nine points at distances of about 200 m away from the towers. The overall horizontal dimensions of the system are several hundred meters. All the lightning discharges observed to date to terminate on this system were of downward type and transported negative charge to ground.

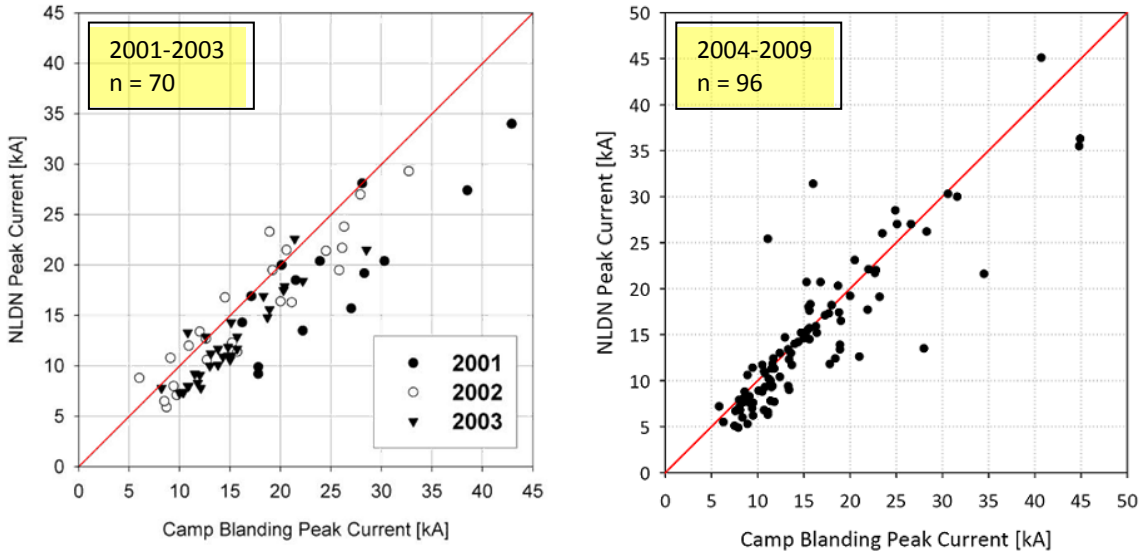

Fig. 3.5. NLDN reported peak currents vs. those directly measured at Camp Blanding, Florida, for two time periods, 2001-2003 (left panel) and 2004-2009 (right panel). In 2001-2003, a power-law propagation model was employed, while for most of the data from 2004-2009, an exponential propagation model was used. Slanted (diagonal) lines represent the ideal situation when the NLDN-reported and directly-measured peak currents are equal to each other. Adapted from Nag et al. (2011).

Similar scatter plots for peak currents reported by the European Cooperation for Lightning Detection (EUCLID) network vs. those directly measured at the Gaisberg Tower, Austria, are shown in Fig. 3.6. The data shown are for strokes in upward lightning (see Chapter 8), which (like strokes in triggered lightning) are similar to subsequent strokes in downward lightning.

It is possible that peak currents reported for first strokes by lightning locating systems are underestimated to a larger degree than for subsequent strokes. Assuming that (a) the radiation field peak is roughly proportional to the product of the current and return-stroke speed and (b) the field-to-current conversion equation is adjusted to a typical speed for subsequent strokes, one can infer that this equation will yield lower currents for first strokes, because the mean speed for first strokes, 9.6×10^7 m/s (n = 17), is lower than that, 1.2×10^8 m/s (n = 46), for subsequent strokes (Idone and Orville, 1982) (see also Chapter 5).

Besides systems of NLDN type (such as the European systems participating in EUCLID or nationwide (JLDN) and regional systems in Japan), there are other lightning locating systems that are also reporting lightning peak currents inferred from measured fields, including LINET (mostly in Europe), USPLN (in the U.S., but similar systems operate in other countries), WTLN (in the U.S. and other countries), WWLLN (global), and GLD360 (global). Peak current estimation errors for the latter systems are presently unknown, although calibration of the WTLN (based on rocket-triggered lightning data) is currently in progress (Mallick et al., 2013a).

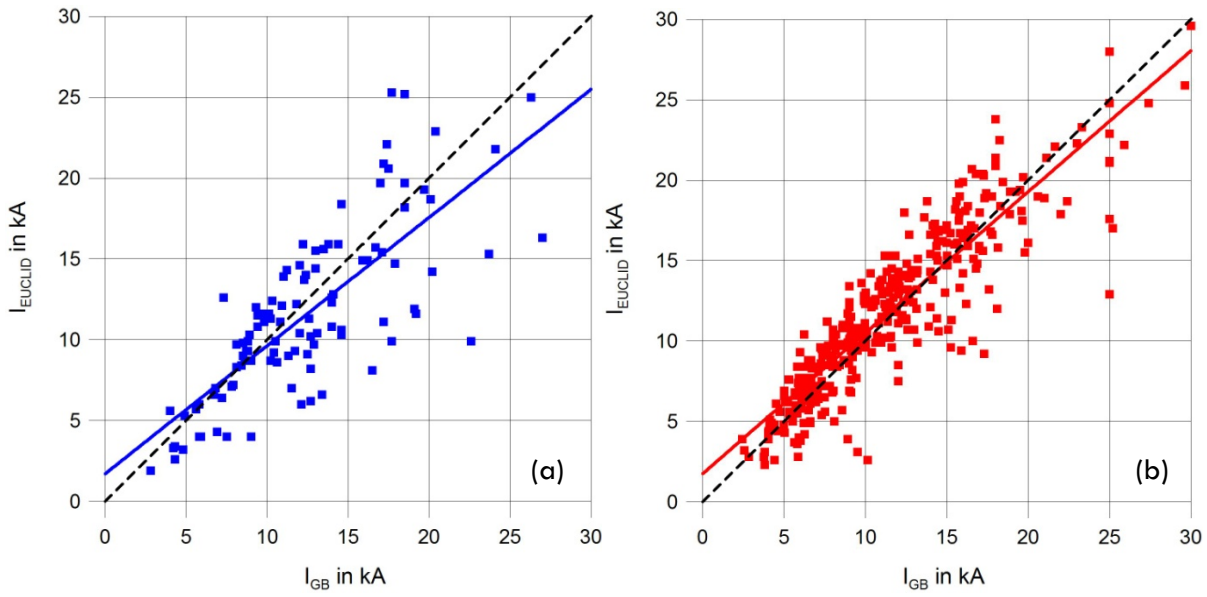

Fig. 3.6. EUCLID-reported peak currents (I_{EUCLID}) vs. those directly measured at the Gaisberg Tower, Austria (I_{GB}). (a) 0.23 field-to-current conversion factor, no propagation model (n = 385); (b) 0.185 field-to-current conversion factor, exponential propagation model (n = 106). Broken (diagonal) lines represent the ideal situation when the EUCLID-reported and directly-measured peak currents are equal to each other. Slanted solid lines are linear regression lines (least-squares fits to the data). Adapted from Diendorfer et al. (2008).

3.6. Channel-Base Current Equations

Direct effects of lightning current injection and induced effects from nearby lightning are often evaluated by numerical simulation involving assumed lightning current waveforms at the channel base. A variety of equations are used to approximate such waveworms. The typical subsequent-stroke current waveform at the channel base is often approximated by the Heidler function (Heidler, 1985a,b):

$$I(0,t) = \frac{I_0}{\eta}\frac{(t/\tau_1)^n}{(t/\tau_1)^n + 1} e^{-t/\tau_2} \qquad (3.11)$$

where I_0, η, τ_1, n, and τ_2 are constants. This function allows one to change conveniently the current peak, maximum current derivative, and associated electrical charge transfer nearly independently by changing I_0, τ_1, and τ_2, respectively. Equation (3.11) reproduces the observed concave rising portion of a typical current waveform, as opposed to the once more commonly used double-exponential function, introduced independently by Bruce and Golde (1941) and Stekolnikov (1941), which is characterized by an unrealistic convex wavefront with a maximum current derivative at t = 0. A current equation capable of reproducing a concave, convex, or linear wavefront was used by Rakov and Dulzon (1987). Sometimes the sum of two Heidler functions with different parameters is used to approximate the desired current waveshape. Diendorfer and Uman (1990), for example, described the subsequent-stroke current waveform at the channel base as the sum of two functions given by (3.11). The first function is characterized by I_0 = 13 kA, η = 0.73, τ_1 = 0.15 μs, n = 2, and τ_2 = 3.0 μs and the second one by I_0 = 7 kA, η = 0.64, τ_1 = 5 μs, n = 2, and τ_2 = 50 μs. The resultant current peak is 14 kA, and the maximum current rate of rise is 75 kA/μs. The channel-base current waveform used by Nucci et al. (1990), Rakov and Dulzon (1991), Thottappillil et al. (1997), and Moini et al. (2000) for the calculation of lightning return stroke electric and magnetic fields is the sum of a Heidler function and a double-exponential function. For this latter waveform, the current peak

is 11 kA, and the maximum current rate-of-rise is 105 kA/μs. Diendorfer and Uman (1990) also described the first-stroke current waveform (30 kA, 80 kA/μs) as the sum of two Heidler functions.

De Conti and Visacro (2007) employed Heidler functions to model the median rise-to-peak characteristics of first and subsequent negative return-stroke currents observed on towers on Mount San Salvatore, Switzerland, and at Morro do Cachimbo, Brazil. Gamerota et al. (2012) extended that study and other similar studies (e.g., Heidler and Cvetic, 2002; Andreotti et al., 2005; Silveira et al., 2010; Javor and Rancic, 2011) of negative return-stroke current waveform characteristics to include continuing current, as well as full-flash charge transfer and action integral (specific energy), for both positive and negative flashes, and for both median (typical) and severe cases.

3.7. Summary

From direct current measurements, the median return-stroke peak current is about 30 kA for negative first strokes in Switzerland, Italy, South Africa, and Japan, and typically 10-15 kA for subsequent strokes in Switzerland and for triggered and upward (object-initiated) lightning. Corresponding values from measurements in Brazil are 45 kA and 18 kA. Additional measurements are needed. The "global" distributions of lightning peak currents for negative first strokes currently recommended by CIGRE and IEEE (see Fig. 3.2) are each based on a mix of direct current measurements and less accurate indirect measurements, some of which are of questionable quality. However, since the "global" distributions have been widely used in lightning protection studies and are not much different (within 20% for currents up to 40 kA and within 40% for currents up to 90 kA for the CIGRE distribution) from that based on direct measurements only (median = 30 kA, $\sigma_{lg}I = 0.265$ for Berger et al.'s distribution), continued use of these "global" distributions for representing negative first strokes is recommended. For negative subsequent strokes, distribution 4 (median = 12 kA, $\sigma_{lg}I = 0.265$) in Fig. 3.1 should be used. For positive lightning strokes, distribution 2 (median = 35 kA, $\sigma_{lg}I = 0.544$) in Fig. 3.1 is recommended, although the data are very limited and may be influenced by the presence of strike object located on the mountain top. Direct lightning current measurements on instrumented towers should be continued. Currently, direct current measurements are performed on instrumented towers in Austria, Brazil, Canada, Germany, and Switzerland, although the overwhelmimg majority of observed flashes (except for Brazil) are of upward type.

Recommended lightning current waveshape parameters are still based on Berger et al.'s (1975) data (see Table 3.6), although the current rate-of-rise parameters estimated by Anderson and Eriksson (1980) from Berger et al.'s oscillograms are likely to be significantly underestimated, due to limitations of the instrumentation used by Berger et al. Triggered-lightning data for current rates of rise (see Table 3.7) can be applied to subsequent strokes in natural lightning. Relatively strong correlation is observed between the lightning peak current and impulse charge transfer and between the current rate-of-rise characteristics and current peak, and relatively weak or no correlation between the peak and risetime.

The field-to-current conversion procedure employed by the U.S. National Lightning Detection Network (NLDN) and other similar lightning locating systems has been calibrated only for negative subsequent strokes, with the median absolute error being 10 to 20%. Peak current estimation errors for negative first strokes and for positive lightning are presently unknown. Preliminary results of comparison of peak currents obtained by summing directly measured currents in nine downleads (at ground level) of lightning protection system of one of the launch pads (LC39B) at the Kennedy Space Center, Florida, with NLDN-reported peak currents suggest that NLDN current estimation errors for negative first strokes do not exceed 40%. Besides systems of NLDN type (such as the European systems participating in EUCLID or nationwide and regional systems in Japan), there are other lightning locating systems that are also reporting lightning peak currents inferred from measured fields, including LINET (mostly in Europe), USPLN (in the U.S., but similar systems operate in other countries), WTLN (in the U.S. and other countries), WWLLN (global), and GLD360 (global). Peak current estimation errors for the latter systems are presently unknown.

4. Continuing Currents

Most of the continuing current (CC) characteristics presented in this section come from observations of natural cloud-to-ground flashes with high-speed cameras obtained over the last decade. These findings are also discussed in the context of earlier results (see Chapters 4 and 5 of Rakov and Uman, 2003, and references therein) obtained using photographic/TV methods and/or broadband electric field measurements.

In using high-speed cameras, the presence and the duration estimates of CC are based on the assumption that the luminosity of the channel is due to the electric current that flows through it. In fact, Diendorfer et al. (2003) found a strong linear correlation (determination coefficient R^2 = 0.96) between brightness and current of the initial continuous current in upward initiated flashes (see Chapter 8) to the Gaisberg Tower (the range of 10 to 250 A). Based on the fact that continuing current values in CG flashes are usually in this range, it is generally assumed that the variations observed in the brightness of the channel are proportional to variations in the current that flows along the channel.

High-speed cameras can estimate the duration of CC that is as short as a few milliseconds. However, CC durations may be underestimated at large observation distances or in the presence of rain (Saba et al., 2006a). In order to minimize underestimation, only flashes occurring at distances less than 50 km were included in the review presented here. The data presented here are for strokes with visible channels, where it is possible to identify the presence of the CC.

Estimates of the CC magnitudes and charge transfers were derived from electric field measurements.

4.1. Presence of Continuing Currents

CC can last from a few to hundreds of milliseconds, and it can be classified as long (duration greater than 40 ms) (Brook et al., 1962; Kitagawa et al., 1962), short (between 10 and 40 ms) (Shindo and Uman, 1989), and very short (between 3 and 10 ms) (Ballarotti et al., 2005). In order to avoid contamination by what could be just return-stroke pulse tails, the observation of CG channels with luminosity duration less than 3 ms is not considered to be a CC event.

Long CC (duration longer than 40 ms) are responsible for most serious lightning damage associated with thermal effects, such as burned-through ground wires and Optical Fiber Ground Wires (OPGW) of overhead power lines, initiating forest fires, as well as blowing fuses used to protect distribution transformers, holes in the metal skins of aircraft, etc. (e.g., Fisher and Plumer, 1977; Rakov and Uman, 1990a; Chisholm et al., 2001).

A review of statistics on the occurrence of long CC in negative flashes observed with different instrumentation and in different locations is given by Rakov and Uman, 1990a. In general, the percentage of flashes containing at least one stroke followed by long CC varies from 20 to 50%.

Saraiva et al., 2010 using the same instrumentation (high-speed video cameras) in two different locations, São Paulo, Brazil and Arizona, USA, found a similar percentage of negative flashes containing at least one long CC: 34% in São Paulo and 27% in Arizona. However, there were large storm-to-storm variations.

Since large storm-to-storm variations are usually observed, studies analyzing several storms using the same technique will give a more reliable figure of the presence of long CC in negative flashes.

A study of the characteristics of a large number of negative cloud-to-ground flashes from 124 different storms based on high-speed video records was recently done in Brazil. 2459 out of 4495 negative strokes (55%) were followed by some CC (very-short, short or long), and 759 out of 971 negative flashes (78%) contained at least one stroke followed by some CC. The percentage of flashes containing at least one stroke followed by a long CC was 27% (Medeiros et al., 2012).

The presence of long CC (lasting more than 40 ms) after first strokes is very rare in negative CG flashes. Ballarotti et al. (2012) observed that only 2.4% (19/809) of first strokes in multi-stroke flashes were followed by long CC. This percentage is in agreement with the one found by Rakov and Uman (1990a) (2%) using broadband E-field and TV recordings. For single-stroke flashes, however, long CC was present in 14% of the 162 flashes in the study by Medeiros et al. (2012).

The presence of CC in positive flashes is very common. Beasley (1985), in his review of observations of positive CG flashes, reports that in some past studies (Rust et al., 1981; Fuquay et al., 1982; Beasley et al., 1983) there were large electric field changes that could be interpreted as CC in positive CG flashes. In fact, high-speed video observations of positive cloud-to-ground flashes (Schumann and Saba, 2012) indicate that 166 out of 171 positive strokes (97%) were followed by some CC (very-short, short or long). The percentage of flashes containing at least one long CC was 68% (100 out of 148). Further, relatively high percentages were observed in different geographical locations: 85% (40 out of 47) in southeast Brazil, 72% (23 out of 32) in south Brazil, 67% (10 out of 15) in South Dakota, and 52% (23 out of 44) in Vienna, Austria.

Table 4.1 summarizes the overall percentage of CC present in negative and positive strokes and flashes derived from recent studies based on high-speed video records mentioned above. Note that the percentages of positive flashes or strokes containing CC are much higher than in negative flashes/strokes. The percentages for positive flashes and positive strokes are very similar due to the fact that a large fraction of the positive flashes (81%) produces just a single stroke (Saba et al., 2010) (see also Chapter 7).

Table 4.1: Summary of the occurrence of CC in negative and positive strokes and flashes (sample sizes are given in the parentheses).

Polarity	Number	% with some CC ≥ 3ms)	% with Long CC (>40 ms)
Negative flashes	971	78%(759)	27%(259)
Negative strokes	4495	55% (2459)	7%(328)
Positive flashes	148	97% (144)	68% (100)
Positive strokes	171	97% (166)	62% (106)

4.2. Distribution of Continuing Current Duration

The cumulative probability distributions of CC duration for negative and positive flashes are presented in Fig. 4.1. Note that the probability to exceed any given duration of CC in positive CG flashes is much higher than in negative CG flashes.

Table 4.2 shows 5%, 50%, and 95% values for all CC (≥ 3 ms) and for long CC (> 40 ms) for both positive and negative CG flashes. Values obtained by Kitagawa et al. (1962) for long CC in negative CG flashes distribution are also shown.

Although there is a significant difference between the 5, 50 and 95% values in Table 4.2 for negative and positive CC when all CC durations are considered, these values are similar if only long CC duration is considered.

The maximum measured CC duration value for a negative flash found in the literature is 714 ms (Ballarotti et al., 2012). They observed only 6 cases of continuing current longer than 500 ms, representing 0.28% of the 2,180 CC events (or 0.68% of the 883 flashes). However, the percentage of CC longer than 500 ms in positive CG flashes is much higher, 6% of the 148 CC events (Schumann and Saba, 2012).

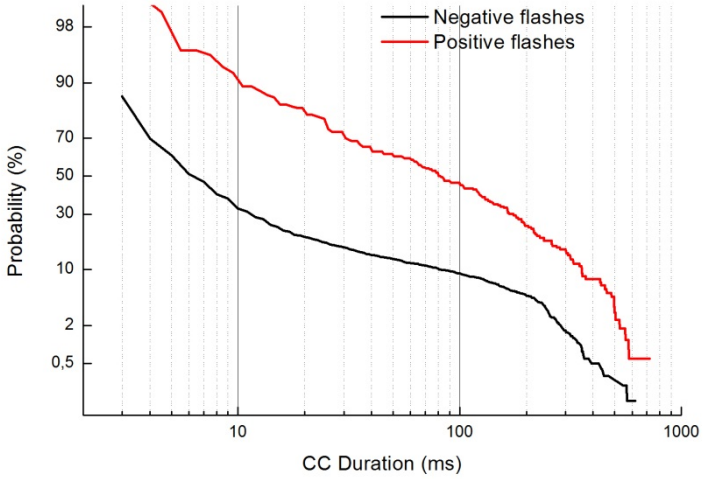

Fig. 4.1 Cumulative probability distributions of CC durations greater than or equal to 3 ms in negative and positive strokes.

Table 4.2: Summary of CC duration for positive and negative CG flashes.

Continuing Current Duration (ms)	Location	# of Storms	# of Events	Arithmetic Mean	Percentage [a] Exceeding Tabulated Value		
					95%	50%	5%
Negative CG flashes							
All CC (≥3 ms) Ballarotti et al. (2012)	S. Paulo, Brazil	1022	2180	31	2*	6	204
Long CC (>40 ms) Ballarotti et al. (2012)	S. Paulo, Brazil	102	304	173	45	145	366
Long CC (>40 ms) Kitagawa et al. (1962)	New Mexico, US	1	40	206	48	188	435
Positive CG flashes							
All CC (≥3 ms) Schumann et al. (2012)	Brazil/Austria/US	46	166	142	7	81	484
Long CC (>40 ms) Schumann et al. (2012)	Brazil/Austria/US	46	106	212	55	165	519

[a] *Based on values taken from the cumulative probability distribution curves.*

** Extrapolated value.*

4.3. Return Stroke Peak Current Preceding and Following Continuing Current

In this section we summarize the results of studies of the relationship between peak current and the duration of CC in ground flashes (Saba et al., 2006b; Saraiva et al. 2010). Similar studies were done comparing electric field peak and charge values for strokes initiating CC with those not initiating CC (e.g., Brook et al., 1962; Livingston and Krider, 1978; Shindo and Uman, 1989; Rakov and Uman, 1990a), with generally similar findings but with smaller datasets. Fig. 4.2 shows a scatterplot of the peak current (I_p) of negative strokes estimated by the LLS versus the duration of the CC that followed it. Note that this scatterplot shows a so-called "exclusion zone" for negative strokes, discussed by Saba et al. (2006b). That is, negative strokes that produce estimated peak currents greater than 20 kA are never followed by a CC longer than 40 ms, while negative strokes that produce peak currents less than 20 kA can be followed by CC of any duration.

Fig. 4.2 also includes data for 141 positive strokes for comparison. Note that positive strokes can produce both a high peak current (I_p > 20 kA) and a long CC (> 40 ms), a feature that has not been found in any negative stroke. Note also in Fig. 4.2 (upper right corner of the plot), that the positive stroke followed by the longest (800 ms) CC had one of the largest estimated peak current values (142 kA).

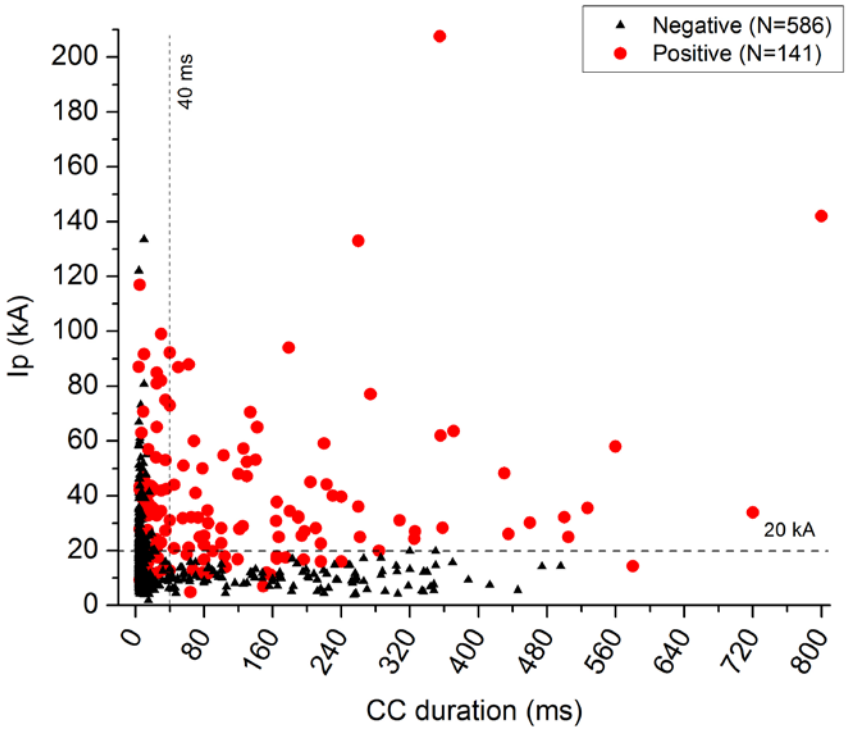

Fig. 4.2 Peak current (I_p) versus CC duration for 586 negative strokes and 141 positive strokes.

A pattern in the initiation of long CC was first suggested by Rakov and Uman (1990a). According to their suggestion, this pattern has the following characteristics: (i) strokes initiating long CC tend to have a smaller initial electric field peak than regular strokes, the latter defined as neither initiating long CC nor preceding those doing so nor following a long CC interval; (ii) strokes that precede those initiating a long CC are more likely to have a relatively large electric field peak than regular strokes and (iii) strokes that initiate long CC are usually preceded by a relatively short interstroke interval. This pattern in the initiation of long CC is also valid for the long CC initiated by a stroke that follows a new channel (Ferro et al., 2009).

4.4. Continuing Current Waveshapes and M-components

Although CCs are usually assumed in lightning protection standards to have a constant current value (e.g., IEC 62305, 2010), the CC intensity exhibits significant variations with time. These current variations can be either M-components (approximately symmetrical relatively short duration current pulses superimposed on the background steady current) or long duration variations that define the overall CC waveshape (Fig. 4.3). Both were first studied through direct current measurements by Fisher et al. (1993) for negative triggered lightning. They have grouped the current-versus-time graphs into four waveshape types. More recently, high-speed video data have made it possible to study waveshapes of CC in both negative and positive natural cloud-to-ground lightning (Campos et al., 2007, 2009).

The high-speed video records were used to examine the luminosity variation with time for specific pixels on each frame. Assuming that the luminosity is directly proportional to the channel current (Diendorfer et al., 2003), the results were interpreted in terms of CC variation with time. Findings from these studies indicate that natural CG flashes exhibit two more waveshape types, in addition to those suggested by Fisher et al. (1993). More than 30 M-components have been observed in one extremely long negative CC. Furthermore, the average number of M components per CC is very different for different polarities: while for negative flashes Campos et al. (2007) observed 5.5 M components per CC, Campos et al. (2009) observed 9.0 for positive flashes.

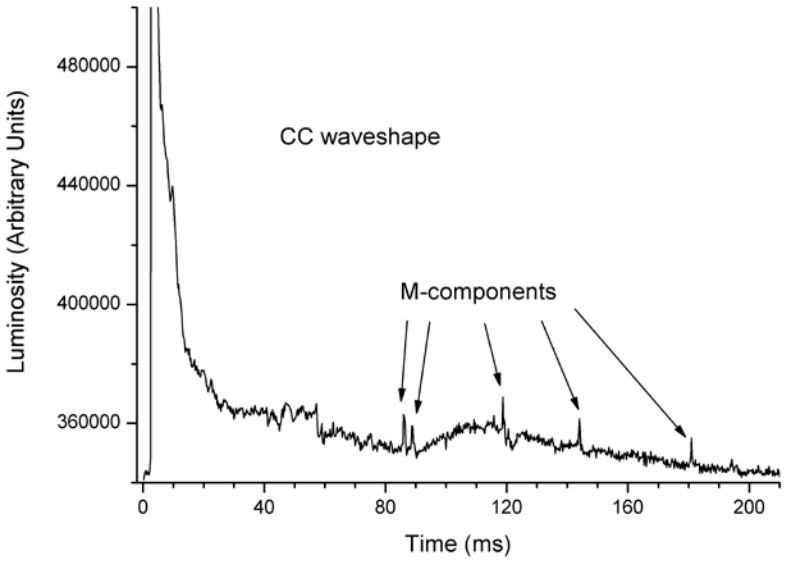

Fig. 4.3 Example of continuing current with M-components. The M-components are indicated by arrows.

4.5. Continuing Current Magnitude and Charge Transfer

Continuing current magnitudes can be most precisely determined via direct measurements for triggered lightning or lightning that strikes an instrumented tower (e.g., Fisher et al., 1993; Diendorfer et al., 2009). In the absence of such measurements, continuing currents can be detected by their signature in measured ground-level static or quasi-static electric fields. The continuing-current signature is a slow increase in the magnitude of the electric field change due to the steady charge transfer to ground during the continuing current. Because of the r^3 electrostatic field decay with distance from the electric dipole formed by the lightning charge source and its image, estimates are restricted to close range lightning (distances less than 50 km or so) (Kitagawa et al., 1962; Shindo and Uman, 1989; Ross et al., 2008).

The estimates of CC magnitude presented in this section for negative and positive ground flashes were calculated using the CC signature in measured ground-level quasi-static electric fields (slow E-field variation) on top of a 27-m tall structure located in southeast Brazil (Medeiros et al., 2012; Schumann and Saba, 2012). In order to find the field enhancement factor due to the presence of the structure, simultaneous measurements of the field change were made on top of the tall structure and on the ground. The enhancement factor was found to be equal to 3. The decay time constant of the sensor was also measured and used to reconstruct what would be the actual electric field changes if the decay time constant were infinitely large. All cases presented here had their CC duration confirmed by high-speed video records.

Some significant uncertainties can arise from the determination of the range to the center of charge removal. Although the distance from the sensor to the flash ground contact point can be given by lightning location systems with accuracy of the order of 1 km or less, it can also be offset from the charge removal centroid by horizontal distances on the order of kilometers (Rakov et al., 1990; Ross et al., 2008).

For each CC event the total charge transferred was calculated and then divided by the total duration in order to get the average current. A cumulative probability distribution plot of 81 CC magnitudes for negative flashes is shown in Fig. 4.4. The arithmetic mean value of the CC magnitudes is 321 A. Maximum and minimum values are 1400 A and 22 A, respectively. The 5%, 50%, and 95% values in the probability distribution shown in Fig. 4.4 are 788 A, 199 A, and 45 A, respectively. Note that relatively-low-magnitude long continuing currents transfer considerably larger charges than high-amplitude return-stroke pulses.

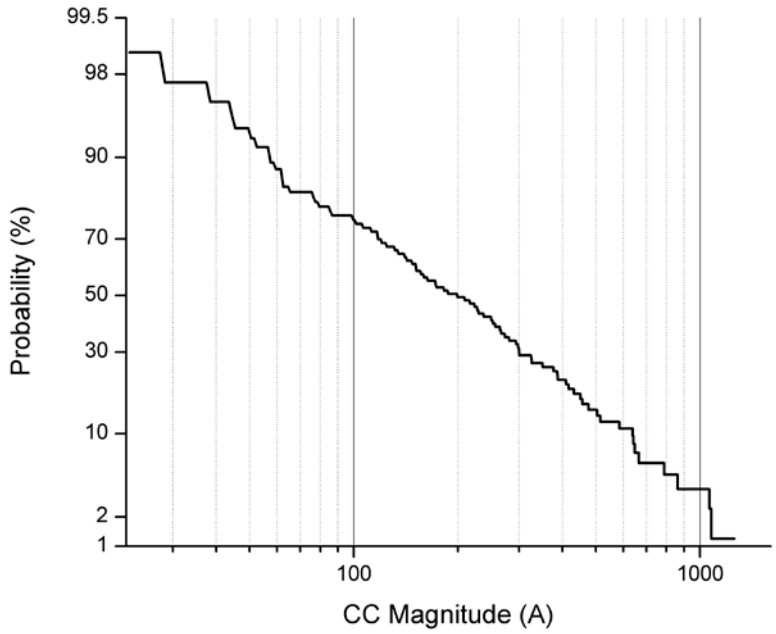

Fig. 4.4 Cumulative probability distribution of CC magnitudes for negative CG flashes.

For positive cloud-to-ground flashes recorded in southeast Brazil, the magnitude of the total charge lowered by 5 CC ranged from a minimum of 30 C to a maximum of 3070 C. The continuing current for positive CC ranged from 400 A to 35.8 kA (Schumann and Saba, 2012).

Using the same technique, but with multiple station electric field measurements in Japan, Brook et al. (1982) earlier pointed out that positive CG flashes often had CC greater than 10 kA, an order of magnitude larger than for negative flashes. The higher CC magnitudes for positives flashes inferred from electric field measurements are corroborated by direct current measurements found in the literature. For example, Matsumoto et al. (1996), measuring currents of direct strikes to transmission line towers, reported on CC having a magnitude of 10 kA and lasting as long as 35 ms. For both positive and negative (more often for positive) winter lightning in Japan charge transfers of the order of 1000 C were reported from direct current measurements by Miyake et al. (1992).

4.6. Summary

The percentage of positive flashes or strokes containing CC is much higher than that of negative flashes or strokes. Positive strokes tend to be followed by longer and more intense CC than negative strokes. Positive strokes can produce both a high peak current and a long CC, a feature that has not been found in any negative stroke. CC in natural CG flashes exhibit a variety of waveshapes that may be grouped into six categories. The average number of M components per CC differs significantly from one polarity to the other: while an average of 5.5 M components per CC were observed for negative flashes, an average of 9.0 M components per CC were observed for positive flashes. Strokes initiating long CC in negative flashes often have a smaller peak current and are preceded by high peak current return strokes and by relatively short interstroke intervals. Relatively-low-magnitude long continuing currents transfer considerably larger charges than high-amplitude return-stroke pulses.

5 Lightning Return Stroke Propagation Speed

5.1. Introduction

Lightning return stroke speed is an important parameter in lightning protection studies. Some researchers (e.g., Lundholm, 1957; Wagner, 1963) have suggested that the return-stroke speed should increase with increasing peak current. If such relationship indeed existed, it could be used in relating return-stroke peak current to the electric potential of the preceding leader and estimating the lightning striking distance (e.g., Hileman, 1999, pp. 221-222). Further, the return-stroke speed is a parameter in the models used in evaluating lightning-induced effects in power and communication lines (e.g., Rachidi et al., 1996). Finally, an explicit or implicit assumption of the return-stroke speed is involved in inferring lightning currents from remotely measured electric and magnetic fields (see Section 3.5). It is known that the return-stroke speed may vary along the lightning channel. As a result, optical speed measurements along the entire channel are not necessarily representative of the speed within the bottom 100 m or so, that is, at early times when the peaks of the channel-base current and of remote electric and magnetic fields (and of their derivatives) are formed.

The optically measured return-stroke speed probably represents the speed of the region of the upward-moving return-stroke tip where power losses are greatest, the power per unit length being the product of the current and the longitudinal electric field in the channel. The peak of the power loss wave likely occurs earlier in time than the peak of the current wave (e.g., Gorin, 1985; Jayakumar et al., 2006). Since the shape of the return-stroke light pulse changes significantly with height, there is always some uncertainty in tracking the propagation of such pulses for a speed measurement. For example, if the light pulse peak is tracked, then an increase in pulse risetime translates into a lower speed value than if an earlier part of the light pulse is tracked. It is thought that the error involved in identifying the time of the initial exposure (the time when light intensity first exceeds the background level) on streak photographs, as a basis for the speed measurements, is not large, especially near ground. Techniques for measuring return-stroke speed are discussed, for example, by Idone and Orville (1982).

In this Chapter, the available experimental data on return-stroke speed for both natural and rocket-triggered negative lightning will be presented. Data for both the entire visible part of the channel and the bottom 100 m or so will be discussed. Limited measurements of return-stroke speed for positive lightning will be considered. It will be shown that the often assumed relationship between the return-stroke speed and peak current is generally not supported by experimental data. Additional information about the return-stroke speed can be found in Rakov (2007) and in references therein.

5.2. Return-Stroke Speed Averaged Over the Visible Part of the Channel

Negative lightning. Schonland et al. (1935) found that the first return stroke speed at the channel base was typically near 1×10^8 m/s, and at the top of the main channel it was typically near 5×10^7 m/s. A summary of more recently measured return-stroke speeds averaged over the lowest some hundreds of meters of the channel for both natural and rocket-triggered lightning is given in Table 5.1. In natural lightning, the two-dimensional return-stroke speed (for both first and subsequent strokes combined) was reported by Idone and Orville (1982) from streak-camera measurements to vary from 2.9×10^7 to 2.4×10^8 m/s, almost an order of magnitude. The sample of Idone and Orville (1982) includes speeds for 17 first and 46 subsequent return strokes, with the mean values within about 1.3 km being 9.6×10^7 m/s and 1.2×10^8 m/s, respectively. Thus, the return-stroke speed for first strokes is observed to be lower than that for subsequent strokes, although the difference is not very large. Boyle and Orville (1976) reported return-stroke speeds for 12 strokes varying from 2.0×10^7 to 1.2×10^8 m/s. A similar wide speed range for natural lightning was found from photoelectric measurements by Mach and Rust (1989, Fig. 13). The more recently measured return-stroke speeds presented in Table 5.1 are generally higher than the earlier results of Schonland et al. (1935), probably due in part to the fact that the recent measurements were made closer to the ground where the return-stroke speed tends to be higher.

In triggered lightning, the return-stroke speed range was found to be 6.7 x 10^7 to 1.7 x 10^8 m/s from streak-camera measurements (three-dimensional speed) (Idone et al. 1984) and 6 x 10^7 to 1.6 x 10^8 m/s from photoelectric measurements in the lowest channel section longer than 500 m ("long-channel" two-dimensional speed) (Mach and Rust, 1989, Figs. 8 and 14). Accompanying photoelectric measurements in channel sections less than 500 in length ("short-channel" two-dimensional speed) resulted in a somewhat wider range of speeds of 6 x 10^7 to 2 x 10^8 m/s (see Fig. 8 of Mach and Rust (1989)).

Positive lightning. Mach and Rust (1993), from photoelectric measurements, reported on two-dimensional propagation speeds for 7 positive and 26 negative natural-lightning return strokes. They presented their speed measurements in two groups (similar to speed measurements of Mach and Rust (1989) discussed above): one included values averaged over channel segments less than 500 m (four positive flashes were analyzed over segments 332 to 433 m long) and the other included values averaged over channel segments greater than 500 m (seven positive flashes were analyzed over segments 569 m to 2300 m long). For the "short-segment" group, Mach and Rust (1993) found an average speed of 0.8 x 10^8 m/s for positive return strokes and 1.7 x 10^8 m/s for negative return strokes.

Two-dimensional measurements of positive return-stroke speed were also reported by Idone et al. (1987) for one positive return stroke that was part of an eight-stroke rocket-triggered lightning flash in Florida (KSC), the other seven strokes being negative, and by Nakano et al. (1987, 1988) for one natural positive lightning stroke in winter in Japan. Idone et al.'s (1987) measurements yielded a value about 10^8 m/s for the positive stroke and values ranging from 0.9 x 10^8 to 1.6 x 10^8 m/s for the seven negative strokes, all averaged over a channel segment of 850

Table 5.1. Summary of measured return stroke speeds in natural and triggered negative lightning. Adapted from Rakov et al. (1992).

Reference	Min. Speed, m/s	Max. Speed m/s	Mean Speed, m/s	St. Dev. m/s	Sample Size	Comments
Natural Lightning						
Boyle and Orville (1976)	2.0 x 10^7	1.2 x 10^8	0.71 x 10^8	2.6 x 10^7	12	Streak camera, 2-D speed
Idone and Orville (1982)	2.9 x 10^7	2.4 x 10^8	1.1 x 10^8	4.7 x 10^7	63	Streak camera, 2-D speed
Mach and Rust (1989, Fig. 7)	2.0 x 10^7 8.0 x 10^7	2.6 x 10^8 >2.8 x 10^8	1.3±0.3 x 10^8 1.9±0.7 x 10^8	5 x 10^7 7 x 10^7	54 43	Long channel Short channel (Photoelectric, 2-D)
Triggered Lightning						
Hubert and Mouget (1981)	4.5 x 10^7	1.7 x 10^8	9.9 x 10^7	4.1 x 10^7	13	Photoelectric, 3-D speed
Idone et al. (1984)	6.7 x 10^7	1.7 x 10^8	1.2 x 10^8	2.7 x 10^7	56	Streak camera, 3-D speed
Willett et al. (1988)	1.0 x 10^8	1.5 x 10^8	1.2 x 10^8	1.6 x 10^7	9	Streak camera, 2-D speed
Willett et al. (1989a)	1.2 x 10^8	1.9 x 10^8	1.5 x 10^8	1.7 x 10^7	18	Streak camera, 2-D speed
Mach and Rust (1989, Fig. 8)	6.0 x 10^7 6.0 x 10^7	1.6 x 10^8 2.0 x 10^8	1.2±0.3 x10^8 1.4±0.4 x10^8	2 x 10^7 4 x 10^7	40 39	Long channel Short channel (Photoelectric, 2-D)

m in length near ground. Nakano et al. reported a significant speed variation with height, discussed in Section 5.4.

5.3. Return-Stroke Speed in the Lowest 100 m of the Channel

We now review the optical measurements of lightning return-stroke speed within the bottom 100 m or so of the channel. This channel segment corresponds to the time when the initial peaks of the channel-base current (the typical 10-to-90% risetime of subsequent return-stroke currents is 0.3 to 0.6 μs; Fisher et al., 1993, Fig. 6) are formed. It is this value of speed that is needed for estimating the current peak from measured radiation field peak and distance (see Section 3.5).

Wang et al. (1999c) reported on two-dimensional speed profiles within 400 m of the ground for two return strokes in triggered lightning. These speed profiles were obtained in 1997 at Camp Blanding, Florida, using the digital optical imaging system ALPS having a time resolution of 100 ns and a spatial resolution of 30 m. The return-stroke speeds within the bottom 60 m of the channel were found to be 1.3×10^8 and 1.5×10^8 m/s. Weidman (1998), from photoelectric measurements in 1996 at Camp Blanding, Florida, and in 1996-1998 in Tucson, Arizona, reported mean return-stroke speeds in the lowest 100 m of the lightning channel of 8.8×10^7 and 7.8×10^7 m/s for 14 triggered and 9 natural lightning strokes, respectively.

Olsen et al. (2004), using a vertical array of four photodiodes, estimated return-stroke speeds in the bottom 170 m of the channel for five strokes in one flash triggered at Camp Blanding, Florida. Return-stroke speed values estimated tracking the 20% of the peak point on the front of return-stroke light pulse for three different segments of the lightning channel, 7 to 63 m, 63 to 117 m, and 117 to 170 m, are summarized in Table 5.2. For the lowest channel segment, 7 to 63 m, the speed values are 1.2 to 1.3×10^8 m/s. For higher channel segments, speed values are generally higher, varying from 1.6 to 1.8×10^8 m/s over the 63 to 117 m segment and from 1.2 to 1.7×10^8 m/s over the 117 to 170 m segment.

Thus, based on all the pertinent measurements available to date, the return-stroke speed in the bottom few tens of meters to 100 m of the lightning channel, that is, at the time when the initial peak of the channel-base current is formed is typically one-third to two-thirds of the speed of light.

Table 5.2. Return-stroke speeds ($\times 10^8$ m/s) estimated tracking the 20% point on the light-pulse front for triggered lightning flash F0336 (Olsen et al., 2004).

Height range, m	Stroke order					Estimated error, %
	1	2	4	5	6	
7 – 63	1.3	1.2	1.2	1.2	1.2	10
63 – 117	1.6	1.8	1.8	1.8	1.6	15
117 – 170	1.7	1.2	1.5	1.6	1.5	21

No data are available for stroke 3.

5.4. Variation of Return-Stroke Speed with Height

Idone and Orville (1982) found that the negative return-stroke speed usually decreases with height, for both first and subsequent strokes, by 25% or more over the visible part of channel relative to the speed near ground. In computing lightning electromagnetic fields, the return-stroke speed is often assumed to be constant (particularly for subsequent strokes) over the radiating channel section (e.g., Rakov and Uman, 1998). Gorin (1985) suggested a non-monotonic return-stroke speed profile. According to his nonlinear distributed-circuit model for a first stroke, the speed initially increases to its maximum over a channel length of the order of some hundreds of meters and decreases thereafter. The initial speed increase in Gorin's (1985) model is associated with the so-called break-through phase (also called the final jump or switch-closing phase) thought to be responsible for the formation of the

initial rising portion of the return-stroke current pulse. Srivastava (1966) proposed, based on the experimental data published by Schonland (1956), a bi-exponential expression for the first return-stroke speed as a function of time, according to which the speed rises from zero to its peak and falls off afterwards. Variation of the return-stroke speed with height for triggered-lightning strokes 2, 4, 5, and 6 in Table 5.2 suggests that the speed indeed initially increases and then decreases with increasing height.

We now briefly discuss observed variations of speed with height for return strokes in positive lightning. Nakano et al. (1987, 1988) reported a significant decrease in two-dimensional speed with increasing height over a 180-m section of the channel, from 2 x 10^8 m/s at 310 m to 0.3 x 10^8 m/s at 490 m. On the other hand, Mach and Rust (1993) found no significant speed change with height for positive return strokes. Clearly, more data on positive return-stroke speed are needed.

5.5. Return-Stroke Speed vs. Peak Current

Some researchers (e.g., Lundholm 1957; Wagner 1963) have suggested that the return-stroke speed should increase with increasing peak current. This suggestion, implying that the return-stroke wave is highly non-linear so that the wave speed is a function of wave amplitude, appears to be not supported by experimental data. In particular, Willett et al. (1989a) and Mach and Rust (1989) found a lack of correlation between the return-stroke propagation speed and the return-stroke peak current (varying from 6 to 43 kA) in triggered lightning in Florida. Idone et al. (1984) did observe “a nonlinear relationship” between these two parameters in triggered lightning in New Mexico, but it disappears if one excludes the relatively small events that are characterized by return-stroke peak currents less than 6-7 kA in order to make Idone et al.’s (1984) sample similar to those of Willett et al. (1989a) and Mach and Rust (1989). If there is a relationship between the return-stroke speed and return-stroke current, as might be expected on physical grounds, it is influenced by many factors and, as a result, characterized by a large scatter. Rakov (1998) inferred, from a comparison of the behavior of traveling waves on a lossy transmission line and the observed characteristics of the lightning return stroke process, that the return stroke is similar to a “classical” (linear) traveling wave. Ionization does occur during the return-stroke process but has a relatively small effect on the wave propagation characteristics, which, according to Rakov (1998), are primarily determined by the transmission-line parameters ahead of the front as opposed to being determined by the wave magnitude. As a result, the return-stroke wave suffers appreciable attenuation and dispersion. Thus, the often assumed relationship (e.g., Chowdhuri et al., 2005, Fig. 4) between the return-stroke speed and peak current is generally not supported by experimental data.

5.6. Summary

The average propagation speed of a negative return stroke (first or subsequent) below the lower cloud boundary is typically between one-third and one-half of the speed of light. It appears that the return-stroke speed for first strokes is lower than that for subsequent strokes, although the difference is not very large (9.6 x 10^7 vs. 1.2 x 10^8 m/s). For positive return strokes, the speed is of the order of 10^8 m/s, although data are very limited. The negative return-stroke speed within the bottom 100 m or so is expected to be between one-third and two-thirds of the speed of light. The negative return stroke speed usually decreases with height for both first and subsequent strokes. There exists some experimental evidence that the negative return stroke speed may vary non-monotonically along the lightning channel, initially increasing and then decreasing with increasing height. There are contradicting data regarding the variation of positive return stroke speed with height. The often assumed relationship between the return-stroke speed and peak current is generally not supported by experimental data.

6 Equivalent Impedance of the Lightning Channel

6.1. General Considerations

Lightning-channel impedance is an important parameter that can influence the current injected into the strike object. It may also be needed for specifying the reflection coefficient at the lightning current injection point.

Direct-strike effects. When the actual current distribution in the lightning channel is of no concern (electromagnetic coupling effects are neglected), lightning is often approximated by a Norton equivalent circuit (e.g., Carlson, 1996). This representation includes an ideal current source equal to the lightning current that would be injected into the ground if that ground were perfectly conducting (a short-circuit current, I_{sc}) in parallel with a lightning-channel impedance Z_{ch} assumed to be constant. In the case when the strike object can be represented by lumped grounding impedance, Z_{gr}, this impedance is a load connected in parallel with the lightning Norton equivalent (see Fig. 6.1a). Thus, the "short-circuit" lightning current I_{sc} effectively splits between Z_{gr} and Z_{ch} so that the current flowing from the lightning-channel base into the ground is found as $I_{gr} = I_{sc} Z_{ch}/(Z_{ch} + Z_{gr})$. Both source characteristics, I_{sc} and Z_{ch}, vary from stroke to stroke, and Z_{ch} is a function of channel current, the latter nonlinearity being in violation of the linearity requirement necessary for obtaining the Norton equivalent circuit. Nevertheless, Z_{ch}, which is usually referred to as equivalent impedance of the lightning channel, is assumed to be constant.

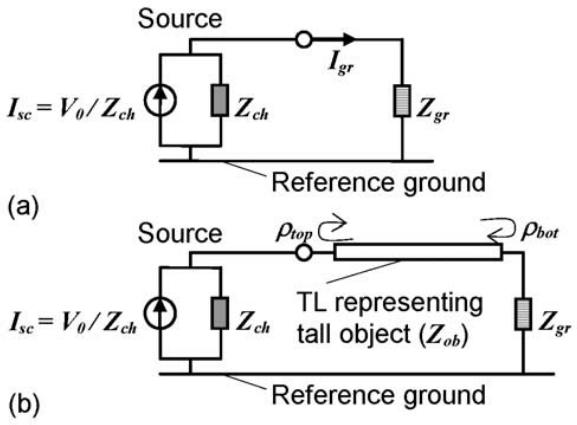

Fig. 6.1. Engineering models of lightning strikes (a) to lumped grounding impedance and (b) to a tall grounded object, in which lightning is represented by the Norton equivalent circuit, labeled ''source''. The source output currents injected into the lumped grounding impedance Z_{gr} in (a) and into an electrically-long object whose characteristic impedance is Z_{ob} in (b) are consistent with the lumped-voltage-source models presented in Figs. 6.2a and 6.2b, respectively. Adapted from Baba and Rakov (2005a).

Equivalent impedance of the lightning channel also influences the transient process in the strike object, if that object is electrically long; that is, has dimensions that are comparable to or greater than some of the shortest wavelengths of the source current, which are usually associated with the initial rising portion of the lightning return stroke current waveform. As an example, representation of lightning by a Norton equivalent circuit for analyzing lightning interaction with a tall object is shown in Fig. 6.1b. It is important to re-iterate that the equivalent circuits shown in Figs. 6.1a and b are only suitable for studying direct lightning strike effects (for example, using the EMTP; Scott-Meyer, 1982), when the actual distribution of current in the lightning channel is of no concern.

Lightning-induced effects. In studying lightning-induced effects, the distribution of current along the lightning channel is needed for computing electric and magnetic fields. In this latter case, the representations shown in Figs. 6.2a and b can be used instead, where the lightning channel is assumed to be a transmission line energized by a lumped voltage source, $V_0 = I_{sc} Z_{ch}$ (Baba and Rakov, 2005a). In this case, the equivalent impedance of the lightning channel is the same as its characteristic impedance. A series ideal current source can be also used in the case of lumped strike object (Fig. 6.1a), provided that no reflections are involved, but not in the case of tall (electrically-long) grounded strike object (Fig. 6.1b). This is because an ideal current source has infinitely large impedance, making the lightning channel electrically isolated from the strike object when ground reflections arrive at the source point. A lumped shunt current source is not suitable in the case of tall strike object either, because it would inject different currents in the lightning channel and strike object (connected in series) when their characteristic impedances are assumed to be different. In both representations shown in Fig. 6.2, distributed-shunt-current sources (Rachidi et al., 2002) or specification of longitudinal current without inserting any impedance at the current injection point (Thottappillil and Theethayi, 2006) can be used instead of the lumped voltage sources, but knowledge of Z_{ch} is still needed for specifying the reflection coefficient at the top of the strike object (in configuration shown in Fig. 6.2b).

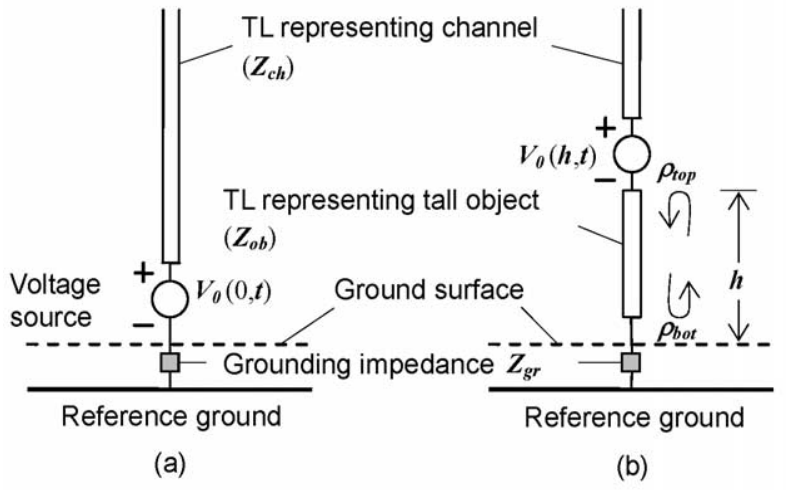

Fig. 6.2. Lightning strikes (a) to flat ground or electrically-short object and (b) to a tall grounded object of height h, represented in each case by a lossless transmission line connected in series with a lumped voltage source generating an arbitrary voltage waveform, $V_0(0, t)$ or $V_0(h, t)$. Z_{ch} is the characteristic impedance of the transmission line representing the lightning channel, and Z_{ob} is that representing the tall strike object. Adapted from Baba and Rakov (2005a).

Note that a vertical conductor above ground (see Fig. 6.2a) is actually a nonuniform transmission line whose characteristic impedance increases with increasing height. The resultant distributed impedance discontinuity causes distributed reflections back to the source that is located at ground level. As a result, even in the absence of ohmic losses, the current amplitude appears to decrease with increasing height (Baba and Rakov, 2005b).

Summary. The equivalent impedance of the lightning channel is needed for specifying the source in circuit models used for calculations of either direct-strike (see Fig. 6.1) or induced (see Fig. 6.2) lightning effects. It may also be needed for specifying the reflection coefficient at the lightning current injection point (see Fig. 6.2b). In Section 6.2, we will present the available limited data on the equivalent impedance of the lightning channel.

6.2. Inferences from Experimental Data

It is possible to estimate the equivalent impedance of the lightning channel from measurements of lightning current waveforms at a very tall object, if the characteristic impedance of the object and the grounding impedance are known or can be reasonably assumed. Such measurements were performed at the 540-m high Ostankino tower in

Moscow. Typical lightning current waveforms, reported by Gorin and Shkilev (1984), at heights of 47, 272, and 533 m above ground are shown in Fig. 6.3. The median peak currents from their measurements at 47 and 533 m were 18 and 9 kA, respectively. The observed differences in peak current suggest that the effective grounding impedance of the tower is much smaller than its characteristic impedance and that the latter impedance is appreciably lower than the equivalent impedance of lightning channel. Gorin and Shkilev (1984) used current oscillograms recorded near the tower top (at 533 m), for the cases in which the current risetime was smaller than the time (about 3.5 μs) required for a current wave to travel (at the speed of light) from the tower top to its base and back, to estimate the equivalent impedance of the lightning channel, assumed to be a real number. Their estimates varied from 600 ohm to 2.5 kiloohm, when the characteristic impedance of the tower was assumed to be 300 ohm and the grounding resistance was assumed to be zero (the low-current, low-frequency value was about 0.2 ohm; Gorin et al. (1977)).

It has been observed, for rocket-triggered lightning, that the average return stroke peak current is not much influenced by the impedance "seen" at the strike point, ranging from as low as 0.1 ohm (Rakov et al., 1998) to 200 ohm or so (Schoene et al., 2009), which implies that the equivalent lightning-channel impedance is of the order of kiloohms, consistent with the findings of Gorin and Shkilev (1984). Further, Wagner and Hileman (1961), from theoretical considerations, suggested that what they referred to as the surge impedance of the stroke should vary from 900 ohm to 2 kiloohm, with larger values corresponding to lower-current strokes. Finally, Rakov (1998), from lossy transmission line modeling, estimated the characteristic impedance of the channel created by the dart leader, which is "seen" by frequency components between 100 kHz and 1 MHz of the return-stroke wave, to be about 0.5-1 kiloohm. Thus, it appears that the equivalent impedance of the lightning channel should be appreciably higher than the surge impedance, $(L/C)^{1/2}$, of an overhead wire, which is about 400 ohm.

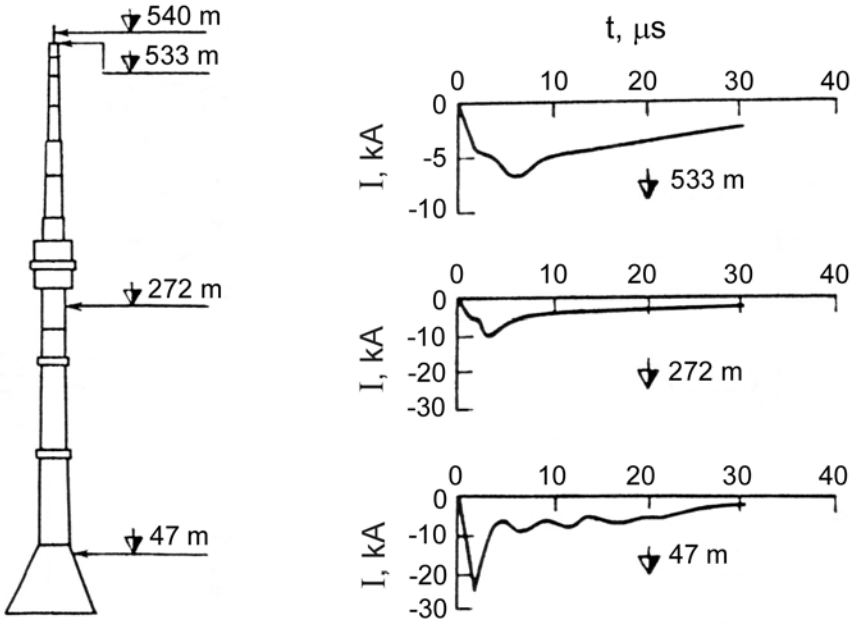

Fig. 6.3. Typical return-stroke current waveforms of upward negative lightning recorded near the top (at 533 m), in the middle (at 272 m), and near the bottom (at 47 m) of the 540-m high Ostankino tower in Moscow. Differences in current waveforms at different heights are indicative of the tower behaving as a distributed circuit. Adapted from Gorin and Shkilev (1984).

6.3. Concluding Remarks

The equivalent impedance of the lightning channel is needed for specifying the source in circuit models used in studies of either direct-strike or induced lightning effects. It may also be needed for specifying the reflection coefficient at the lightning current injection point. The limited estimates of this impedance from experimental data suggest values ranging from several hundred ohm to a few kiloohm. In many practical situations the impedance "seen" by lightning at the strike point is some tens of ohm or less, which allows one to assume infinitely large equivalent impedance of the lightning channel. In other words, lightning in these situations can be viewed as an ideal current source. In case of direct lightning strike to an overhead conductor of a power line with 400 ohm surge impedance (effective impedance 200 ohm, since 400 ohm is "seen" in either direction), the ideal current source approximation may still be suitable. Representation of lightning by a current source with internal impedance of 400 ohm, similar to that of an overhead wire (e.g., Motoyama et al., 1998), is probably not justified. It is worth mentioning again that the lightning channel impedance should be a function of channel conditioning level and current (e.g., Wagner and Hileman, 1961; Gorin, 1985; Rakov, 1998), which is not presently taken into account in engineering calculations.

7. Positive and Bipolar Lightning Discharges

7.1. Introduction

Downward positive lightning, which is initiated by a downward leader and effectively lowers positive charge from the cloud to ground, accounts for about 10% of all cloud-to-ground discharges (e.g., Rakov, 2003b). Due to their relative paucity, positive lightning discharges are considerably less studied and understood than their negative counterparts. The charge structure and evolution of thunderclouds that produce positive lightning, as well as in-cloud processes that can lead to its initiation (e.g., Nag and Rakov, 2012), largely remain a mystery. Positive lightning discharges have recently attracted considerable attention for the following reasons (see Rakov (2003b) and references therein):

1) The highest recorded lightning currents (near 300 kA) and the largest charge transfers to ground (hundreds of coulombs or even more) are associated with positive lightning.

2) Positive lightning can be the dominant type of cloud-to-ground lightning during the cold season and during the dissipating stage of a thunderstorm.

3) Positive lightning has been found to be preferentially related to transient luminous events known as sprites in the middle and upper atmosphere.

4) Reliable identification of positive discharges by lightning locating systems (LLS), such as the U.S. National Lightning Detection Network (NLDN), has important implications for various meteorological and other studies that depend on LLS data.

5) Several properties of positive lightning (e.g., number of strokes per flash, occurrence of continuing current, leader propagation mode, and branching) appear to be distinctly different from those of negative lightning.

Positive charge can be also transferred to ground by so-called bipolar lightning that sequentially lowers charges of both polarities to ground. Bipolar lightning is generally not considered to be a significant component of the overall lightning activity, although this type of lightning discharge may not be less common than positive lightning (Rakov, 2005). Bipolar lightning discharges are usually initiated by upward leaders from tall objects. However, natural downward flashes also can be bipolar (Jerauld et al., 2009; Fleenor et al., 2009; Saba et al., 2013). Additional information on positive and bipolar flashes of upward type is found in Chapter 8. Continuing currents in positive lightning are discussed in Chapter 4.

Although the overall percentage of positive lightning discharges is relatively low, there are five situations, listed below, that appear to be conducive to the more frequent occurrence of such discharges. The genesis of positive lightning in these situations is not yet fully understood.

a) The dissipating stage of an individual thunderstorm.

b) Winter thunderstorms.

c) Trailing stratiform regions of mesoscale convective systems (MCSs).

d) Severe storms.

e) Thunderclouds formed over forest fires or contaminated by smoke.

7.2. General characterization

The following is a list of observed lightning properties that are thought to be characteristic of positive lightning discharges.

a) Positive flashes are usually composed of a single stroke, whereas about 80% of negative flashes contain two or more strokes, with three to five being typical (see Section 2.5). Multiple-stroke positive flashes do occur but they are relatively rare.

b) Positive return strokes tend to be followed by continuing currents that typically last for tens to hundreds of milliseconds (e.g., Fuquay, 1982; Rust et al., 1981,1985; Saba et al., 2010). Brook et al. (1982), from multiple-station electric field measurements, inferred continuing currents in positive flashes in excess of 10 kA, at least one order of magnitude larger than for negative flashes, for periods up to 10 ms. Campos et al. (2009) recently showed that, similar to negative lightning, continuing currents in positive lightning are accompanied by M-components. Additional information on continuing currents and M-components in positive lightning is found in Chapter 4.

c) From electric field records, positive return strokes often appear to be preceded by significant in-cloud discharge activity lasting, on average, in excess of 100 (Fuquay, 1982; Schumann et al., 2013) or 200 ms (Rust et al., 1981). This observation suggests that a positive discharge to ground can be initiated by a branch of, or otherwise produced by, an extensive cloud discharge (Kong et al., 2008; Saba et al., 2009). Negative cloud-to-ground discharges are less often preceded by such long-lasting in-cloud discharge activity.

d) Several researchers (e.g., Fuquay, 1982; Rust, 1986) reported that positive lightning discharges often involve long horizontal channels, up to tens of kilometers in extent. This might be due to their more intimate relation to cloud discharges.

e) It appears that positive leaders can move either continuously or intermittently (in a stepped fashion), as determined from time-resolved optical images. This is in contrast with negative leaders, which are always optically stepped when they propagate in virgin air.

To summarize, positive discharges to ground are usually composed of a single stroke, often appear to be preceded by significant in-cloud discharge activity, and tend to be followed by continuing currents. In contrast to negative leaders, positive leaders seem to be able to move either continuously or in a stepped fashion, although the stepping mechanism is different for these two types of leaders.

7.3. Multiplicity

The term multiplicity is often used to denote the number of strokes per flash, not necessarily along the same channel to ground. As noted above, positive flashes are usually composed of a single stroke, whereas about 80% of negative flashes contain two or more strokes (see Section 2.5). Occurrence of positive flashes with different number of strokes from different studies is summarized in Table 7.1 and occurrence of positive subsequent strokes in a previously-created channel in Table 7.2.

Table 7.1. Occurrence of Positive Flashes With Different Number of Strokes. Adapted from Nag and Rakov (2012).

Reference	Location	Sample size	Occurrence (percentage) of flashes with different number of strokes				Average multiplicity
			Single-stroke	Two-stroke	Three-stroke	Four-stroke	
Heidler and Hopf (1998)	Germany (1988 - 1993)	44	33 (75%)	8 (18%)	2 (5%)	1 (2%)	1.3
Heidler et al. (1998)	Germany (1995 - 1997)	32	28 (88%)	4 (13%)	0	0	1.1

Fleenor et al. (2009)	U.S. Cental Great Plains (Kansas and Nebraska)	204	195 (96%)	9 (4%)	0	0	1.0
Saba et al. (2010)	Brazil, Arizona, Austria	103	83 (81%)	19 (18%)	1 (1%)	0	1.2
Saba et al. (2010)	Brazil	70*	54 (77%)	15 (21%)	1 (1%)	0	1.2
Nag and Rakov (2012)	Florida	52	42 (81%)	9 (17%)	1 (2%)	0	1.2

* Subset for Brazil only of the 103 events recorded in Brazil, Arizona, and Austria.

Table 7.2. Occurrence of Subsequent Strokes in Positive Flashes That Follow a Previously-Created Channel. Adapted from Nag and Rakov (2012).

Reference	Location	Occurrence (percentage) of subsequent strokes in a previously-created channel	Sample size (total number of subsequent strokes)	Remarks
Ishii et al. (1998)	Japan	0 (0%)	17	Winter storms; five-station electric field records
Fleenor et al. (2009)	U.S. Cental Great Plains (Kansas and Nebraska)	5 (56%)	9	Summer storms; video records, electric field records (LASA), NLDN
Saba et al. (2010)	Brazil, Arizona, Austria	1 (4.8%)	21	Summer storms; high-speed video records, lightning locating systems
Nag and Rakov (2012)	Florida	3 (38%)	8	Summer (2 flashes) and winter (1 flash) storms; electric field records, NLDN

LASA = Los Alamos Sferic Array

7.4. Current Waveform Parameters

A reliable distribution of positive lightning peak currents applicable to objects of moderate height on the flat ground is presently unavailable. The sample of 26 directly measured positive lightning currents analysed by Berger et al. (1975) (see Table 7.3) is commonly used as a primary reference both in lightning research and in lightning protection studies. However, this sample is apparently based on a mix of 1) discharges initiated as a result of junction between a descending positive leader and an upward-connecting negative leader within some tens of meters of the tower top and 2) discharges initiated as a result of a very long (1–2 km) upward negative leader from the tower making contact with an oppositely charged channel inside the cloud. These two types of positive discharges, which differ by the height above the tower top of the junction between the upward-connecting leader and the oppositely charged overhead channel (descending positive leader or positively-charged in-cloud discharge channel), are expected to produce very different current waveforms at the tower, as illustrated in Figs. 7.1a and 7.1b. The “microsecond-scale” current waveform shown in Fig. 7.1a is probably a result of processes similar to

those in downward negative lightning, whereas the “millisecond-scale” current waveform shown in Fig. 7.1b is likely to be a result of the M-component mode of charge transfer to the ground (see Section 2.3), although in the latter case current peaks can be considerably higher than for ordinary M-components. It is possible that such millisecond-scale waveforms are characteristic of tall objects capable of generating very long upward-connecting leaders. The above view of the 26 positive lightning discharges documented in detail by K. Berger is an update on the previous CIGRE assumption that those events are related “principally to upward flashes” (Anderson and Eriksson, 1980).

Table 7.3. Lightning current parameters for positive flashes. Adapted from Berger et al. (1975).

Parameters	Units	Sample Size	Percent Exceeding Tabulated Value		
			95%	50%	5%
Peak current (minimum 2 kA)	kA	26	4.6	35	250
Charge (total charge)	C	26	20	80	350
Impulse charge (excluding continuing current)	C	25	2.0	16	150
Front duration (2 kA to peak)	μs	19	3.5	22	200
Maximum di/dt	kA/μs	21	0.20	2.4	32
Stroke duration (2 kA to half peak value on the tail)	μs	16	25	230	2000
Action integral ($\int i^2 dt$)	A^2s	26	2.5×10^4	6.5×10^5	1.5×10^7
Flash duration	ms	24	14	85	500

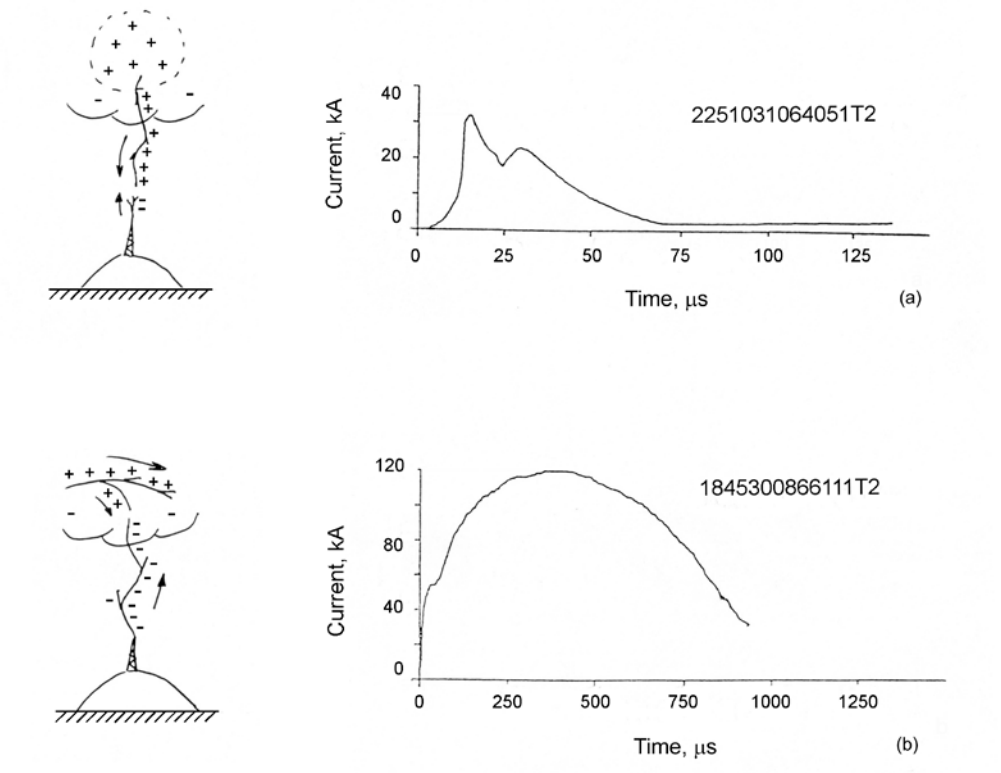

Fig. 7.1. Examples of two types of positive lightning current vs. time waveforms observed by K. Berger: (a) microsecond-scale waveform, similar to those produced by downward negative return strokes, and a sketch illustrating the lightning processes that might have led to the production of this waveform; (b) millisecond-scale waveform and a sketch illustrating the

lightning processes that might have led to the production of this current waveform. Arrows indicate directions of the extension of lightning channels. Adapted from Rakov (2003b).

On the other hand, the distribution of positive lightning peak currents inferred from electric or magnetic fields recorded by multiple-station LLSs, such as the NLDN, are influenced by the uncertainties of the conversion of the measured field to current (see Section 3.5). The NLDN formula that is used for this conversion is based on the linear regression equation relating the NLDN-measured field peak to the directly measured current peak for negative triggered lightning strokes and is extrapolated to natural positive strokes. Additionally, the lower end of the positive lightning peak current distribution based on LLS data is contaminated by misidentified cloud-flash pulses (e.g., Cummins et al., 1998).

Because of the absence of other direct current measurements for positive lightning return strokes, it is still recommended to use the peak current distribution based on the 26 events recorded by K. Berger (see Fig. 3.1 and Table 7.3), even though some of those 26 events are likely to be not of return-stroke type. However, caution is to be excersized, particularly for the waveshape parameters listed in Table 7.3, for which sample sizes are smaller than for peak currents. Clearly, additional measurements for positive lightning return strokes are needed to establish reliable distributions of peak current and other parameters for this type of lightning.

For the 26 positive lightning events examined by K. Berger, the peak current exhibits relatively strong correlation with the impulse charge (correlation coefficient = 0.77) and action integral (correlation coefficient = 0.84) and essentially no correlation with the front duration. The correlation coefficient with the maximum rate-of-rise (0.49) and stroke duration (0.58) are relatively weak.

Gamerota et al. (2012), who developed lightning current waveforms for numerical simulation of lightning effects, recommended for the severe (1%) positive return stroke case a waveform with a peak of 350 kA, time to current peak of 11 μs, and time to decay to half-peak value of 40 μs. They also noted that the latter parameter is not well defined for positive first strokes and attributed the large charge transfers and action integrals observed in positive lightning to continuing currents.

7.5. Summary

In spite of recent progress, our knowledge of positive lightning remains considerably poorer than that of negative lightning. Many questions regarding the genesis of positive lightning and its properties cannot be answered without further research. Although positive lightning discharges account for 10% or less of global cloud-to-ground lightning activity, there are five situations that appear to be conducive to the more frequent occurrence of positive lightning. These situations include (1) the dissipating stage of an individual thunderstorm, (2) winter thunderstorms, (3) trailing stratiform regions of mesoscale convective systems, (4) some severe storms, and (5) thunderclouds formed over forest fires or contaminated by smoke. The highest directly measured lightning currents (near 300 kA) and the largest charge transfers (hundreds of coulombs or more) are associated with positive lightning. Two types of impulsive positive current waveforms have been observed. One type is characterized by risetimes of the order of 10 μs, comparable to those for first strokes in negative lightning, and the other type by considerably longer risetimes, up to hundreds of microseconds. The latter waveforms are apparently associated with very long, 1 to 2 km, upward negative connecting leaders. Because of the absence of other direct current measurements for positive lightning return strokes, it is still recommended to use the peak current distribution based on the 26 events recorded by K. Berger (see Fig. 3.1 and Table 7.3), even though some of those 26 events are likely to be not of return-stroke type. However, caution is to be excersized, particularly for the waveshape parameters listed in Table 7.3, for which sample sizes are smaller than for peak currents. Clearly, additional measurements for positive lightning return strokes are needed to establish reliable distributions of peak current and other parameters for this type of lightning. Positive flashes are usually composed of a single stroke, although up to four strokes per flash were observed. Positive return strokes often appear to be preceded by significant in-cloud discharge activity and tend to be followed by significant continuing currents.

8. Upward lightning discharges

8.1 Introduction

Grounded vertical objects produce relatively large electric field enhancement near their upper extremities so that upward-moving connecting leaders from these objects start earlier than from the surrounding ground and, therefore, serve to make the object a preferential lightning attachment point. A comprehensive review of the interaction of lightning with tall objects is given by Rakov (2003a). With increasing height of an object an increase in the number of lightning discharges is observed with an increasing percentage of upward initiated flashes. Objects with heights ranging from 100 to 500 m experience both types of flashes, upward and downward. The high number of lightning events to tall towers makes those objects preferential for direct lightning current measurements (see Sections 3.1-3.4).

8.2 Concept of Effective Height of Tall Objects

To account for the observation of increased lightning incidence to towers of moderate height (less than 100 m) on high mountains a so called "effective height" that is larger than the physical height of the object is assigned to the structure. The effective height accounts for the additional field enhancement at the tower top due to the presence of the mountain. Pierce (1971) and Eriksson and Meal (1984) proposed two statistical and empirical methods to estimate the effective height of tall objects, based on experimental observations of the lightning incidence to a given tower. According to Eriksson (1987) the total number of flashes N_{all} to a tall structure is given by:

$$N_{all} = N_g \cdot 24 \cdot h^{2.05} \cdot 10^{-6} \tag{8.1}$$

where h is the structure height in meters and N_g is the ground flash density (per km^2 per year) in the region where the object is situated. An equation for percentage of upward flashes P_u as a function of structure height was proposed by Eriksson and Meal (1984) as:

$$P_u = 52.8 \cdot \ln(h) - 230 \tag{8.2}$$

[In derivation of empirical formulas (8.1) and (8.2), an effective height of 350 m was used for Berger's towers, instead of their physical height of 70 m.] Zhou et al. (2010) proposed a method to estimate the effective height based on a model taking into account the overall geometry (structure + mountain), the electric field distribution around the mountaintop, and the upward flash inception criterion proposed by Rizk (1990). They called it the "Rizk-model method".

Table 8.1 presents the effective heights of some structures estimated by Pierce and Eriksson and calculated using the Rizk-model method. As seen from Table 8.1, the effective height depends on both mountain height and the tower height, and it is always larger than the physical height of the tower. Variations of the upward positive leader speed and mountain base radius have been identified by Zhou et al. (2010) as most influencing parameters in estimating the effective height based on the Rizk-model method.

Table 8.1. An overview of lightning studies conducted at instrumented tall objects, including effective height estimates. Adapted from Rakov (2011).

Object	Location	Height, m	Terrain	Effective Height, m	Selected References
Empire State Building	New York City, USA	410	Flat	410	McEachron (1939, 1941), Hagenguth and Anderson (1952)

Object	Location	Height, m	Terrain	Effective Height, m	Selected References
Two towers 400 m apart[a]	Mount San Salvatore, Lugano, Switzerland	70	Mountain 640 m above Lake Lugano, 912 m above sea level	270 (Pierce 1971), 350 (Eriksson 1978) 198 (Zhou et al., 2010)	Berger and Vogelsanger (1965, 1966, 1969), Berger (1967, 1972, 1977, 1978), Berger et al. (1975)
Ostankino TV Tower	Moscow, Russia	540	Flat	540	Gorin et al. (1975; 1977), Gorin and Shkilev (1984)
Two TV towers[b]	Sasso di Pale, near Foligno, central Italy and Monte Orsa, near Varese, northern Italy	40	Mountains 980 and 993 m above sea level	500 (Eriksson 1978) 120 (Zhou et al., 2010)	Garbagnati and Lo Piparo (1970, 1973, 1982a,b) Garbagnati et al. (1974; 1975; 1978; 1981)
CSIR research mast	Pretoria, South Africa	60	Hill 80 m above surrounding terrain, 1400 m above sea level	148 (Eriksson 1978) 113 (Zhou et al., 2010)	Eriksson (1978, 1982)
CN Tower	Toronto, Canada	553	Flat	553	Hussein et al. (1995), Janischewskyj et al. (1997)
Peissenberg Tower	Hoher Peissenberg, Munich, Germany	160	Mountain about 288 m above surrounding terrain, 988 m above sea level[c]	324 (Zhou et al., 2010)	Beierl (1992), Fuchs et al. (1998) Flache et al. (2008)
St. Chrischona Tower	Basel, Switzerland	248	Mountain 493 m above sea level	468 (Zhou et al., 2010)	Montandon (1992, 1995)
Cachimbo Tower	Brazil	60	Mountain 200 m above surrounding terrain, 1600 m above sea level	145 (Zhou et al., 2010)	Lacerda et al. (1999), Schroeder et al. (2002), Visacro et al. (2004)
Gaisberg Tower	Salzburg, Austria	100	Mountain 1287 m above sea level	274 (Zhou et al., 2010)	Diendorfer et al. (2000, 2002, 2009), Zhou et al. (2010, 2011a,b, 2012)
Fukui chimney	Fukui, Japan	200	Flat	200	Miyake et al. (1992), Asakawa et al. (1997)
Meteorological tower	Maki, Japan	150	Flat	150	Goto and Narita (1995)

Object	Location	Height, m	Terrain	Effective Height, m	Selected References
Säntis Tower	Switzerland	124	Mountain 2,505 m above sea level	Unknown ($P_u \rightarrow 100\%$)	Romero et al. (2012a, 2013a)
Windmill and its protection tower (45 m apart)	Uchinada, Japan	100 and 105	Hill 40 m above sea level	Unknown ($P_u = 96\%$)	Wang et al. (2008a, 2011), Lu et al. (2009)

[a] The first tower, made of wood and equipped with a grounded lightning rod, was erected in 1943. The second tower, made of steel was erected in 1950. In 1958, the wooden tower was replaced by a tower made of steel (F. Heidler, personal communication, 2000).

[b] Most data have been obtained on Monte Orsa which is only 10 km from Monte San Salvatore.

[c] The tower is located below the mountain top, at about 937 m above sea level (F. Heidler, personal communication, 1999).

New approaches to estimate the number of upward flashes from tall structures based on the analysis of the data provided by lightning locating systems (LLS) were presented recently by Smorgonskiy et al. (2011) and Ishii et al. (2011).

8.3 Initiation of Upward Lightning

It is generally assumed that an object-initiated discharge (upward leader) begins when the electric field intensity over some critical distance from the top of the object exceeds the breakdown value. Based on the analysis of the electric field changes resulting from 14 upward lightning flashes initiated from a windmill and its lightning protection tower in Japan, Wang et al. (2008a) suggested to classify upward lightning discharges into the two types “self-triggered” (initiated without any preceding nearby lightning activity) and “other-triggered” (triggered by nearby lightning activity). Zhou et al. (2012) use the terms “self-initiated” and “nearby-lightning-triggered” flashes, respectively, to classify the two types of upward lightning.

Wang et al. (2011) classified 53% (28/53) of flashes as self-triggered and 47% (25/53) as triggered by in-cloud or nearby CG lightning. During summer seasons in Rapid City, South Dakota, USA, almost 100% (80 out of 81) of upward lightning flashes were triggered by a nearby flash, with the positive return stroke being the dominant triggering event (Warner et al., 2011). In contrast, Zhou et al. (2012) report that 87% (179/205) of the upward flashes at the Gaisberg Tower (GBT) were initiated without any preceding nearby discharge activity, whereas 13% (26/205) were initiated from the tower top with immediately preceding nearby lightning activity. The majority (85%) of those nearby-lightning-triggered upward flashes occurred during convective season. The above observations indicate that there are strong regional and seasonal dependencies of the mechanism of initiation of upward lightning, and this could be the reason why none of the presently available methods to estimate the expected number of upward flashes from a tall structure provides satisfactory results.

8.4 Seasonal Occurrence of Upward Lightning

Seasonal occurrence of upward lightning is observed to be somewhat different from the seasonal occurrence of downward lightning. Upward lightning to the GBT was reported by Diendorfer et al. (2009) to be more or less uniformly distributed over the year (see Fig. 8.1) and independent of the overall lightning activity, which shows a pronounced lightning season in summer. During an eight-year period (2000 – 2007) 56% of negative upward lightning from the GBT were recorded during the cold season (fall and winter) compared to 44% recorded during the warm season (spring and summer). Note that in other geographical regions the seasonal occurrence of upward lightning initiated from tall structures can be quite different from observations at the GBT.

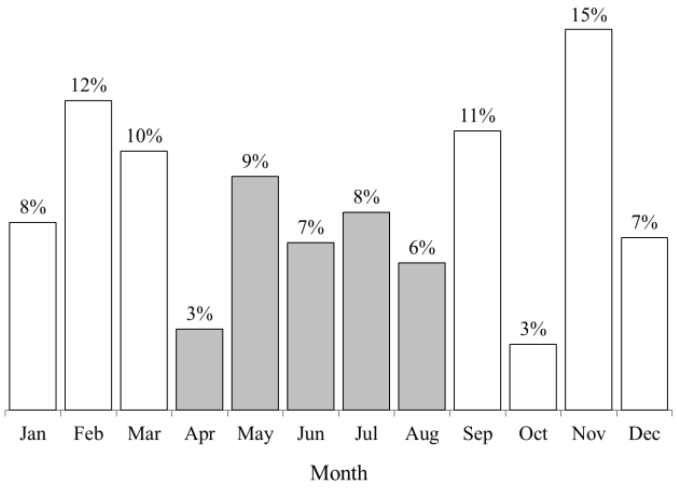

Fig. 8.1. Monthly lightning activity observed at the Gaisberg Tower from 2000 to 2007. Shaded diagram bars represent the convective season (April – August) and unshaded bars represent the cold (non-convective) season (September – March). Adapted from Diendorfer et al. (2009).

8.5 General Characterization of Upward Negative Lightning

Upward negative discharges are initiated by upward positive leaders from the tops of elevated objects (see Fig. 2.1b). Object-initiated negative lightning discharges always involve an initial stage (IS) that may or may not be followed by downward leader/upward return stroke sequences (RS). The latter are similar to subsequent leader/return stroke sequences in natural downward lightning and to downward leader/upward return stroke sequences in rocket-triggered lightning.

A schematic overall current waveform of upward-initiated lightning with three current pulses superimposed on the ICC and two RSs following the initial stage (IS) after a period of no current flow is shown in Fig. 8.2.

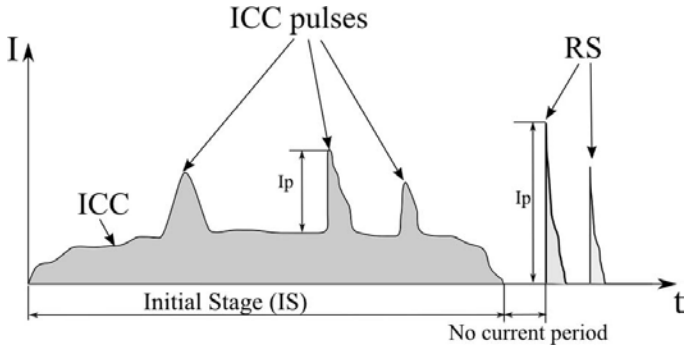

Fig. 8.2. Schematic current record of upward-initiated flash. Labeled are the initial continuous current (ICC) with three superimposed ICC pulses, a period of no current flow, and two return strokes (RS). Adapted from Diendorfer et al. (2009).

The percentage of upward flashes with return strokes was found to be 50% for the Empire State Building (Hagenguth and Anderson, 1952), 20–25% for the two towers on Mount San Salvatore (Berger, 1978), 27% for the Ostankino tower (Gorin and Shkilev, 1984) and 30% for the Gaisberg Tower (Diendorfer et al., 2009). Interestingly, the percentage of rocket-triggered flashes with return strokes is significantly higher, 70 – 75% (Wang et al., 1999;

Rakov, 2009). On the other hand, about 50% of 457 flashes recorded at the Gaisberg Tower from 2000 to 2009 did not contain any pulses with peaks greater than 2 kA, either superimposed on the ICC, or following the ICC. The initial stage in object-initiated lightning is similar to the initial stage in rocket-triggered lightning. The initial stage, in a sense, replaces the downward stepped leader/upward return stroke sequence (first stroke) characteristic of natural downward lightning.

Overall characteristics of the initial stage for both object-initiated and rocket-triggered negative lightning are summarized in Table 8.2.

Table 8.2. Overall characteristics (geometric mean values) of the initial stage of natural upward and rocket-triggered negative lightning. Adapted from Miki et al. (2005), Diendorfer et al. (2009), and Diendorfer et al. (2011).

Data Set	Sample Size	Duration, (ms)	Charge Transfer, (C)	Average Current, (A)	Action Integral, (10^3, A^2s)
Rocket-triggered lightning, Florida	45	305	30.4	99.6	8.5
Peissenberg Tower, Germany	21	290	38.5	133	3.5
Fukui Chimney, Japan [a)]	36	>82.5	>38.3 (>36.8)	465	40 (34)
Gaisberg Tower, Austria (2000)	74	231	29.1	126	1.5
Gaisberg Tower, Austria (2000-2007) Diendorfer et al. (2011)	457	266 (N=431)	33	113 (N=431)	7.0

a) Values in the parentheses are calculated from the current data limited to 2 kA in order to make the Fukui data (upper current measurement limit of 13 kA) comparable to the other data sets (upper current measurement limit of 2-2.1 kA)

Diendorfer et al. (2009) analyzed three categories of upward negative flashes, namely ICC_{RS} (ICC is followed by one or more RS), ICC_P (ICC is not followed by any RS but with one or more ICC pulses >2 kA), and ICC_{Only} (ICC is not followed by any RS and no ICC pulse > 2 kA occurred). For the ICC_P type discharges the geometric mean transferred charge of 69 C is more than three times larger than the 21 C determined for ICC_{Only} flashes. The maximum transferred charge measured in a single flash to the GBT was 405 C and 1.5% (10/625) of the flashes transferred charges exceeding 300 C, and all those events with large amounts of transferred charge occurred during cold season (Diendorfer et al. 2011).

8.6 Impulsive currents in negative upward lightning

Parameters of ICC pulses. In many cases the initial stage contains current pulses superimposed on the slowly varying continuous current (see Fig. 8.2). Some of these pulses have peaks in the kiloamperes range, comparable to current peaks of smaller return strokes. A statistical comparison between the initial-stage pulses and the M-component pulses following return strokes in rocket-triggered lightning indicates that both types of pulses are due to similar physical processes (Wang et al., 1999). On the other hand, the initial stage pulses in object-initiated lightning exhibit larger peaks, shorter rise times, and shorter half-peak widths than do the initial-stage pulses in rocket-triggered lightning (see Table 8.3).

Table 8.3. Parameters (geometric mean values) of initial-stage current pulses in upward-initiated lightning. Also given are the corresponding parameters of M-component currents in rocket-triggered lightning. Adapted from Miki et al. (2005).

Data Set	Sample Size	Magnitude (A)	Duration (μs)	Risetime (μs)	Half-Peak Width (μs)
Fukui Chimney, Japan	231	781	514	44.2	141
Peisenberg Tower, Germany	124	512	833	60.9	153
Gaisberg Tower, Austria	348-377	> 377 (N=351)	1199 (N=377)	<110 (N=344)	276 (N=348)
Rocket-triggered lightning, Florida	247-296	113 (N=296)	2590 (N=254)	464 (N=267)	943 (N=247)
Rocket-triggered lightning M-components, Florida	113-124	117 (N=124)	2100 (N=114)	422 (N=124)	816 (N=113)

Flache et al. (2008) analyzed high-speed video images of upward flashes initiated by the Peissenberg tower in Germany and found that six (86%) of seven ICC pulses with shorter risetimes developed in a newly illuminated branch, whereas 25 (96%) of 26 ICC pulses with longer risetimes occurred in already luminous channels. These results support the hypothesis that longer risetimes are indicative of the M-component mode of charge transfer to ground, while shorter risetimes are associated with (dominated by) the leader/RS mode. More recently, Zhou et al. (2011b) proposed the term “mixed mode” of charge transfer to ground for the ICC pulses previously referred to as the “leader/RS mode” by Flache et al. (2008). In the ”mixed mode”, a leader/RS sequence in one channel occurs simultaneously with the continuous current flowing to ground in another channel. The mixed mode is usually associated with relatively-low-level upward branching that is common in object-initiated lightning, but not in rocket-triggered lightning in Florida. Thus, the mixed-mode concept can explain the occurrence of ICC pulses in object-initiated lightning with larger peaks, shorter risetimes, and shorter half-peak widths than those in rocket-triggered lightning, as reported by Miki et al. (2005).

Parameters of return strokes (peak current and charge transfer). Return strokes in upward lightning are assumed to be similar to subsequent strokes in natural cloud-to-ground lightning. Table 8.4 shows a comparison of return-stroke current peaks (in kA) and transferred charge (in coulombs) in natural upward (object-initiated), natural downward, and rocket-triggered lightning.

Table 8.4. Peak current and charge transfer (median values) of return strokes in natural upward, natural downward, and rocket-triggered lightning flashes.

Reference	Location	Sample size	Peak Current (kA)	Stroke Charge (C)
Return strokes in upward initiated flashes				
Diendorfer et al. (2009)	Austria, Gaisberg Tower	615	9.2	0.51
Fuchs *et al.* (1998)	Germany, Peissenberg Tower	35	8.5	
Gorin and Shikilev (1984)	Russia	58 76	9 18[a]	
Berger (1978)	Switzerland, Monte San Salvatore	176	10	0.77 (N=579)
Hagenguth and Anderson (1952)	New York, Empire State Building	84[b]	10	0.15 (N=83)[c]
Return strokes in natural downward flashes				
Anderson and Eriksson (1980)	Switzerland	114	12	
Berger et al. (1975)	Switzerland	135	12	0.95 (N=117)
Return strokes in rocket-triggered lightning				
Schoene et al. (2009)	Florida, Camp Blanding	144	12.4[d]	1.1[e] (N=122)
Fisher *et al.* (1993)	Florida (KSC) and Alabama	45	13	
Depasse (1994)	Florida France	305 54	12.1 9.8	- 0.59 (N=24)

[a] Overestimates due to a transient process in the tower
[b] Two events out of 84 were of positive polarity
[c] Sample includes one or two events of positive polarity. Charge was determined only up to half-peak value on the tail of the current waveform
[d] Geometric mean value
[e] Geometric mean value of charge transfer within 1 ms

Recently, direct current measurements were obtained on the 124-m Säntis Tower in Switzerland (Romero et al., 2012a-c, 2013a,b). More than 200 flashes (about 30 of which were positive) were recorded during the first 2 years of operation, apparently all of them of upward type. For 2034 negative current pulses (some of them superimposed on steady currents) with peaks greater than 2 kA and risetimes shorter than 8 μs, the median peak current was found to be 6 kA.

8.7 Characteristics of Upward Positive Lightning

Upward positive lightning usually involves an upward negative leader initiated from the top of a tall structure (see Fig. 2d). Berger and co-workers were the researchers who first presented a comprehensive study of positive discharges including both upward positive and downward positive flashes (Berger et al., 1975; Berger 1978). Very few systematic studies of upward positive lightning have been reported since Berger's work (e.g., Garbagnati and Lo Piparo, 1982; Fuchs et al., 1998; Heidler et al., 2000). Miki (2006) presented simultaneous current and optical observations of upward positive flashes at the Fukui chimney in Japan and, more recently, Miki et al. (2010) observed 16 upward positive discharges, initiated from wind turbines at Nikaho Kougen Wind Farm in the coastal area of the Sea of Japan. At the GBT positive upward lightning accounted for 4% (26/652) of the total flashes recorded from 2000 to 2009 (Zhou et al., 2012) and 19 (73%) out of these 26 upward positive flashes occurred during non-convective season. At the Säntis Tower, in the period from June 2010 to January 2012, about 15% of the recorded flashes (30 out of 201) were of positive polarity (Romero et al., 2012b). Most of the positive flashes were recorded in summer months (23 in June-August, 6 in May, and 1 in January). Ishii and Natsuno (2011) measured 304 current waveforms at wind turbines at 25 sites in Japan during 2008-2011 (no data were recorded during May-September). They found that 21% of the currents were positive. Wang and Takagi (2012) reported that 11% of 36 upward flashes striking a windmill or/and its lightning protection tower in winter in Japan were of positive polarity.

Table 8.5. Lightning current parameters (median values) of upward positive flashes. The sample size is given in the parenthesis.

References	Location	Peak Current (kA)	Flash Duration (ms)	Charge Transfer (C)	Action Integral ($\times 10^3$ A^2s)
Berger (1978)	Berger's Tower, Switzerland	1.5 (132)	72 (138)	26 (137)	-
Miki et. al. (2010)	Nikaho Kougen Wind Farm, Japan	6.5 (16)	40 (16)	30.2 (16)	-
Zhou et al. (2012)	Gaisberg Tower, Austria	5.2 (26)	82 (26)	58 (26)	160* (26)
Romero et al. (2013b)	Säntis Tower, Switzerland	11 (30)	80 (30)	169 (30)	390 (30)

*The value of action integral (0.16 x 10^3 A^2s) given by Zhou et al. (2012) is a misprint.

In case of upward positive flashes, observed current pulses of high repetition rate superimposed on the initial portion of initial continuous current were inferred by Zhou et al. (2012) to be associated with the upward negative stepped leader process, in agreement with high speed camera observations reported by Miki et al. (2011). Both Miki et al. (2011) and Zhou et al. (2012) have shown that the estimated upward negative stepped leader channel charge density is on the order of mC/m, which is significantly larger than typically used in leader propagation models. A comparison of lightning parameters of upward positive flashes reported from different studies is given in Table 8.5.

From comparison of Tables 8.5 and 8.2, median charge transfers for upward positive flashes are comparable (except for that for the Säntis Tower flashes) to their counterparts for the initial stage of upward negative flashes,

while upward positive flashes have shorter durations. This implies a higher average current for upward positive flashes. Note also that median action integrals in Table 8.5 are considerably larger than for the initial stage of upward negative flashes (see Table 8.2).

8.8 Characteristics of Upward Bipolar Lightning

Bipolar lightning is defined as a lightning event in which the current waveform measured at the channel-base exhibits a polarity reversal within the same flash. McEachron (1939) first reported this kind of flashes from his measurements at the Empire State Building in New York, and later Hangenguth and Anderson (1952) presented a total of 11 bipolar flashes for a 10-year observation period. Berger (1978) observed 68 upward bipolar flashes (6%) out of 1196 discharges at Mount San Salvatore in Switzerland between 1963 and 1973. Gorin and Shkilev (1984) reported six (6.7%) of 90 upward discharges initiated from the Ostankino tower in Moscow to be bipolar, and two bipolar flashes were observed on the Peissenberg tower in Germany by Heidler et al. (2000). Miki et al. (2004) observed 43 (20%) bipolar flashes of 213 upward flashes observed at the Fukui chimney in Japan. Wang and Takagi (2008b) reported on 3 upward bipolar lightning flashes observed from a windmill and its lightning protection tower. Ishii and Natsuno (2011) measured 304 current waveforms at wind turbines at 25 sites in Japan during 2008-2011 (no data were recorded during May-September). They found that 6% of the currents were bipolar. Wang and Takagi (2012) reported that 25% of 36 upward flashes striking a windmill or/and its lightning protection tower in winter in Japan were bipolar.

Zhou et al. (2011a) analyzed 21 upward-initiated bipolar lightning flashes observed at the Gaisberg Tower in 2000-2009. At this tower, bipolar lightning flashes constitute 3% (21/652), and 13 (62%) of the 21 bipolar flashes occurred in non-convective season (September-March). Based on the classification suggested by Rakov and Uman (2003), 13 (62%) of the 21 bipolar flashes belong to Type 1 associated with a polarity reversal during the initial stage current, 5 belong to Type 2 associated with different polarities of the IS current and the following return strokes, 1 belongs to Type 3 associated with return strokes of opposite polarity following the IS, and 2 were not assigned to any of the above types. In agreement with observations in other studies, the initial polarity reversal from negative to positive occurred more often (76% or 16/21) than from positive to negative. The geometric mean (GM) and arithmetic mean (AM) of the total absolute charge transfer are 99.5 C and 125 C, with the GM and AM total flash durations being 320 ms and 396 ms, respectively.

Bipolar upward-initiated flashes are different from downward bipolar lightning flashes reported by Fleenor et al. (2009) and Jerauld et al. (2009). To date, the knowledge of the physics of bipolar lightning is still poorer than that of negative or positive lightning, although continuing measurements of lightning currents on tall towers should provide more insights in the near future. At least when tall structures are involved, bipolar lightning flash occurrence is similar to that of positive lightning (Rakov, 2005).

8.9 Summary

Tall objects (higher than 100 m or so) located on flat terrain and objects of moderate height (some tens of meters) located on mountain tops experience primarily upward lightning discharges that are initiated by upward-propagating leaders. Upward (object-initiated) lightning discharges always involve an initial stage that may or may not be followed by downward-leader/upward-return-stroke sequences. The initial-stage current often exhibits superimposed pulses whose peaks range from tens of amperes to several kiloamperes (occasionally a few tens of kiloamperes).

Object-initiated lightning events may occur relatively independent from downward lightning during non-convective season and it has been observed that frequently several flashes were initiated from a tall object within a period of some hours. Diendorfer et al. (2006) reported on 20 negative flashes to the Gaisberg Tower during one night in February 2005 (winter season) transferring a total charge of more than 1,800 coulombs to ground.

At tall objects, the probability of occurrence of bipolar lightning is about the same as for positive lightning. Possible reasons for the observed differences from downward lightning and the high complexity of upward lightning are the multiple upward branches of leaders initiated from the tower tip and the relatively short upward leader channels approaching charged regions above the object.

9. Geographical and seasonal variations in lightning parameters

9.1 Introduction

A possible dependence of lightning parameters on geographical location has been pointed out for many years, in particular the peak current of first strokes (e.g., Anderson and Eriksson, 1980; Pinto et al., 1997). However, no conclusive evidence has been reported until now, in part due to the difficulties in obtaining statistically significant data samples and in part due to the effects caused by differences in instrumentation and data analysis methodology present in the observations made at different locations.

In this section we shall discuss the possible dependence of negative cloud-to-ground (CG) lightning parameters on geographical location and season, specifically a) the return stroke peak current and front duration (for both first and subsequent strokes), b) flash multiplicity, interstroke interval, number of channels per flash, and c) continuing current (intensity and duration). For other parameters of negative lightning flashes, such as M-components and return-stroke speed, there is insufficient information available for a reliable analysis.

As regards positive CG lightning parameters, there is insufficient information for a reliable analysis of dependence on geographical location. It is worth mentioning that, in spite of this fact, there are evidences suggesting a relationship between some positive flash parameters and the type of thunderstorm, and also different current waveforms have been observed in the coastal area of the Sea of Japan at different seasons (for a review, see Rakov and Uman, 2003). Assuming that there is a difference in the prevalent type of thunderstorms in different locations, the above data imply a dependence on the geographical location. Additional information on characteristics of lightning as a function of season, location, and storm type is found in Section 2.8 of Rakov and Uman (2003).

Although it is well known that flash density (Pinto et al., 2007; Orville et al., 2011) and polarity (Rakov and Uman, 2003; Orville et al., 2011) dramatically vary with geographical location and season, it has been a subject of controversy whether or not this is the case for other lightning parameters. This controversy, which has been discussed in the literature for many years, is a direct result of the complexity of the physical processes responsible for the various observed lightning features and the inherent limitations of lightning detection techniques. Before attributing any variation of lightning parameters to regional or meteorological peculiarities, one should make certain that measuring and data processing techniques used in different locations possess similar capabilities so as to allow a meaningful comparison of the different measurements (Rakov et al. 1994). Although any technique has some limitations, for a given lightning parameter these limitations could be more or less important. For this reason, one must be very careful when comparing different observations using different techniques. Another important aspect is related to the level of statistical significance of a given variation, sometimes not completely addressed by the data analysis (Rakov and Uman, 2003). It is also very important in any comparison of CG lightning parameters to exclude any upward and intracloud lightning from the analysis. In some cases and for some techniques, this task could be very difficult if not impossible.

From a physical point of view, geographical or seasonal variations of lightning parameters would be caused by variations in thunderstorm electrical structure that resulted from either geographic or seasonal factors. “Geographic variations” in lightning parameters would be those related to changes in latitude, topography, continentality or other surface features. “Seasonal variation” would be those related to temperature, humidity, general atmospheric circulation or other meteorological features.

To fully understand a given variation in a lightning parameter, we would need to understand how this variation could be explained in terms of thunderstorm structure. However, the complexity of the processes involved makes it difficult, in some cases, to fully comprehend the causes of the variations. In consequence, a detailed statistical analysis and a rigorous technical evaluation are required to avoid obtaining spurious results.

Due to the difficulties mentioned above, and considering the goal of this document, the results presented in this section are limited to negative CG flashes and divided into three sub-sections describing variations in: 1) return stroke peak current and front duration, 2) flash multiplicity, interstroke interval, and number of channels per flash, 3) continuing current intensity and duration. No attempt was made to present a comprehensive review of the literature. Instead, we concentrated on comparing recent observations at different locations that used the same technique. We also included observations based on using similar techniques and resulting in large sample sizes. A comprehensive review of previous results can be found in Rakov and Uman (2003) and CIGRE Report 376 (2008).

Seasonal occurrence of upward and downward lightning in Austria is discussed in Section 8.4.

9.2 Return Stroke Peak Current and Front Duration

Direct current measurements. Direct current observations at short instrumented towers yielded the most precise measurements of first and subsequent return stroke peak current and front duration. However, in many studies the number of events is so small that the statistical significance is limited. Moreover, variations in the measured peak current and front durations can be caused by small differences in instrumentation or data analysis from one study to another, as well as by local topography which influences the effective height of a tower.

The larger sets of first and subsequent return stoke current waveforms measured at relatively short instrumented towers were obtained at Mount San Salvatore, Switzerland (101 negative CG flashes-Berger, 1967, 1975), at Foligno and Monte Orsa, Italy (42 negative flashes-Garbagnati and Lo Piparo, 1982) and at Cachimbo Mountain, Brazil (31 negative CG flashes-Visacro et al., 2004). In addition, Takami and Okabe (2007) measured 120 negative CG flashes (first strokes only) at 60 Japanese transmission line towers. Other measurements of current at short towers are characterized by smaller sample sizes and will not be discussed here.

The towers in Switzerland and Italy are no longer operational. The Brazilian tower operated from 1985 to 1998 (13 years), returning to operation in 2007 when it was upgraded with new instrumentation (additional information is found in Section 3.2). Although the sample size obtained after the upgrade has been too small for inclusion in this analysis, we have included a comment about the new measurements.

Table 9.1 shows the median peak current calculated from the data cited above. Some interesting aspects related to these observations are listed below:

Table 9.1. Median values of first stroke peak current calculated from observations at different instrumented towers.

Location	Peak Current (kA)	Number of Events
Switzerland	30	101
Brazil*	45	31
Japan	29	120
Italy	33	42

*The value in Brazil does not change if the observations after the 2007 upgrade are included. (Visacro et al., 2010).

a. In Brazil, the summer mean peak current value is the same as that for other seasons, while in Switzerland the summer mean peak current value (37 kA) is 20% higher than in other seasons. This suggests possible seasonal dependence.

b. In Brazil, no values below 20 kA were observed in the period from 1985 to 1998. This fact partially explains the larger value for Brazil (50% larger than the Swiss value reported by K. Berger) shown in Table 9.1. Note, however, that values below 20 kA were measured after 2007 (Visacro et al., 2010).

c. The Japanese measurements are restricted to peak currents above 9 kA.

d. In all observations possible contamination by upward flashes cannot be ruled out, although it is unlikely judging from the measured current waveforms.

Clearly, additional direct current measurements for first strokes are needed.

First-stroke peak current estimated by lightning location systems (LLS). First-stroke peak currents reported by lightning location systems are subject to large uncertainties. Despite these uncertainties, relative annual variations of the peak currents reported by a lightning location system could reveal possible dependence of this parameter on season. Pinto et al. (2006) studied the annual variation of peak current in negative flashes observed by the NLDN in the United States and the RINDAT network in the southeastern Brazil. They found the annual variations for both networks to be less than 10% (Fig. 9.1).

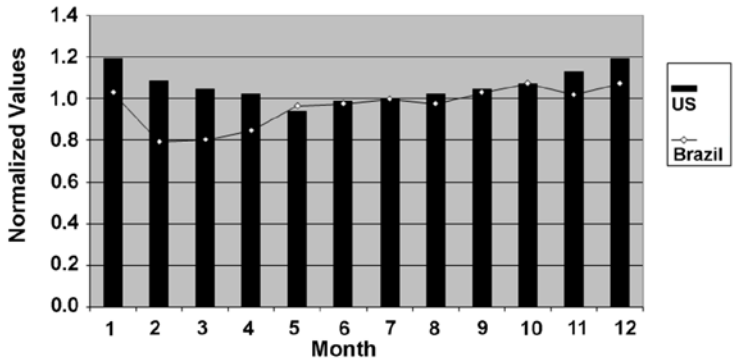

Fig. 9.1. Normalized mean monthly distribution of the negative first-stroke peak current observed by RINDAT in southeastern Brazil from 1998 to 2005 and by NLDN from 1989 to 1999. Adapted from Pinto et al. (2006).

Recently, Saraiva (2011) suggested (based on a preliminary analysis of limited data) that the peak current of negative flashes increases by about 10% as the height of the 35 dBZ echo increases from 8 to 15 km. This prediction is in need of confirmation with larger data samples.

First return stroke front duration. First return stroke front duration T-10 defined as the time between the 10% and 90% values of the first peak in the current wave front can be measured with precision only at instrumented towers. Table 9.2 shows the median values of front duration obtained in Switzerland (Berger et al., 1975), Brazil (Visacro et al., 2004), Japan (Takami and Okabe, 2007) and Italy (Garbagnati and Lo Piparo, 1982), The differences are less than or within one standard deviation or so of each other, suggesting that there is no dependence on locations.

Table 9.2. Median values of front duration (T-10) for first strokes calculated from measurements at different instrumented towers.

Location	Front Duration T-10 (μs)	Number of Events
Switzerland	4.4	101
Brazil*	5.6	31
Japan	4.8	120
Italy	7.2	42

*The value for Brazil changes to 5.1 μs if the observations after 2007 (n = 7) are included (Visacro et al., 2010).

Subsequent return strokes. Table 9.3 shows median values of peak current and front duration (T-10) for subsequent strokes calculated from measurements in Switzerland, Brazil, and Italy. The differences for peak currents are larger than those for front duration, the latter being less than or of the order of one standard deviation.

Table 9.3. Median values of peak current and front duration (T-10) for subsequent strokes calculated from measurements at different instrumented towers.

Location	Peak Current (kA)	Front Duration T-10 (μs)	Number of Events
Switzerland	12.0	0.9	135
Brazil*	16.3	0.7	59
Italy	18.0	0.9	33

*The values for Brazil change respectively to 17.5 kA and 0.6 μs if the observations after 2007 (n =12) are included (Visacro et al., 2010).

The above data appear to suggest that variations in the first and subsequent stroke peak current may exist for different geographical locations. However, one cannot rule out the possibility that a significant part of the observed variation results from differences in the instrumentation and/or data analysis. Additional measurements are needed. Further, the observations of front duration seem to suggest no dependence on geographical location.

9.3 Flash Multiplicity, Interstroke Interval, and Number of Channels per Flash

Flash Multiplicity and Interstroke Interval. High speed cameras in conjunction with microsecond-scale electric and magnetic field records is the most precise technique for recording flash multiplicity, interstroke Interval, and number of channels per flash. Saraiva et al. (2010) recently studied the flash multiplicity of negative flashes in Arizona (United States) and São Paulo (Brazil) using the same high-speed camera. Fig. 9.2 compares the number of strokes per flash in Arizona and São Paulo. Note that the percentage of flashes with a given number of strokes is very similar in both regions. The figure also shows that the most frequent value of the multiplicity was 2 in both locations. The percentage of single-stroke flashes is also almost the same in both regions (approximately 20%), and the average number of strokes per flash was 3.9 in both Arizona and Sao Paulo.

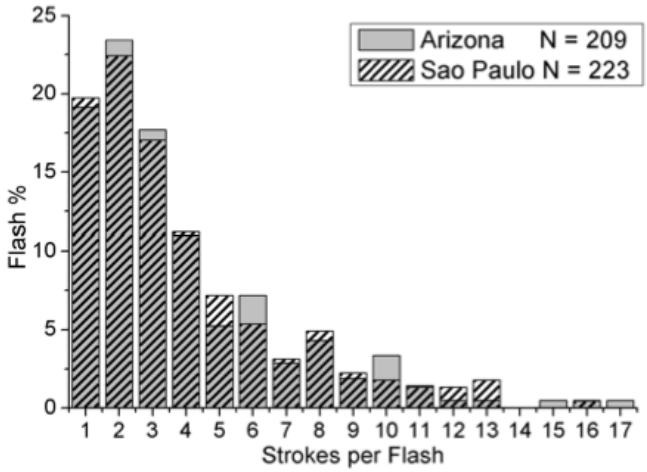

Fig. 9.2. Percentage of flashes with different number of strokes per flash (multiplicity) observed in Arizona and São Paulo. Adapted from Saraiva et al. (2010).

Electric field measurements with sufficient time resolution is another technique capable of obtaining accurate values of multiplicity. Observations using this technique have been done in Sri Lanka by Cooray and Jayaratne (1994), in Sweden by Cooray and Perez (1994) and in Malaysia by Baharudin et al. (2012). Further, Rakov and Uman (1990a, b) and Thottappillil et al. (1992), working in Florida, employed both electric field measurements and multiple-station TV observations. For a review of most of these studies see Ballarotti et al. (2012). All results suggest similar values of the percentage of single stroke flashes and multiplicity values in the range of 3 to 5 (see Table 2.1).

However, Saraiva (2011) recently showed that when the multiplicity data are sorted according to the different storm types present in Arizona and São Paulo during the observation period, an appreciable storm-to-storm lightning parameter variation is observed in both places. This is in agreement with past observations in Russia (Rakov and Dulzon, 1986). Data from lightning location system observations in Austria (Diendorfer et al., 1998) and United States (Orville et al., 2002, 2011; Rakov and Huffines, 2003) and from slowly rotating streak-camera observations in the United States (Kitterman, 1980) also suggest significant variation in multiplicity for different thunderstorms. Saraiva (2011) suggested that the multiplicity of negative flashes could be correlated with the horizontal extent of the main negative charge region within the parent thunderstorm (as estimated by the area enclosed by the 35 dBZ reflectivity contours at the level of the -10 °C isotherm). It is possible that different flash multiplicities found in different regions could be a function of the occurrence of different storm types in those regions. More studies are needed to test these hypotheses.

Saraiva et al. (2010) who used an accurate stroke-count technique, reported interstroke intervals for negative flashes in different regions. A high-speed camera was used to measure 1210 interstroke intervals in Arizona and São Paulo. The values ranged from a few ms to 782 ms. The geometric mean interstroke interval (60 ms) was essentially the same in both locations. Many other authors have reported geometric mean values of interstroke intervals around 60 ms (Shindo and Uman, 1989; Cooray and Jayaratne, 1994; Rakov et al., 1994; Saba et al., 2006; among others). This value is also the same as observed by Schulz et al. (2005) in Austria in a 10-year study using data from a lightning location system. Fig. 9.3 shows histograms of interstroke intervals in Arizona and São Paulo. Additional information on interstroke intervals (and on flash duration) is found in Section 2.6.

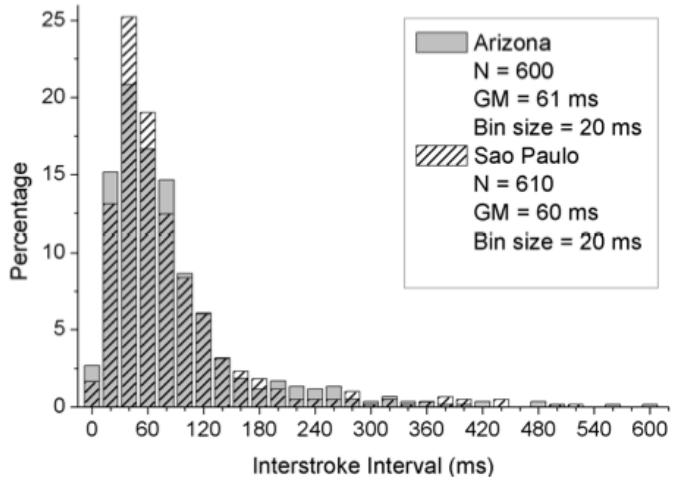

Fig. 9.3. Distributions of interstroke intervals in Arizona and São Paulo. Adapted from Saraiva et al. (2010).

Number of Channels per Flash. Another parameter investigated for changes in different geographical locations was the average number of ground contacts (ground terminations) per flash. Saraiva et al. (2010) found that about half of the 344 flashes observed in Arizona and São Paulo exhibited one or more ground terminations. Fig. 9.4 shows how the numbers of ground contacts in those two locations are distributed. The results for Arizona and São Paulo are very similar, with the average number of ground contacts in both locations being 1.7. This is in agreement with previous observations reported for Florida and New Mexico (Rakov et al., 1994). Additional information on the number of channels per flash is found in Section 2.7.

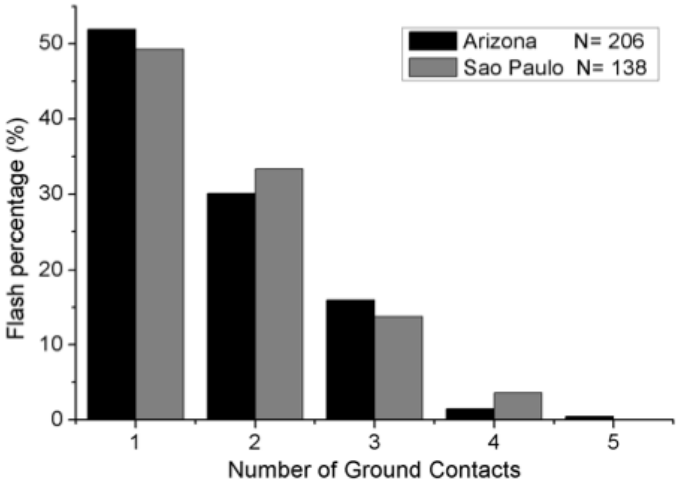

Fig. 9.4. Percentage of flashes that produce a given number of ground contacts in Arizona and São Paulo. Adapted from Saraiva et al. (2010).

9.4 Continuing Current Intensity and Duration

Three studies have investigated the average intensity and duration of continuing currents (CC) of negative flashes using large data sets obtained from electric field observations. The observations were done in New Mexico (Brook et al., 1962), Florida (Shindo and Uman, 1989), and São Paulo, Brazil (Ferraz et al., 2009) and are compared in

Fig. 9.5, where the data of Ferraz et al. were compensated for a relatively short decay time constant. Two slanted lines in Fig. 9.5 represent average CC intensities in the United States (50 A) and in Brazil (800 A).

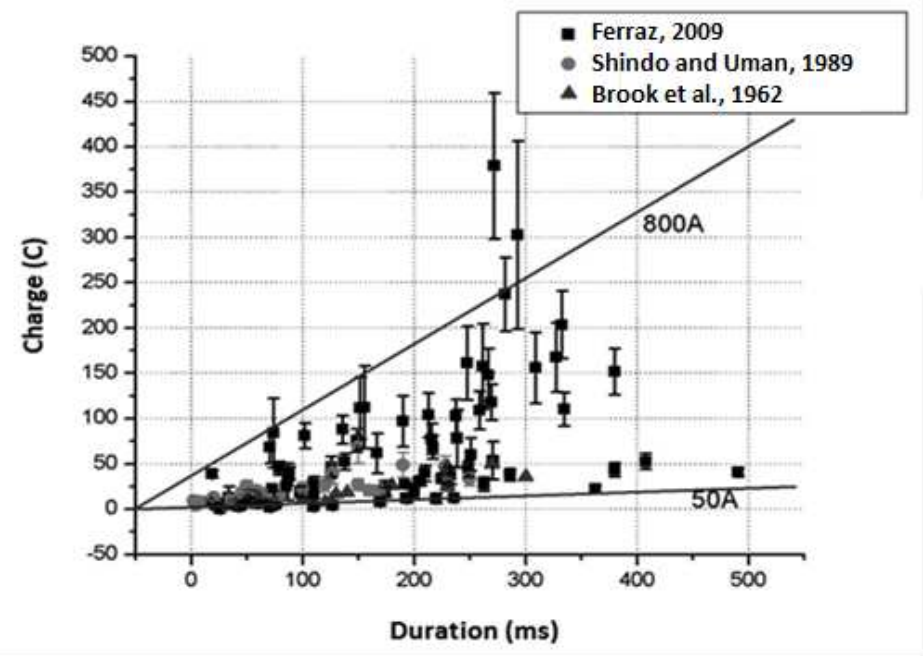

Fig. 9.5. Charge versus duration for negative CC. Adapted from Ferraz et al. (2009).

The results suggest that the CC average intensity in Brazil is larger than in United States, although more data at other locations are needed before a definitive conclusion can be made.

Figs. 9.6 and 9.7 show distributions of CC durations from Arizona and São Paulo (Saraiva et al, 2010). These were inferred from the duration of the channel luminosity following the return stroke. All data were obtained with the same high speed camera. Fig. 9.6 shows the distributions of durations for very-short and short CCs. The only noticeable differences between the CCs observed in Arizona and São Paulo is in the range of 12 to 40 ms (short CC) and this is likely due to the small sample size. Fig. 9.7 shows the distributions of durations for long CCs, which were about 10% of the overall CC data set.

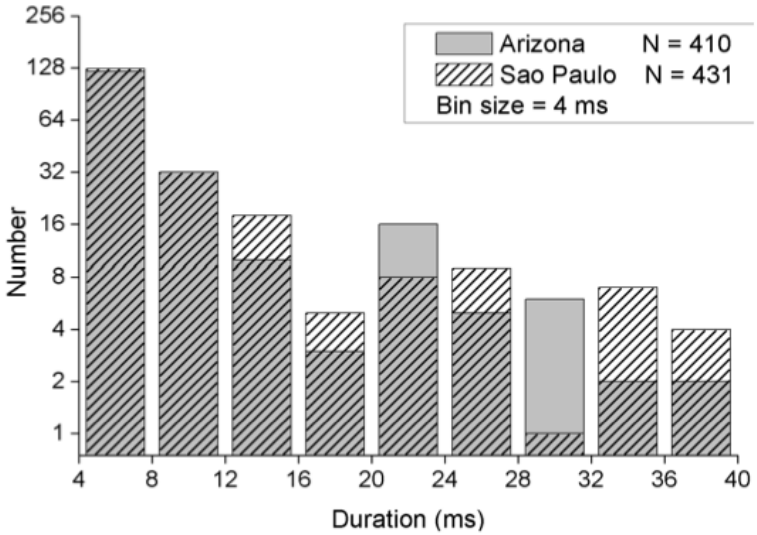

Fig. 9.6. Distributions of very-short and short CC durations in Arizona and Sao Paulo. The distributions are very similar. The only differences appear between 12 and 40 ms, in the range of short CC. Adapted from Saraiva et al. (2010).

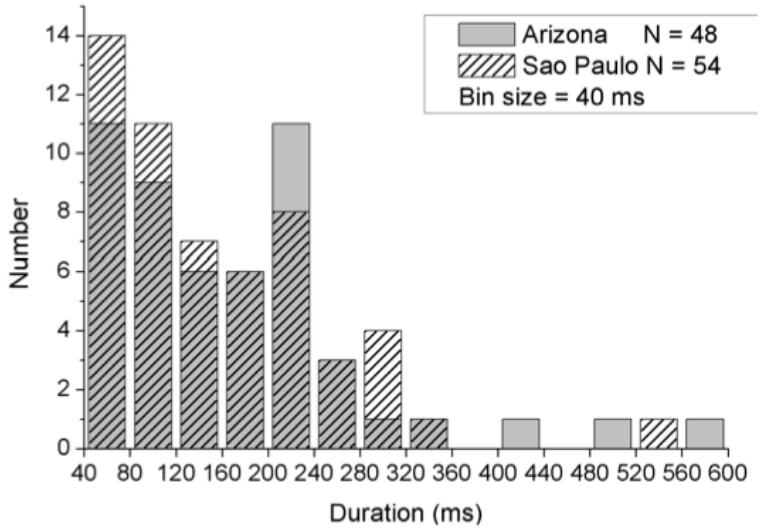

Fig. 9.7. Distributions of long continuing current durations in Arizona and São Paulo. There are no significant differences between the two distributions. Adapted from Saraiva et al. (2010).

In summary, available data obtained using the same technique in different regions do not support any dependence of the CC duration on geographical location.

9.5 Summary

From the information available in the literature at the present time, there is no evidence of a dependence of negative CG lightning parameters on geographical location, except maybe for current intensity (first and subsequent stroke peak currents), for which relatively insignificant (less than 50%), from the engineering point of view, variations may exist. It is important to note, however, that it cannot be ruled out that the observed differences in current measurements are due to reasons other than "geographical location", with limited sample size for some observations being of particular concern. Similarly, no reliable information on seasonal dependence is available. In summary, at the present time, the available information is not sufficient to confirm or refute a hypothesis on dependence of negative CG lightning parameters on geographical location or season. Clearly, exceptions could exist, such as the large, long duration current waveforms observed by Miyake et al. (1992) in winter in the coastal area of the Sea of Japan. Further studies are necessary, however, to clarify if the observed exceptions represent actual variations in flash characteristics with the geographical location or represent extreme values of a common distribution.

10. Lightning parameters needed for different engineering applications

This chapter was envisioned to serve as a "bridge" between the description of lightning parameters found in the preceding chapters and the existing standards and other literature on specific applications of those parameters. No attempt is made to present detailed descriptions of the various procedures in which lightning parameters are used as an input. Instead, references to the pertinent CIGRE documents, standards, and published papers are given.

10.1 Introduction

Lightning parameters are of interest in different fields of research and engineering applications, such as airborne vehicles, construction and oil industry engineering, power network components and wind turbines. The protection against lightning for each application follows specific standards. Several aspects have been covered by previous CIGRÉ Brochures 63 (1991), 118 (1997), 172 (2000), 360 (2008), 287 (2006), 441 (2010) and reports, such as that by Cooray et al. (2011), and by the ongoing activities of other working groups (e.g. WG C4.408 Lightning Protection of Low-Voltage Networks, WG C4.409 Lightning Protection of Wind Turbine Blades, WG C4.410 Lightning Striking Characteristics for Very High Structures, WG C4.23 Guide to Procedures for Estimating the Lightning Performance of Transmission Lines, WG C4.26 Evaluation of Lightning Shielding Analysis Methods for EHV and UHV DC and AC Transmission Lines).

The aim of this chapter is to briefly summarize the main lightning parameters that have an influence in the power engineering calculations with emphasis on the studies presented in the recent literature.

This chapter first addresses some general considerations on lightning effects and parameters. Then, following the structure of CIGRÉ Brochure 172 (2000), the chapter focuses on power networks, including protection of transmission lines, protection of distribution lines, testing of surge arresters and other surge protection devices, and protection of other ground-based installations (substations). Additionally reviewed are the lightning parameters needed for designing the protection of ordinary structures. Other objects and systems, including airborne vehicles, wind turbines, and electronic circuits, are outside the scope of this chapter.

10.2 General Considerations

Before addressing the parameters of major relevance in specific applications, this section considers, following Visacro (2012a), some general aspects related to lightning effects and lightning parameters responsible for those effects.

The impact of lightning effects on power plants (and other objects and systems) can be considered from two different perspectives: their severity, in terms of their potential to cause physical damage or operational failures, and the frequency with which these effects occur.

The lightning ground flash density (see Section 2.4), which is considered to be a characteristic of lightning activity in a certain region, as opposed to being considered a lightning parameter, is by far the most relevant factor in any kind of application related to lightning protection of ground-based installations. The risks to potential “victims” are practically proportional to this density. There is a trend to replace the ground flash density by the ground stroke density or by ground strike point density, both of which can be determined from data provided by LLS. The ground stroke density is needed in those applications where the effects of both first and subsequent strokes are relevant, notably those related to induced effects of nearby lightning flashes. The ground strike point density can be also estimated from the known local ground flash density by applying a correction factor of about 1.5 to 1.7 to it in order

to account for multiple channel terminations on ground within a flash (see Section 2.7). Bouquegneau et al. (2012) proposed a conservative value of 2 for this correction factor to be used in lightning risk calculations.

The severity of lightning effects depends on the characteristics of the lightning event and on the response of the "victim" (electrical system or structure) subjected to the lightning stress. Focusing on the event, a fundamental point to consider is that the source of the most damaging lightning effects is the lightning current, as discussed in Visacro (2012a). Such effects are derived either from the most severe events of direct lightning strikes to the "victims", which are subjected to the whole lightning current or part of it, or from the less severe, but much more frequent events associated with coupling electromagnetic fields of nearby flashes. Thus, it is important to consider the specific features of currents in the different types of lightning events.

The most common downward negative flashes have currents that, at the ground level, exhibit pulses of high magnitude and short duration, corresponding to the first and subsequent return strokes, and slowly-varying currents of low amplitude and long duration, consisting of continuing and superimposed M-component currents that frequently follow subsequent strokes. The pulses of first and subsequent strokes are quite different (see Chapter 3). The first-stroke current starts with a concave front followed by an abrupt rise around the half-peak that leads to the first peak. This is typically followed by a second peak, usually higher than the first and, then, the current decays slowly with some subsidiary peaks, ceasing typically after 1 to 3 ms (Visacro et al. 2010). Similar features are observed at the wavefront of measured remote lightning electric fields (Krider and Radda, 1975). Representative double-peaked current waveforms of first strokes are presented in Fig. 3.3 and in Visacro (2005a). Compared to first negative return strokes, the currents of most subsequent return strokes show a single peak, shorter front time, time-to-half-peak and lower transferred charge. Parameters for analytical expression of representative waveforms of first- and subsequent-stroke currents by means of a set of Heidler functions are presented in De Conti and Visacro (2007) (see also Section 3.6). According to Table 3.5, the median parameters of first-stroke pulses for maximum current, front duration, time-to-half-peak and transferred charge are 30 kA, 5.5 μs, 75 μs, and 5.2 C, respectively, while for subsequent-strokes the corresponding median values are 12 kA, 1.1 μs, 32 μs, and 1.4 C. As mentioned in Chapter 4, continuing currents of negative downward flashes have durations of a few to hundreds of milliseconds and typical magnitudes of a few hundreds of amperes, although values varying from around 20 A to several kiloamperes have been reported. In spite of their small amplitude (relative to return-stroke pulses), they can transfer large amounts of charge from the cloud to ground, exceeding several hundreds of coulombs in some cases.

Chapter 7 addresses the positive downward lightning. It draws attention to the paucity of data about this event and possible influence of the strike object located on the mountain top on the distributions of current parameters of this event reported by Berger et al. (1975). Typically, positive lightning consists of a single stroke, whose peak current is larger and time parameters are longer than for negative first strokes. According to Table 7.3, the median values for peak current, front duration, time-to-half-peak, and transferred charge are 35 kA, 22 μs, 230 μs, and 80 C, respectively. Apparently, larger and longer continuing currents are observed in positive lightning compared to those of downward negative lightning, as discussed in Chapter 4.

Fig. 8.2 depicts the typical current record of upward negative lightning that always involves an initial relatively low intensity and long duration continuous current (typical average values of around 100 to 500 A and of around 80 to 300 ms, respectively, according to Table 8.2). In many cases the initial stage of upward lightning contains current pulses superimposed on the slowly varying continuous current, some of them with peaks in the kiloamperes range, comparable to current peaks of smaller return strokes. Fewer than half of the events contain return strokes whose current magnitudes and waveforms are similar to those of subsequent strokes. Upward negative lightning can transfer large amounts of charge to ground, frequently several tens of coulombs. Upward positive lightning events are relatively rare and their specific energy is much higher than that of negative upward lightning, according to Table 8.5.

In order to discuss the severity of lightning effects, it is worth addressing the two main types of damaging lightning effects in the context of power engineering, the physical damage associated with the dissipation of energy and overvoltages responsible for insulation failures.

Physical Damage. The heating resulting from the energy dissipated while the lightning current flows into and through a "victim" circuit is the source of damage. The lightning parameter that is most closely related to this effect is the specific energy or action integral. The response of a "victim" is represented by its equivalent resistance. The dissipated energy, and therefore associated damage, can be roughly estimated as the product of the specific energy by this resistance, whatever the type of lightning event and current variation with time (pulse or continuing current). In this respect, the time duration is a very important parameter. In many cases, even low-current, but long duration events, such as upward lightning and long continuing currents, can produce high values of specific energy and hence highly destructive effects. The equivalent resistance of the "victim" circuit plays a major role in determining the extent of damage. Even "victims" with low equivalent resistance such as metallic conductors can suffer damage, as frequently observed in OPGW cables of overhead lines. In this particular case, the effect is mainly attributed to long continuing currents, and the associated charge transfer is considered to be the lightning parameter most closely related to the damage at the interface between the lightning plasma channel and the metallic object, which effectively has a constant voltage drop for all levels of current.

The most severe damage is that from direct strikes, since the currents induced by nearby flashes, typically of low amplitude and short duration, are unlikely to impart enough energy to cause damage, with the exception of low voltage systems with sensitive components, although, even in this case, the damage is usually preceded by insulation failure. The median values of specific energy of first and subsequent negative strokes in downward lightning given in Table 3.5 are 5.5×10^4 and 6.0×10^3 A^2s, respectively, while for positive strokes the value of 6.5×10^5 A^2s is indicated in Table 7.3. According to Table 8.2, the geometric mean value of the specific energy of the initial stage of upward negative lightning varies from 1.5×10^3 to 4×10^4 A^2s.

Overvoltages. Insulation failures can be caused by either direct lightning strikes to electrical systems or nearby flashes. The disruptive discharge responsible for this effect depends on the lightning overvoltage developed across the insulators. Notably, the occurrence of a flashover requires the instantaneous value of the overvoltage to remain above a given threshold, which strongly depends on the insulator withstand electrical strength, during a sufficiently long time interval. Basically, only the return-stroke current pulses are able to cause such high overvoltages in electrical systems. Thus, the amplitude and shape of the overvoltage wave are the factors that define the occurrence (or non-occurrence) of flashover across insulators, and these two parameters depend on the amplitude and waveshape of the lightning return-stroke current. Specification of the lightning source in studies of either direct-strike or induced lightning effects is discussed in Chapter 6.

For overvoltages developed in response to direct strikes, the peak current and the current waveshape have major influence. The time parameters at the wavefront can also influence the overvoltage peak, and the time-to-half-peak has some influence on the overvoltage magnitude after the peak, although the magnitude in the wave tail is more influenced by the "victim" parameters, such as the impedance of the ground connections and their distances from the strike point. In power engineering, lightning effects on high voltage transmission lines is a subject of major interest. Usually, only first strokes are considered as the source of lightning-related insulation failures of such lines because their median peak current is 2 to 3 times larger than that of subsequent strokes. Recent results by Silveira and Visacro (2012, 2013) show that subsequent strokes can also be responsible for failures and outages of 69- and 138-kV lines. Due to the low insulation level of distribution lines, most of (if not all) direct strikes to those lines are expected to lead to flashover.

Concerning lightning-related insulation failures due to nearby flashes, the amplitudes and waveforms of overvoltages they induce depend basically on the average time derivative of the lightning current (Nucci et al., 1993; Silveira et al., 2009), whose associated time-varying magnetic fields illuminates the "victim". The retardation of the current wave propagating along the lightning channel also influences the overvoltage along with the distance of the strike point and the "victim" parameters, since the contributions to the induced voltage from the current

elements along the channel reach the “victim” at different times. Thus, the peak current, the front time, the waveshape, and the velocity of propagation of the current wave along the channel are the most influential lightning parameters. Current waveform parameters are discussed in Chapter 3 and return-stroke speed in Chapter 5. The maximum current derivative is often stressed as an important parameter for induced voltage, but it is possible to argue that, although it does contribute, it lasts for too short time to influence significantly the overvoltage amplitude. Both first and subsequent strokes can be sources of significant induced overvoltages, since both have high values of current derivative at the wavefront. Although the peak current of first strokes has a median value that is about 3 times larger than that of subsequent strokes, the latter have median front-times around 5 to 8 times shorter. The induced voltages of nearby flashes are the main cause of distribution-line failures. Depending on the conditions, the highest overvoltages induced in such lines can be caused by either first or subsequent strokes, as discussed by Piantini and Janiszewski (2009), Silveira and Visacro (2009), and Silveira et al. (2011).

Due to the shape of the return-stroke current wave, the wavefront of the induced overvoltage of first and subsequent strokes tends to be steep, reaching the peak almost at the same time as the current peak, and, then, to decay quickly, once the time derivative of current at the ground level after the peak becomes low. This decay is not very sharp due the retardation of the current that travels along the channel with a finite velocity. The maximum contribution of current elements above ground to the induced overvoltage delays the time required for the current wave to propagate along the channel from the attachment point plus the time required for the inducing field of that element to propagate from the element position to the line. Thus, their maximum contribution to the induced voltage is time shifted with respect to that of elements at the ground level, delaying the overvoltage decrease after the peak. To summarize, the parameters that influence the average time derivative of current, notably the peak current, the front time, and the waveshape, are the lightning parameters that govern the induced overvoltage amplitude, along with the velocity at which the current wave propagates along the channel. The combined effect of those parameters determines the overvoltage.

Main lightning parameters needed in calculations of lightning performance, for specification of lightning testing procedures, and for designing lighting protection are discussed in the following five sections.

10.3 Transmission Lines

The protection of transmission lines is based mainly on the use of shield wires (or overhead ground wires, OHGWs) and selective use of surge arresters. Some special methods have also been successfully used for improving the lightning performance (IEEE Std 1243-1997). The grounding system has generally a great influence on the effectiveness of the protection means.

Effective shield wire protection is characterized by low probability of both shielding failures and backflashovers. Modeling and procedures for the estimation of these probabilities have been addressed by both CIGRÉ documents and IEEE Standards. The two reference documents are

- CIGRÉ WG 33-01, “Guide to Procedures for Estimating the Lightning Performance of Transmission Lines”, CIGRÉ Technical Brochure, No. 63, October 1991;
- IEEE Std 1243-1997, IEEE Design Guide for Improving the Lightning Performance of Transmission Lines, 1997.

CIGRÉ Brochure 63 (1991) presents the procedures based on using the statistical distribution of the first return-stroke current peaks of downward negative flashes, shown in Fig. 3.2. Anderson and Eriksson (1980) noted that the two sub-distributions (below and above 20 kA) can be viewed as corresponding to the shielding failure and backflashover regimes, respectively. A single distribution, also shown in Fig. 3.2, was adopted by IEEE Std 1243-1997.

The shielding analysis needs a model that describes the attractive effects of the various transmission line configurations. The so-called electrogeometric model (EGM) is employed in both CIGRÉ Brochure 63 (1991) and

IEEE Std 1243-1997. The striking distance, r, the cornerstone of EGM, is most often computed (for phase conductors and shield wires) as $r = 10 \times I^{0.65}$, where r is in meters and I is the first-stroke peak current in kA (e.g., IEEE Std 1243-1997). CIGRÉ also makes reference to models based on the simulation of the leader progression (LPM). The influence of various models on the maximum shielding failure current of overhead transmission line is analyzed by Mikropoulos and Tsovilis (2010). Recently, CIGRÉ WG C4.405 has reviewed the lightning interception models (Cooray et al., 2011).

The calculation of the shielding failure flashover rate (SFFOR) is based on the integration of the product of the exposure area of the phase conductors and the probability density function of the lightning current amplitude between an upper value and a lower value of the lightning current amplitude. The upper value is defined by the reduction to zero of the exposure area. The lower value is determined on the basis of the estimation of the voltage across the line insulation and the evaluation of the line critical impulse flashover voltage (CFO). The IEEE procedure suggests an approximate calculation of the voltage across the line insulators by using the conductor surge impedance under corona and the CFO of the line insulation for the critical current calculation (Baldo et al., 1981; Darveniza and Vlastos, 1988). The IEEE procedure takes into account the shielding failure flashovers that result from subsequent strokes following the same path as a sub-critical first stroke, to form an additional $SFFOR_S$ term. CIGRÉ adopts a simplified procedure that only considers the first-stroke peak current distribution, but also suggests more sophisticated procedures that take into account: I) the whole line response considering the line configuration and II) different ways for the calculation of the line critical impulse flashover voltage. The first point can be approached by representing the line response by means of Electromagnetic Transient Programs (e.g., Ametani and Kawamura, 2005; Martinez and Castro-Aranda, 2005) or using elaborate electromagnetic models (e.g., Visacro and Soares, 2005b; Soares et al., 2005). Concerning the second point, CIGRÉ suggests approaches based on the use of i) insulation voltage/time curve (similar to the IEEE approach), ii) integration method (Witzke and Bliss, 1950a,b; Akopian, 1954; Jones, 1954; Kind, 1958; Rusck, 1958a; Caldwell and Darveniza, 1973; Alstad et al.,1979) and iii) physical models representing the corona inception, streamer and leader phases along the line insulation (Pigini et al., 1989; Suzuki and Miyake, 1977; Motoyama 1996).

When a lightning strikes the tower or the overhead ground wire, the current in the tower and ground impedances causes the rise of the tower voltage. A considerable fraction of the tower and shield wire voltage is coupled by mutual surge impedance to the phase conductors. The tower and shield wire voltages are much larger than the phase conductor voltages. If a voltage difference from phase to tower exceeds a critical value, a flashover occurs, called “backflash” or “backflashover”. The corresponding minimum lightning current that produces such a flashover is called “critical current”. The calculation of the critical current for backflashover depends, in general order of sensitivity, on the following parameters:

- Amplitude of the lightning current (generally the peak value of the first return stroke)
- Flashover criteria for the insulation and air gaps
- Presence of surge arresters across some or all insulators
- Surge impedance coupling among phases and groundwires, evaluated using transmission line models and considering the additional coupling from arrester-protected insulators
- Steepness (di/dt) at the peak of the current wave, which is generally assumed to be the maximum di/dt
- Waveshape, including both time to peak and time to half-peak value
- Footing impedance, influenced by high frequency and soil ionization effects
- Tower inductance or surge impedance model
- Representation of nearby towers and grounding systems
- Representation of nearby power system components (e.g. transformers).

Sometimes (Chowdhuri et al., 2002), the induction effects of the electromagnetic field of the lightning channel are additionally taken into account for the estimation of the insulator voltage. Induction effects related to current flow in the tower past the phase conductors have been observed and modeled in several ways.

The procedure adopted by CIGRÉ for the calculation of the line backflashover rate (BFR), the same as described by Hileman (1999), is specifically aimed at calculating the critical current and the resultant BFR value. In particular, the CIGRÉ procedure analytically estimates the backflashover critical current by making reference to the representation of the travelling wave phenomena that take place for both cases of a lightning strike to a tower or to an overhead ground wire. The BFR is given by the probability of exceeding the critical current multiplied by the number of flashes to the shield wires, taking into account that the crest voltage and the flashover voltage are both functions of the time-to-crest of the lightning current. The approach adopted by the IEEE is based on the estimation of the voltage across the line insulation at two specific time instants (IEEE Working Group, 1985 and 1993), namely: a first evaluation of the full impulse-voltage waveshape peak (at 2 μs) considering only the stricken tower, and a second evaluation on the tail (at 6 μs) considering relevant adjacent towers. In order to estimate the backflash critical current, these values are compared with an estimation of the volt-time curve of the line insulation, evaluated at the two-way span travel time for the 2-μs peak voltage.

Note that the procedures to calculate both rates, SFFOR and BFR, are based on using the local ground flash density N_g to determine the number of strikes to the line. Visacro et al. (2005c) used the historical data from lightning location systems to obtain the continuous variation of N_g along the line to improve the estimates of the number of strikes.

The CIGRÉ and IEEE procedures are compared in Nucci (2009). The main differences, when present, lie in the fact that some approaches/methods proposed so far within CIGRÉ can be considered to be more general than those proposed within IEEE, in that they take into account more variables of the problem. Within the IEEE – thanks in part to the inherently simpler approach – a computer code, called FLASH (v.19), has been made available, which can serve either as a professional tool capable of providing an approximate, yet very useful, answer on the lightning performance of typical overhead transmission lines or as a reference for beginner researchers when simple cases are dealt with.

Both the tower and ground models are fundamental parts of the lightning performance analysis of overhead lines. Several approaches have been presented in the recent literature addressing tower models (e.g., Ametani, 1994; Meliopoulos et al., 1997; Baba and Ishii, 2000; Motoyama and Matsubara, 2000; Gutierrez et al., 2004; Grcev and Rachidi, 2004; De Conti et al., 2006). The minor role of the OHGW in grounding impedance, using a distributed circuit approach, is clarified in CIGRÉ Brochure 275 (2005). The main factors that influence the grounding behavior have been analyzed in Visacro (2007) and revised in Visacro et al. (2009). The current-dependent response of electrodes is addressed in Sekioka (2005) and the effect of the frequency-dependent soil parameters on this response is addressed in Visacro and Alipio (2012b). A recent review of the assessment of backflashover occurrence rate on the HV transmission line towers and of the influence of the tower footing impulse resistance based on analytical developments is available in Sarajcev and Goic (2012). The same issue is covered in Visacro et al. (2012c) and Silveira et al. (2012) based on electromagnetic modeling. The relevant effect of the frequency dependence of soil resistivity and permittivity on backflashover rates of transmission lines is considered in Visacro et al. (2012d).

The use of surge arresters is covered by CIGRÉ Brochure 440 (2010) -- Use of Surge Arresters for Lightning Protection of Transmission Lines, reference to which is made in section 10.5.

Negative first strokes have traditionally been considered to produce the worst stress on transmission-line insulation (e.g., Chowdhuri et al., 2005). Subsequent negative strokes have significantly lower peak current but faster rate of current rise. Subsequent strokes may stress the system insulation more than typical or large first stroke in some cases, particularly those involving low footing resistances and tall structures with high inductance. The influence of subsequent strokes on backflashover has been recently analyzed for 69-kV and 138-kV lines in Silveira et al. (2012, 2013). The insulation stress produced by subsequent strokes of multiple-stroke flashes that are characterized by the largest peak current in the flash has been found by Visacro et al. (2012e) to be an additional threat, due to the combination of relatively high peak current and high steepness.

Both positive (Chapter 7) and negative (Chapter 3) strokes should be considered in the lightning performance simulations of overhead power lines. Positive strokes may also cause more thermal damage because of their significantly higher charge transfer.

10.4 Distribution Lines

For distribution lines, the CIGRÉ and IEEE reference documents are

- Joint CIRED-CIGRÉ WG C4.402, “Protection of MV and LV networks against lightning - part I: common topics”, CIGRÉ Technical Brochure, No. 287, February 2006 and “Protection of medium voltage and low voltage networks against lightning part 2: lightning protection of medium voltage networks”, No. 441, 2010.
- IEEE Std 1410-2010 (Revision of IEEE Std 1410-2004) “Guide for improving the lightning performance of electric power overhead distribution lines”, 2011.

The lightning performance of overhead distribution lines is generally represented by curves indicating how many lightning faults per year a distribution line may experience, as a function of line insulation level. These curves are used by power engineers for improving system reliability and power quality.

Lightning may cause flashovers on distribution lines from both direct strikes and nearby flashes. Direct lightning strikes to power distribution lines cause insulation flashover in the great majority of cases. However, experience and observations show that many of the lightning-related outages of low-insulation lines are due to lightning that hits the ground in proximity of the line. Moreover, due to the limited height of distribution lines of medium and low voltage distribution networks compared to that of the structures in their vicinity, indirect lightning strikes are more frequent than direct ones, and for this reason the literature on this subject (see the bibliography of IEEE Std 1410-2011) focuses mostly on such a type of lightning events.

The evaluation of the lightning performance of distribution systems is greatly affected by:

- model adopted to describe the lightning attachment;
- adopted distributions of the lightning current parameters;
- modeling of the lightning induction mechanism;
- statistical procedure.

The attachment models are similar to those adopted for transmission lines, taking into account the reduced height of the line, and usually relying on the calibration line experience of Eriksson (1987).

The distributions of the lightning current parameters should refer to flashes to ground. However, as already described in the previous chapters, the statistical distributions currently adopted have been mostly obtained from measurements at instrumented towers. In addition to the effects of the reflections at the top and at the base of the tower (Guerrieri et al., 1998; Bermudez et al., 2003; Rakov 2001; Visacro and Silveira, 2005a), tower or overhead transmission line measurements tend to attract lightning flashes with larger first return stroke currents. The influence of the tower on the lightning current distributions has been addressed in Sargent (1972), Mousa and Srivastava (1989), Rizk (1994a,b), Pettersson (1991), Sabot (1995), and Borghetti et al. (2003, 2004). Borghetti et al. (2003) illustrated the effects of the use of the unbiased distribution to ground. The return-stroke velocity is also a significant parameter in estimating lightning-induced voltages. The inclination of the channel has been analytically represented in Matsubara and Sekioka (2009). De Conti et al. (2010) and Silveira et al. (2010) analyzed the effects of the lightning current waveform, with particular reference to the concavity of the front and the presence of a second peak.

For the modeling of the induction mechanism and the statistical procedure applied to the case of an infinitely-long single-conductor overhead line with and without a grounded shielding (or neutral) conductor, IEEE Std 1410-2010 proposes the application of the statistical method proposed by Wagner and McCann (1942), and the use of the simplified formula by Rusck (1958b) that provides the estimation of the maximum amplitude of the lightning induced

voltages on the line. Such an equation takes into account the lightning current amplitude and the distance between the strike location and the line, assuming that the current waveshape is a step function and the ground is a perfectly conducting plane. IEEE Std 1410-2010 also presents the procedure that has been described in the CIGRÉ documents summarized in CIGRÉ Brochures 287 (2006) and 441 (2010). Such a procedure is based on the application of the Monte Carlo method and on an accurate evaluation of the induced voltages due to indirect lightning events (e.g., Nucci, 1995a,b; Nucci and Rachidi, 2003). The procedure allows one to take into account the effects of the current waveshape, with particular reference to the time to peak probability distribution, and also the effects of the finite conductivity of the soil, the specific characteristics of the line and its topology (Borghetti et al., 2007, 2009). Borghetti et al. (2007) presented a comparison between the two above-mentioned procedures.

The Influence of the attachment height on first-stroke induced voltages is addressed in Piantini and Janiszewski (1996, 2003) and Silveira and Visacro (2008).

Besides the stroke location relative to the line, also the current parameters have significant effects on the effectiveness of surge arresters and periodically grounded overhead or underbuilt shield wires as protection means against induced overvoltages, as shown in CIGRÉ Brochure 441 (2010) and analyzed, for example, in Yokoyama et al. (1985), Paolone et al. (2004), Piantini (2008), Silveira et al. (2011), and Piantini and Janiszewski (2013).

For distribution lines equipped with surge arresters and an overhead ground wire, the lightning performance is mainly affected by direct strikes. An analysis of this particular case has been recently presented in Michishita and Hongo (2012) and demonstrates the importance of the study of current parameters for subsequent strokes since with surge arresters at intervals of 100 or 200 m the flashover rate associated with subsequent strokes is higher than that associated with first strokes.

10.5 Surge Arresters and Other Surge Protection Devices

The recent CIGRÉ Brochure 440 (2010) is devoted to the use of line surge arresters (LSA). A LSA is composed of many varistors in series. The volume of metal oxide in a LSA establishes the energy characteristics that give them a limited ability to withstand temporary overvoltages. The active part of the surge arrester (varistors) must withstand power frequency voltage, temporary overvoltages (TOV), slow front overvoltages, and fast front transient overvoltages, as described in IEC 60099 standards. For LSA with an external series air gap (EGLA), the Metal Oxide Resistor must withstand TOV in the period after flashover on the series air gap caused by a lightning overvoltage, as described in IEC 60099-8.

There are differences regarding energy duty for the arrester, depending on whether or not the line is protected by overhead shield wires. When the line is efficiently protected with shield wires, the high peak current lightning strokes will terminate on the shield wires and the majority of the stroke charge will be diverted to ground. Only a small fraction of the total lightning current will circulate through the arresters into the surge impedance of the phase conductors. The shape of the line arrester current will be different from the shape of the injected current. Specifically, the line arrester current tail will be shorter and less energy will be injected into the arrester.

For unshielded lines or lines with shield or neutral conductors below the phases, a phase conductor can be hit directly by high peak current lightning strokes. This may cause a severe stress on the line surge arresters. The shape of the line arrester current will be similar to the shape of the injected current. The energy absorbed by the arrester will be essentially proportional to the charge transfer as the voltage drop across the arrester is nearly constant. This energy duty may be reasonable for negative flashes, but may exceed the energy duty of LSA for positive flashes that transfer considerably more charge than negative ones. The risk of failure of arresters due to energy breakdown is an important parameter to make a rational and economical design for an unshielded, LSA-protected line using either non-gapped (NGLA) or externally gapped (EGLA) arresters.

The influence of the lightning parameters, such as lightning current-wave duration, on the surge arrester minimum energy absorption capability is analyzed in Stenstrom and Lundquist (1999), Savic (2005), and Nakada (1997). The total lightning charge, including multiple strokes, is the primary parameter for the absorbed arrester energy.

However, due to the non-linear voltage-current characteristic of the arrester, the amplitude of the lightning current is also essential for the results. Therefore, the influence of the current amplitude was also investigated by varying the stroke current for a given total charge. The charge of the continuing current between strokes does not usually contribute to the absorbed arrester energy as this tends to find alternate paths to ground through the line terminations. In some cases, the ground impedance is important in the energy duty calculation, as illustrated in Stenstrom and Lundquist (1999) and Bassi and Janiszewski (2003).

10.6 Other Ground-Based Installations

In this section, we consider substations and similar installations, whose lightning protection systems usually consist of:

- lightning interception system, such as shield wires and vertical masts;
- overvoltage protection.

Direct strikes to equipment, live conductors, etc. must be avoided if there is no overvoltage protection within the limit distance of the strike point. Therefore, a shielding system is often needed. Basically, the design of this system should be based on similar consideration as for the shielding of overhead lines discussed above. The protection of the lines and substation should be coordinated. Lightning faults on towers tend to generate incoming voltages with steep fronts that may not be attenuated by corona effects before they arrive at the substation terminals. Direct strike lightning protection may also be desirable to prevent charge ablation damage on ground-based equipment such as SF_6 ductwork that otherwise has sufficient metal cross section area to carry typical station fault and lightning currents.

IEEE Guide Std. 998-1996 is devoted to the methods typically applied to minimize direct lightning strikes to equipment and buswork within substations (IEEE Std. 998, 1996).

According to CIGRÉ Brochure 172 (2000), when considering overvoltage protection (mainly location and selection of surge arresters), the following parameters are important:

- number of incoming and outgoing lines;
- probability of shielding failures and backflashovers for connected overhead lines;
- distance between substation and point of backflashover or shielding failure on the line;
- substation configuration and extension (GIS, open air, busbar system/layout, cable lengths etc.);
- acceptable risk of equipment failure.

Usually, the incidence of lightning flashes in the vicinity of the substation (one or a few line spans away), and the knowledge of their distribution, are decisive for the design and location of surge protective devices. Also, the various operating conditions for the substation (number of lines, various busbar arrangements etc.) must be considered. In many cases, the most critical situation is considered in order to obtain a conservative design of the protection system.

The relationship between current peak and front duration (defined as the ratio of the initial peak of current waveform and its maximum rate-of-rise, as opposed to “traditional” front durations considered in Chapter 3) has been taken into account in Okabe and Takami (2011) in estimating lightning failure rates at substations. Overvoltages caused by backflashovers at Gas Insulated Switchgears (GIS) are affected by the front duration of the lightning current, in contrast with overvoltages at transformers in UHV substations that are less influenced by the front duration.

Transformer fuse operation is known to occur due to core saturation from long duration lightning current waves or multiple-stroke flashes with continuing currents.

The topic of insulation characteristics of GIS elements for non-standard lightning impulses is addressed in CIGRÉ Brochure 360 (2008).

10.7 Lightning Parameters Needed for the Protection of Ordinary Structures

The IEC Standard 62305 series (2010) provides the principles to be followed in designing the lightning protection of ordinary structures, including their installations, services and contents, as well as persons. The scope of the IEC 62305 series is restricted to fixed common structures located on earth, such as buildings and industrial facilities. For these structures, the earth termination system is an essential part of the external lightning protection system. Because mobile systems, such as vehicles or boats and moveable systems such as tents or containers, do not have earth termination systems comparable to those of fixed structures, they are excluded from the IEC standard 62305 series. The lightning protection measures of such systems are given by special regulations. The lightning parameters needed for designing the protection, however, are almost the same in both cases.

According to IEC Standard 62305-1 (2010), the lightning current (i) is the primary source for physical damage, disturbances, and malfunctions and the lightning threat is associated with the following four current parameters:

- Peak current i_{max};
- Maximum current steepness $(di/dt)_{max}$;
- Charge $Q = \int i\, dt$;
- Specific energy $W/R = \int i^2\, dt$ (also referred to as the action integral).

All these parameters are discussed in detail in Chapters 3, 4, 7, and 8 for different lightning types and lightning processes.

The peak current is important for the design of the earth termination system. When the lightning current enters the earth, the current flowing through the earthing impedance produces a voltage drop. The peak current determines the maximum of this voltage drop. The peak current also governs the maximum force between metallic conductors when the lightning current flows through two or more paths.

Depending on the line routing and grounding inside the structures, large open loop networks are often formed by the connecting lines to the different electrical devices. The maximum current steepness is responsible for the maximum of the induced voltages in such open loops. Therefore, the maximum current steepness is also responsible for the separation distance needed between the air termination or down conductor system and electrical installations inside the structure to be protected.

The charge transfer Q is closely related to the melting effects at the attachment points of the lightning channel. The energy input at the arc root is roughly given by the anode/cathode voltage drop multiplied by the charge Q. The charge is also responsible for melting and heating effects of SPDs depending on whether it is a voltage-switching or a voltage-limiting type.

The specific energy W/R is responsible for the heating effects when the lightning current flows through a metallic conductor. The specific energy also governs the mechanical stresses when the lightning current or a fraction of it flows through metallic conductors.

These four lightning parameters are needed in separate statistics for the first stroke currents of the positive lightning, the first stroke currents of the negative lightning, and the subsequent stroke currents of the negative lightning. Parameters of negative and positive lightning are discussed in Chapter 3 and Chapter 7, respectively.

Further, the current risetime, the decay time, and the duration of the stroke current are needed because they determine the waveshape of the impulse current components of the return strokes. These parameters should also be given in separate statistics for the first stroke currents of the positive lightning, the first stroke currents of the negative lightning, and the subsequent stroke currents of the negative lightning.

The continuing currents transfer higher charges compared to the impulse currents of the return strokes. Therefore, the continuing currents are the main source for burning holes into metal plates used, for example, in tank structures. For the continuing currents, the needed parameters are the charge, the current amplitude and the duration of the current. For these parameters, the statistics should be given separately for the continuing currents of positive and negative lightning. Continuing currents of both polarities are discussed in Chapter 4.

The majority of the negative lightning flashes are multiple-stroke ones; that is, contain more than one return stroke. In contrast, the positive lightning often consists only of a first stroke which may be followed by a continuing current. Therefore, for the positive and the negative lightning separate statistics are needed for the number of strokes, the total transferred charge and the flash duration. The number of strokes per flash for negative lightning is discussed in Section 2.5 and for positive lightning in Section 7.3 of this document. The flash duration information for negative and positive lightning is found in Tables 2.2 and 7.3, respectively.

The striking distance (rolling sphere radius) is an additional parameter needed for the designing of lightning protection; it is computed (in meters) as $r = 10 \times I^{0.65}$, where I is the first-stroke peak current in kA (IEC Standard 62305-1, 2010; NFPA 780, 2011). Depending on the required effectiveness of protection, four levels of striking distance form the basis to establish dimensions of the air termination systems in IEC Standard 62305-3 (2010). Sensitive facilities should be protected using a Class-I LPS using a rolling sphere radius of 20 m.

The probability that lightning strikes a structure or occurs in its vicinity is needed in order to evaluate the risk according to IEC Standard 62305-2 (2010). The number of strikes depends on the annual ground flash density, which is discussed in Section 2.4 of this document. The ground strike point density can be estimated from the known local ground flash density by applying a correction factor of about 1.5 to 1.7 to it, in order to account for multiple channel terminations on ground within a flash (see Section 2.7). Bouquegneau et al. (2012) proposed a conservative value of 2 for this correction factor to be used in lightning risk calculations. The risk calculation further depends on the dimensions of the object, the surroundings, and the location (e.g., in a flat terrain or on a hill), and allows users to select the most appropriate class of protection.

10.8 Summary

This chapter has briefly summarized the main lightning parameters that are needed in the power engineering calculations, along with relevant references to standards and the recent literature on the subject. Additionally given is a brief overview of lightning parameters needed for designing the lightning protection of ordinary structures.

Conclusions

1. About 80% or more of negative cloud-to-ground lightning flashes are composed of two or more strokes. This percentage is appreciably higher than 55% previously estimated by Anderson and Eriksson (1980), based on less accurate records. The average number of strokes per flash is typically 3 to 5, with the geometric mean interstroke interval being about 60 ms. Roughly one-third to one-half of lightning flashes create two or more terminations on ground separated by up to several kilometers. When only one location per flash is recorded, the correction factor for measured values of ground flash density to account for multiple channel terminations on ground is about 1.5-1.7, which is considerably higher than 1.1 previosly estimated by Anderson and Eriksson (1980). First-stroke current peaks are typically a factor of 2 to 3 larger than subsequent-stroke current peaks. However, about one third of cloud-to-ground flashes contain at least one subsequent stroke with electric field peak, and, by theory, current peak, greater than the first-stroke peak. Larger-than-first subsequent strokes may represent an additional threat to power lines and other systems.

2. From direct current measurements, the median return-stroke peak current is about 30 kA for negative first strokes in Switzerland, Italy, South Africa, and Japan, and typically 10-15 kA for subsequent strokes in Switzerland and for triggered and upward (object-initiated) lightning. Corresponding values from measurements in Brazil are 45 kA and 18 kA. Additional measurements are needed. The "global" distributions of lightning peak currents for negative first strokes currently recommended by CIGRE and IEEE (see Fig. 3.2) are each based on a mix of direct current measurements and less accurate indirect measurements, some of which are of questionable quality. However, since the "global" distributions have been widely used in lightning protection studies and are not much different from that based on direct measurements only (median = 30 kA, $\sigma_{lg}I = 0.265$ for Berger et al.'s distribution), continued use of these "global" distributions for representing negative first strokes is recommended. For negative subsequent strokes, distribution 4 (median = 12 kA, $\sigma_{lg}I = 0.265$) in Fig. 3.1 should be used. For positive lightning strokes, distribution 2 (median = 35 kA, $\sigma_{lg}I = 0.544$) in Fig. 3.1 is recommended, although the data are very limited and may be influenced by the presence of strike object located on the mountain top. Direct lightning current measurements on instrumented towers should be continued. Currently, direct current measurements are performed on instrumented towers in Austria, Brazil, Canada, Germany, and Switzerland, although the overwhelming majority of flashes observed on those towers (except for Brazil) are of upward type.

3. Recommended lightning current waveshape parameters are still based on Berger et al.'s (1975) data (see Table 3.6), although the current rate-of-rise parameters estimated by Anderson and Eriksson (1980) from Berger et al.'s oscillograms are likely to be significantly underestimated, due to limitations of the instrumentation used by Berger et al. Triggered-lightning data for current rates of rise (see Table 3.7) can be applied to subsequent strokes in natural lightning. Relatively strong correlation is observed between the lightning peak current and impulse charge transfer and between the current rate-of-rise characteristics and current peak, and relatively weak or no correlation between the peak and risetime.

4. The field-to-current conversion procedure employed by the U.S. National Lightning Detection Network (NLDN) and other similar lightning locating systems has been calibrated only for negative subsequent strokes, with the median absolute error being 10 to 20%. Peak current estimation errors for negative first strokes and for positive lightning are presently unknown. Besides systems of NLDN type (such as the European systems participating in EUCLID or nationwide (JLDN) and regional systems in Japan), there are other lightning locating systems that are also reporting lightning peak currents inferred from measured fields, including LINET (mostly in Europe), USPLN (in the U.S., but similar systems operate in other countries), WTLN (in the U.S. and other countries), WWLLN (global), and GLD360 (global). Peak current estimation errors for the latter systems are presently unknown.

5. The percentage of positive flashes or strokes containing continuing currents (CC) is much higher than that of negative flashes or strokes. Positive strokes tend to be followed by longer and more intense CC than negative strokes. Positive strokes can produce both a high peak current and a long CC, a feature that has not been found in any negative stroke. CC in natural cloud-to-ground flashes exhibit a variety of waveshapes that may be grouped into six categories. The average number of M components per CC differs significantly from one polarity to the other: while an average of 5.5 M components per CC were observed for negative flashes, an average of 9.0 M

components per CC were observed for positive flashes. Strokes initiating long CC in negative flashes often have a smaller peak current and are preceded by high peak current return strokes and by relatively short interstroke intervals. Relatively-low-magnitude long continuing currents transfer considerably larger charges than high-amplitude return-stroke pulses.

6. The average propagation speed of a negative return stroke (first or subsequent) below the lower cloud boundary is typically between one-third and one-half of the speed of light. It appears that the return-stroke speed for first strokes is lower than that for subsequent strokes, although the difference is not very large (9.6×10^7 vs. 1.2×10^8 m/s). For positive return strokes, the speed is of the order of 10^8 m/s, although data are very limited. The negative return-stroke speed within the bottom 100 m or so (corresponding to current and field peaks) is expected to be between one-third and two-thirds of the speed of light. The negative return stroke speed usually decreases with height for both first and subsequent strokes. There exists some experimental evidence that the negative return stroke speed may vary non-monotonically along the lightning channel, initially increasing and then decreasing with increasing height. There are contradicting data regarding the variation of positive return stroke speed with height. The often assumed relationship between the return-stroke speed and peak current is generally not supported by experimental data.

7. The equivalent impedance of the lightning channel is needed for specifying the source in studies of either direct-strike or induced lightning effects. The estimates of this impedance from limited experimental data suggest values ranging from several hundred ohm to a few kiloohm. In many practical situations the impedance "seen" by lightning at the strike point is some tens of ohm or less, which allows one to assume infinitely large equivalent impedance of the lightning channel. In other words, lightning in these situations can be viewed as an ideal current source. In case of direct lightning strike to an overhead conductor of a power line with 400 ohm surge impedance (effective impedance 200 ohm, since 400 ohm is "seen" in either direction), the ideal current source approximation may still be suitable. Representation of lightning by a current source with internal impedance of 400 ohm, similar to that of an overhead wire, is probably not justified.

8. Although positive lightning discharges account for 10% or less of global cloud-to-ground lightning activity, there are several situations, including, for example, winter storms, that appear to be conducive to the more frequent occurrence of positive lightning. The highest directly measured lightning currents (near 300 kA) and the largest charge transfers (hundreds of coulombs or more) are thought to be associated with positive lightning. Positive flashes are usually composed of a single stroke, although up to four strokes per flash were observed. Subsequent strokes in positive flashes can occur both in a new and in the previously-formed channel. In spite of recent progress, our knowledge of the physics of positive lightning remains considerably poorer than that of negative lightning. Because of the absence of other direct current measurements for positive lightning return strokes, it is still recommended to use the peak current distribution based on the 26 events recorded by K. Berger (see Fig. 3.1 and Table 7.3), even though some of those 26 events are likely to be not of return-stroke type. However, caution is to be excersized, particularly for the waveshape parameters listed in Table 7.3, for which sample sizes are smaller than for peak currents. Clearly, additional measurements for positive lightning return strokes are needed to establish reliable distributions of peak current and other parameters for this type of lightning. Bipolar lightning discharges are usually initiated by upward leaders from tall objects. However, natural downward flashes also can be bipolar.

9. Tall objects (higher than 100 m or so) located on flat terrain and objects of moderate height (some tens of meters) located on mountain tops experience primarily upward lightning discharges that are initiated by upward-propagating leaders. Upward (object-initiated) lightning discharges always involve an initial stage that may or may not be followed by downward-leader/upward-return-stroke sequences. The initial-stage current often exhibits superimposed pulses whose peaks range from tens of amperes to several kiloamperes (occasionally a few tens of kiloamperes). Object initiated lightning events may occur relatively independent from downward lightning during non-convective season, and it has been observed that frequently several flashes were initiated from a tall object within a period of some hours. Diendorfer et al., (2006) reported 20 flashes to the Gaisberg Tower during one night in February 2005 (winter season) transferring a total charge of more than 1,800 coulomb to ground. At tall objects, the probability of occurrence of bipolar lightning is about the same as for positive lightning. Possible reasons for the observed differences from downward lightning and the high complexity of upward lightning are the multiple upward

branches of leaders initiated from the tower tip and the relatively short upward leader channels approaching charged regions above the object.

10. From the information available in the literature at the present time, there is no evidence of a dependence of negative cloud-to-ground lightning parameters on geographical location, except maybe for first and subsequent stroke peak currents, for which relatively insignificant (less than 50%), from the engineering point of view, variations may exist. It is important to note, however, that it cannot be ruled out that the observed differences in current measurements are due to reasons other than "geographical location", with limited sample size for some observations being of particular concern. Similarly, no reliable information on seasonal dependence is available. In summary, at the present time, the available information is not sufficient to confirm or refute a hypothesis on dependence of negative CG lightning parameters on geographical location or season. On the other hand, some local conditions may exist (for example, winter storms in Japan) that give rise to more frequent occurrence of unusual types of lightning, primarily of upward type, whose parameters may differ significantly from those of “ordinary” lightning. Further studies are necessary to clarify those conditions and their possible dependence on geographical location.

11. Lightning parameters needed for specific engineering applications are summarized. The emphasis is placed on the parameters that have an influence in the electric power engineering calculations, although lightning parameters needed for designing lightning protection of ordinary ground-based structures are also discussed.

Acknowledgement. This document was made possible via efforts of all members of the CIGRE WG C4.407, Lightning Parameters for Engineering Applications and volunteers. The Convenor would like to express special thanks to M.M.F. Saba and K. Cummins for preparing Chapter 4, G. Diendorfer for preparing Chapter 8, O. Pinto for preparing Chapter 9, and A. Borghetti, W. Chisholm, F. Heidler, C.A. Nucci, A. Piantini, and S. Visacro for preparing Chapter 10. Y. Li and B. Glushakow helped with editing the text and L.M. White helped with typing.

References

[1] Akopian A. A., V. P. Larionov, and A. S. Torosian. 1954. On impulse discharge voltages across high voltage insulation as related to the shape of the voltage wave. CIGRE Paper 411: 1-15.

[2] Alstad K., J. Huse, H. M. Paulsen, A. Schei, H. Wold, T. Henriksen, and A. Rein. 1979. Lightning impulse flashover criterion for overhead line insulation. Proc. of ISH, Milan, Italy, paper 42.19.

[3] Ametani A., Y. Kasai, J. Sawada, A. Mochizuki, and T. Yamada. 1994. Frequency-dependent impedance of vertical conductors and a multiconductor tower model. IEE Proc. Generat. Transm. Distrib. 141: 339-45.

[4] Ametani A. and T. Kawamura. 2005. A method of a lightning surge analysis recommended in Japan using EMTP. IEEE Trans. Power Del. 20: 867-75.

[5] Anderson, J. G. 1981. Lightning Performance of Transmission Lines. In Transmission Line Reference Book, Palo Alto, CA, USA: Electric Power Research Institute.

[6] Anderson, J. G. 1982. Lightning performance of transmission lines, in Transmission Line Reference Book – 345 kV and Above, 2nd ed., pp. 545-597, Electric Power Research Institute, Palo Alto, Calif.

[7] Anderson, R. B. and A. J. Eriksson. 1980. Lightning parameters for engineering application. Electra 69: 65-102.

[8] Anderson, R. B., A. J. Eriksson, H. Kroninger, D. V. Meal, and M. A Smith. 1984a. Lightning and thunderstorm parameters. In Lightning and Power Systems, London: IEE Conf. Publ. No. 236, 5 p.

[9] Andreotti, A., S. Falco, and L. Verolino. 2005. Some integrals involving Heidler's lightning return stroke current expression. Electr. Eng. 87: 121-8, doi: 10.1007/s00202-004-0240-8.

[10] Asakawa, A., K. Miyake, S. Yokoyama, T. Shindo, T. Yokota, and T Sakai. 1997. Two types of lightning discharges to a high stack on the coast of the Sea of Japan in Winter. IEEE Trans. Power Del. 12: 1222-31.

[11] Baba, Y. and M. Ishii. 2000. Numerical electromagnetic field analysis on lightning surge response of tower with shield wire. IEEE Trans. Power Del. 15: 1010-5.

[12] Baba, Y. and V. A. Rakov. 2005a. On the use of lumped sources in lightning return stroke models. J. Geophys. Res. 110: D03101, doi:10.1029/2004JD005202.

[13] Baba, Y. and V. A. Rakov. 2005b. On the mechanism of attenuation of current waves propagating along a vertical perfectly conducting wire above ground: Application to lightning. IEEE Trans. Electromagn. Compat. 47: 521-32.

[14] Baharudin, Z.A., N. A. Ahmad, J. S. Makela, M. Fernando, and V. Cooray. 2012. Negative cloud-to-ground lightning flashes in Malaysia. J. Atmos. Solar-Terrestr. Phys., submitted.

[15] Baldo, G., A. Pigini, and K. H. Weck. 1981. Nonstandard lightning impulse strength. In document CIGRÉ 33-81, Private communication.

[16] Ballarotti, M. G., C. Medeiros, M. M. F. Saba, W. Schulz, and O. Pinto Jr. 2012. Frequency distributions of some parameters of negative downward lightning flashes based on accurate-stroke-count studies. J. Geophys. Res. 117: D06112, doi:10.1029/2011JD017135.

[17] Ballarotti, M. G., M. M. F. Saba, and O. Pinto Jr. 2005. High-speed camera observations of negative ground flashes on a millisecond-scale. Geophys. Res. Lett. 32: L23802, doi:10.1029/2005GL023889.

[18] Bassi, W. and J. M. Janiszewski. 2003. Evaluation of currents and charges in low-voltage surge arresters

due to lightning strikes. IEEE Trans. Power Del. 18: 90–94.

[19] Bazelyan, E. M., N. L. Aleksandrov, R. B. Carpenter, and Yu. P. Raizer. 2006. Reverse discharges near grounded objects during the return stroke of branched lightning flashes. In Proc. of 28th Int. Conf. on Lightning Protection, Kanazawa, Japan, pp. 187-192.

[20] Bazelyan, E. M., B. N. Gorin, and V. I Levitov. 1978. Physical and Engineering Foundations of Lightning Protection, 223 p., Leningrad: Gidrometeoizdat.

[21] Beasley, W. 1985. Positive cloud-to-ground lightning observations. J. Geophys. Res. 90: 6131-8.

[22] Beasley, W. H., M. A. Uman, D. M. Jordan, and C. Ganesh. 1983. Positive cloud to ground lightning return strokes. J. Geophys. Res. 88: 8475-82.

[23] Beierl, O. 1992. Front shape parameters of negative subsequent strokes measured at the Peissenberg tower. In Proc. 21st Int. Conf. on Lightning Protection, Berlin, Germany, pp. 19-24.

[24] Berger, K. 1967. Novel observations on lightning discharges: Results of research on Mount San Salvatore. J. Franklin Inst. 283: 478-525.

[25] Berger, K. 1972. Methoden und Resultate der Blitzforschung auf dem Monte San Salvatore bei Lugano in den Jahren 1963-1971. Bull. Schweiz. Elektrotech 63: 1403-22.

[26] Berger, K. 1977. The Earth Flash. In Lightning, Vol. 1, Physics of Lightning, ed. R.H. Golde, pp. 119-90. New York: Academic Press.

[27] Berger, K. 1978. Blitzstrom-Parameter von Aufwärtsblitzen. Bull. Schweiz. Elektrotech. Bd. 69: 353-60.

[28] Berger, K., R. B. Anderson, and H. Kroninger. 1975. Parameters of lightning flashes. Electra 80: 23-37.

[29] Berger, K. and E. Garabagnati. 1984. Lightning current parameters. Results obtained in Switzerland and in Italy. URSI Conf., Florence, Italy.

[30] Berger, G., A. Hermant, and A. S. Labbe. 1996. Observations of natural lightning in France. In Proc. of the 23rd Int. Conf. on Lightning Protection, Florence, Italy, vol. 1, pp. 67-72.

[31] Berger, K. and E. Vogelsanger. 1965. Messungen und Resultate der Blitzforschung der Jahre 1955-1963 auf dem Monte San Salvatore. Bull. Schweiz. Elektrotech. Bd. 56: 2-22.

[32] Berger, K., and E. Vogelsanger. 1966. Photographische Blitzuntersuchungen der Jahre 1955-1965 auf dem Monte San Salvatore. Bull. Schweiz. Elektrotech. Bd. 57: 599-620.

[33] Berger, K., and E. Vogelsanger. 1969. New results of lightning observations. In Planetary Electrodynamics, eds. S.C. Coroniti and J. Hughes, pp. 489-510, New York: Gordon and Breach.

[34] Bermudez, J. L., M. Rubinstein, F. Rachidi, F. Heidler, and M. Paolone. 2003. Determination of reflection coefficients at the top and bottom of elevated strike objects struck by lightning. J. Geophys. Res. 108: 4413, doi: 10.1029/2002JD002973.

[35] Biagi, C. J., K. L. Cummins, K. E. Kehoe, and E. P. Krider. 2007. National Lightning Detection Network (NLDN) performance in southern Arizona, Texas, and Oklahoma in 2003–2004. J. Geophys. Res. 112: D05208, doi: 10.1029/2006JD007341.

[36] Borghetti, A., C. A. Nucci, and M. Paolone. 2003. Effect of tall instrumented towers on the statistical distributions of lightning current parameters and its influence on the power system lightning performance assessment. Eur. Trans. Electr. Power 13: 365-72.

[37] Borghetti, A., C. A. Nucci, and M. Paolone. 2004. Estimation of the statistical distributions of lightning current parameters at ground level from the data recorded by instrumented towers. IEEE Trans. Power Del. 19:

1400-9.

[38] Borghetti, A., C. A. Nucci, and M. Paolone. 2007. An improved procedure for the assessment of overhead line indirect lightning performance and its comparison with the IEEE Std. 1410 method. IEEE Trans. Power Del. 22: 684-92.

[39] Borghetti, A., C. A. Nucci, and M. Paolone. 2009. Indirect-Lightning Performance of Overhead Distribution Networks With Complex Topology. IEEE Trans. Power Del. 24: 2206-13.

[40] Bouquegneau, C., A. Kern, and A. Rousseau. 2012. Flash Density Applied to Lightning Protection Standards. In Proc. of 8th Int. Conf. on Grounding and Earthing & Lightning Physics and Effects GROUND & LPE, pp. 91-95, Bonito, Brazil.

[41] Boyle, J. S. and R. E. Orville. 1976. Return stroke velocity measurements in multistroke lightning flashes. J. Geophys. Res. 81: 4461-6, doi:10.1029/JC081i024p04461.

[42] Brook, M., N. Kitagawa, and E. J. Workman. 1962. Quantitative study of strokes and continuing currents in lightning discharges to ground. J. Geophys. Res. 67: 649-59.

[43] Brook, M., M. Nakano, P. Krehbiel, and T. Takeuti. 1982. The electrical structure of the Hokuriku winter thunderstorms. J. Geophys. Res. 87: 1207-15, doi:10.1029/JC087iC02p01207.

[44] Bruce, C. E. R. and R. H. Golde. 1941. The lightning discharge. J. Inst. Elec. Eng. 88: 487-520.

[45] Caldwell, R. and M. Darveniza. 1973. Experimental and Analytical Studies of the Effect of Non-Standard Waveshapes on the Impulse Strength of External Insulation. IEEE Trans. Power App. Syst. PAS-92: 1420-8.

[46] Campos, L. Z. S., M. M. F. Saba, O. Pinto Jr., and M. G. Ballarotti. 2007. Waveshapes of continuing currents and properties of M-components in natural negative cloud-to-ground lightning from high-speed video observations. Atmos. Res. 84: 302-10, doi:10.1016/j.atmosres.2006.09.002.

[47] Campos, L. Z. S., M. M. F. Saba, O. Pinto Jr., and M. G. Ballarotti. 2009. Waveshapes of continuing currents and properties of M-components in natural positive cloud-to-ground lightning. Atmos. Res. 91: 416-24, doi:10.1016/j.atmosres.2008.02.020.

[48] Carlson, A. B. 1996. Circuits. 838 pp., New York: John Wiley & Sons.

[49] Chisholm, W. A., J. P. Levine, and P. Chowdhuri. 2001. Lightning arc damage to optical fiber ground wires (OPGW): parameters and test methods. In 2001 Power Engineering Society Summer Meeting. Conference Proceedings, 1, 88-93, Vancouver, BC, Canada, 15-19 July 2001.

[50] Chowdhuri, P., J. G. Anderson, W. A. Chisholm, T. E. Field, M. Ishii, J. A. Martinez, M. B. Marz, J. McDaniel, T. R. McDermott, A. M. Mousa, T. Narita, D. K. Nichols, and T. A. Short. 2005. Parameters of lightning strokes: a review. IEEE Trans. Power Del. 20: 346-58.

[51] Chowdhuri, P., S. Li, and P. Yan. 2002. Rigorous analysis of back-flashover outages caused by direct lightning strokes to overhead power lines. IEE Proc. Gener. Transm. Distrib. 149: 58-65.

[52] CIGRE WG 33.01, Report 63. 1991. Guide to Procedures for Estimating the Lightning Performance of Transmission Lines, 61 p.

[53] CIGRE TF 33.01.02, Report 94. 1995. Lightning characteristics relevant for electrical engineering: Assesment of sensing, recording and mapping requirements in the light of present technological advancements, 37 p.

[54] CIGRE TF 33.01.03, Report 118. 1997. Lightning exposure of structures and interception efficiency of air terminals, 86 p.

[55] CIGRE TF 33.01.02, Report 172. 2000. Characterization of lightning for applications in electric power

systems, 35 p.

[56] CIGRE WG C4.2.02, Report 275. 2005. Methods for measuring the earth resistance of transmission towers equipped of earth wires,19 p

[57] CIGRE WG C4.402, Report 287. 2006. Protection of MV and LV networks against lightning - part 1: common topics, 53 p.

[58] CIGRE WG C4.302, Report 360. 2008. Insulation co-ordination related to internal insulation of gas insulated systems with SF6 and N2/SF6 gas mixtures under ac condition, 96 p.

[59] CIGRE WG C4.404, Report 376. 2009. Cloud-to-ground lightning parameters derived from lightning location systems: The effects of system performance, 117 p.

[60] CIGRE WG C4.301, Report 440. 2010. Use of surge arresters for lightning protection of transmission lines, 50 p.

[61] CIGRE WG C4.402, Report 441. 2010. Protection of medium voltage and low voltage networks against lightning part 2: lightning protection of medium voltage networks, 39 p.

[62] Cooray, V. and K. P. S. C. Jayaratne. 1994. Characteristics of lightning flashes observed in Sri Lanka in the tropics. J. Geophys. Res. 99: 21,051-6, doi:10.1029/94JD01519.

[63] Cooray, V. and on behalf of CIGRE Working Group C4.405. 2011. Lightning interception - A review of simulation procedures utilized to study the attachment of lightning flashes to grounded structures. Electra 257: 48–55.

[64] Cooray, V., and H. Pérez. 1994. Some features of lightning flashes observed in Sweden. J. Geophys. Res. 99: 10,683-10,688, doi:10.1029/93JD02366.

[65] Cooray, V. and V. Rakov. 2011. Engineering lightning return stroke models incorporating current reflection from ground and finitely conducting ground effects. IEEE Trans. Electromagn. Compat. 53: 773-81.

[66] Cooray, V., V. Rakov, and N. Theethayi. 2007. The lightning striking distance – Revisited. J. Electrost. 65: 296-306.

[67] Crawford D. 1998. Multiple-station measurements of triggered lightning electric and magnetic fields. Masters thesis, Univ. of Fla., Gainesville.

[68] Cummins, K. L. and M. J. Murphy. 2009. An overview of lightning locating systems: History, techniques, and data uses, with an in-depth look at the U.S. NLDN. IEEE Trans. Electromagn. Compat. 51: 499–518.

[69] Cummins, K.L., M. J. Murphy, E. A. Bardo, W. L. Hiscox, R. B. Pyle, and A. E. Pifer. 1998. A combined TOA/MDF technology upgrade of the U.S. National Lightning Detection Network. J. Geophys. Res. 103: 9035-44.

[70] Darveniza, M. and A. E. Vlastos. 1988. The generalized integration method for predicting impulse volt-time characteristics for non-standard wave shapes-a theoretical basis. IEEE Trans. Electr. Insul. 23: 373-81.

[71] De Conti A. R., E. Perez, E. Soto, S. Member, F. H. Silveira, S. Visacro, H. Torres, and S. Member. 2010. Calculation of Lightning-Induced Voltages on Overhead Distribution Lines Including Insulation Breakdown. IEEE Trans. Power Del. 25: 3078-84.

[72] De Conti, A. R., S. Visacro, A. Soares, and M. A. O. Schroeder. 2006. Revision, Extension, and Validation of Jordan's Formula to Calculate the Surge Impedance of Vertical Conductors. IEEE Trans. Electromagn. Compat. 48: 530-6.

[73] De Conti, A. and S. Visacro. 2007. Analytical representation of single- and double-peaked lightning current waveforms. IEEE Trans. Electromagn.Compat. 49: 448-51.

[74] Dellera, L., E. Garbagnati, G. Lo Piparo, P. Ronchetti, and G. Solbiati. 1985. Lightning protection of structures. Part IV: Lightning current parameters. L'ENERGIA ELETTRICA, 11: 447-61.

[75] Depasse, P. 1994. Statistics on artificially triggered lightning. J. Geophys. Res. 99: 18,515-22, doi:10.1029/94JD00912.

[76] Diendorfer, G. 2008. Some comments on the achievable accuracy of local ground flash density values. In Proc. of the Int. Conf. on Lightning Protection, Uppsala, Sweden, Paper 2-8, 6 p.

[77] Diendorfer, G., K. Cummins, V. A. Rakov, A. M. Hussein, F. Heidler, M. Mair, A. Nag, H. Pichler, W. Schulz, J. Jerauld, and W. Janischewskyj. 2008. LLS-estimated versus directly measured currents based on data from tower-initiated and rocket-triggered lightning. In Proc. of 29th Int. Conf. on Lightning Protection, Uppsala, Sweden, June 23-26, 2008, Paper 2-1, 9 p.

[78] Diendorfer, G., R. Kaltenboeck, M. Mair and H. Pichler. 2006. Characteristics of tower lightning flashes in a winter thunderstorm and related meteorological observations. In Proc. 19th Int. Lightning and Detect. Conf. (ILDC) and Lightning Meteorology Conf. (ILMC), Tucson, Arizona, USA.

[79] Diendorfer, G., M. Mair, and W. Schulz. 2002. Detailed brightness versus lightning current amplitude correlation of flashes to the Gaisberg tower. In Proc. 26th Int. Conf. Lightning Protection (ICLP), Krakow, Poland.

[80] Diendorfer, G., M. Mair, W. Schulz, and W. Hadrian. 2000. Lightning current measurements in Austria - Experimental setup and first results. In Proc. 25th Int. Conf. on Lightning Protection, Rhodes, Greece, pp. 44-47.

[81] Diendorfer, G., H. Pichler, and M. Mair. 2009. Some parameters of negative upward-initiated lightning to the Gaisberg tower (2000–2007). IEEE Trans. Electromagn. Compat. 51: 443-52.

[82] Diendorfer, G., W. Schulz, and V. A. Rakov. 1998. Lightning characteristics based on data from the Austrian Lightning Locating System. IEEE Trans. Electromagn. Compat. 40: 452-64, doi:10.1109/15.736206.

[83] Diendorfer, G. and M. A. Uman. 1990. An improved return stroke model with specified channel-base current. J. Geophys. Res. 95: 13,621-44, doi:10.1029/JD095iD09p13621.

[84] Diendorfer, G., M. Viehberger, M. Mair, W. Schulz. 2003. An attempt to determine currents in lightning channels branches from optical data of a high speed video system. In International Conference on Lightning and Static Electricity, Blackpool, United Kingdom, Feb. 2003.

[85] Diendorfer, G., H. Zhou and H. Pichler. 2011. Review of 10 years of lightning measurement at the Gaisberg Tower in Austria. In Proc. 3rd Int. Symposium on Winter Lightning (ISWL), Sapporo, Japan.

[86] Dulzon, A. A. and V. A. Rakov. 1991. A study of power line lightning performance. In Proc. 7th Int. Symp. on High Voltage Engineering, Dresden, Germany, pp. 57-60.

[87] Dwyer, J. R. 2005. A bolt out of the blue. Sci. Am. 292: 64-71.

[88] Eriksson, A. J. 1978. Lightning and tall structures. Trans. South African IEE 69: 2-16.

[89] Eriksson, A. J. 1982. The CSIR lightning research mast-data for 1972-1982. NEERI Internal Report No. EK/9/82, National Electrical Engineering Research Institute, Pretoria, South Africa.

[90] Eriksson, A. J. 1987. The incidence of lightning strikes to power lines. IEEE Trans. Power Del. 2: 859-870.

[91] Eriksson, A. J. and D. V. Meal. 1984. The incidence of direct lightning strikes to structures and overhead lines. In Lightning and Power Systems, London: IEE Conf. Publ. No. 236, pp. 67-71.

[92] Eriksson, A. J., C. L. Penman, and C. L. Meal. 1984. A review of five years' lightning research on an 11 kV

test-line. In Lightning and Power Systems, London: IEE Conf. Publ. No. 236, pp. 62-66.

[93] Ferraz, E. C., M. M. F. Saba, and O. Pinto Jr. 2009. First measurements of continuing current intensity in Brazil. X International Symposium on Lightning Protection, Curitiba, Brazil.

[94] Ferro, M. A., M. M. F. Saba, and O. Pinto Jr. 2009. Continuing current in multiple channel cloud-to-ground lightning. Atmos. Res. 91: 399–403, doi:10.1016/j.atmosres.2008.04.011.

[95] Ferro, M. A. S., M. M. F. Saba, and O. Pinto Jr. 2012. Time-intervals between negative lightning strokes and the creation of new ground terminations. Atmos. Res. 116: 130-3, doi:10.1016/j.atmosres.2012.03.010.

[96] Fisher, F. A., J. A. Plumer. 1977. Lightning protection of aircraft. NASA Ref. Publ., NASA-RP-1008.

[97] Fisher, R. J., G. H. Schnetzer, R. Thottappillil, V. A. Rakov, M. A. Uman, and J. D. Goldberg. 1993. Parameters of triggered-lightning flashes in Florida and Alabama. J. Geophys. Res. 98: 22,887-902, doi:10.1029/93JD02293.

[98] Flache, D., V. A. Rakov, F. Heidler, W. Zischank, and R. Thottappillil. 2008. Initial-stage pulses in upward lightning: Leader/return stroke versus Mcomponent mode of charge transfer to ground. Geophys. Res. Lett. 35: L13812, doi:10.1029/2008GL034148.

[99] Fleenor, S. A., C. J. Biagi, K. L. Cummins, E. P. Krider, and X. M. Shao. 2009. Characteristics of cloud-to-ground lightning in warm-season thunderstorms in the Central Great Plains. Atmos. Res. 91: 333-52, doi:10.1016/j.atmosres.2008.08.011.

[100] Fuchs, F., E. U. Landers, R. Schmid, and J. Wiesinger. 1998. Lightning current and magnetic field parameters caused by lightning strikes to tall structures relating to interference of electronic systems. IEEE Trans. Electromagn. Compat. 40: 444-51.

[101] Fuquay, D. M. 1982. Positive cloud-to-ground lightning in summer thunderstorms. J. Geophys. Res. 87: 7131-40, doi:10.1029/JC087iC09p07131.

[102] Gamerota, W.R., J. O. Elismé, M. A. Uman, and V. A. Rakov. 2012. Current Waveforms for Lightning Simulation. IEEE Trans. Electromagn. Compat. 54: 880-8.

[103] Garbagnati, E., E. Giudice, and G. B. Lo Piparo. 1978. Measurement of lightning currents in Italy - results of a statistical evaluation. ETZ-A 99: 664-8.

[104] Garbagnati, E., E. Giudice, G. B. Lo Piparo, and U. Magagnoli. 1974. Survey of the characteristics of lightning stroke currents in Italy - results obtained in the years from 1970 to 1973. ENEL Rep. R5/63-27.

[105] Garbagnati, E., E. Giudice, G. B. Lo Piparo, and U. Magagnoli. 1975. Rilievi delle caratteristiche dei fulmini in Italia. Risultati ottenuti negli anni 1970-1973. L'Elettrotecnica 62: 237-49.

[106] Garbagnati, E. and G. B. Lo Piparo. 1970. Stazione sperimentale per il rilievo delle caratteristiche dei fulmini. L'Elettrotecnica 57: 288-97.

[107] Garbagnati, E. and G. B. Lo Piparo. 1973. Nuova stazione automatica per il rilievo delle caratteristiche dei fulmini. L'Energia Elettrica 6: 375-83.

[108] Garbagnati, E., and G. B. Lo Piparo. 1982a. Results of 10 years investigation in Italy. In Proc. Int. Aerospace Conf. on Lightning and Static Electricity, Oxford, England, paper A1, 12 p.

[109] Garbagnati, E., and G. B. Lo Piparo. 1982b. Parameter von Blitzstromen. ETZ-A 103: 61-5.

[110] Garbagnati, E., F. Marinoni, and G. B. Lo Piparo. 1981. Parameters of lightning currents. Interpretation of the results obtained in Italy. In Proc. 16 Int. Conf. on Lightning Protection, Szeged, Hungary.

[111] Geldenhys, H. T., A. J. Eriksson, and G. W. Bourn. 1989. Fifteen years of data of lightning current

measurements on 60 m mast. Trans. South African IEE 80: 130-58.

[112] Golde, R. H. 1945. The Frequency of Occurrence and the Distribution of Lightning Flashes to Transmission Lines. Trans. Am. Inst. Electr. Eng. 64: 902-10.

[113] Gorin, B. N. 1985. Mathematical modeling of the lightning return stroke. Elektrichestvo, 4: 10-16.

[114] Gorin, B. N., V. I. Levitov, and A. V. Shkilev. 1977. Lightning strikes to the Ostankino tower. Elektrichestvo 8: 19-23.

[115] Gorin, B.N., G. S. Sakharova, V. V. Tikhomirov, and A. V. Shkilev. 1975. Results of studies of lightning strikes to the Ostankino TV tower. Trudy ENIN 43: 63-77.

[116] Gorin, B. N. and A. V. Shkilev. 1984. Measurements of lightning currents at the Ostankino tower. Elektrichestvo 8: 64-5.

[117] Goto, Y. and Narita, K. 1995. Electrical characteristics of winter lightning. J. Atmos. Terr. Phys. 57: 449-59.

[118] Grcev, L. and F. Rachidi. 2004. On Tower Impedances for Transient Analysis. IEEE Trans. Power Del. 19: 1238-44.

[119] Guerrieri, S., N. C., F. Rachidi, and M. Rubinstein. 1998. On the Influence of Elevated Strike Objects on Directly Measured and Indirectly Estimated Lightning Currents. IEEE Trans. Power Del. 13: 1543-55.

[120] Gutierrez, J. A. R., P. Moreno, J. L. Naredo, J. L. Bermudez, M. Paolone, C. A. Nucci, and F. Rachidi. 2004. Nonuniform Transmission Tower Model for Lightning Transient Studies. IEEE Trans. Power Del. 19: 490-6.

[121] Hagenguth, J.H. and J. G. Anderson. 1952. Lightning to the Empire State Building. AIEE Trans. 71 (Pt. 3): 641-9.

[122] Heidler F. 1985a. Analytische Blitzstromfunktion zur LEMP- Berechnung, (in German). paper 1.9, pp. 63-66, Munich, September 16-20.

[123] Heidler, F. 1985b. Traveling current source model for LEMP calculation. In Proc. 6th Int. Zurich Symp. on Electromagnetic Compatibility, Zurich, Switzerland, pp. 157-162.

[124] Heidler, F. and J. Cvetic. 2002. A class of analytical functions to study the lightning effects associated with the current front. Eur. Trans. Elect. Power 12: 141–50.

[125] Heidler, F., F. Drumm, and C. Hopf. 1998. Electric fields of positive earth flashes in near thunderstorms. Proc. 24th Int. Conf. on Lightning Protection, Birmingham, U. K., Staffordshire University, pp. 42–47.

[126] Heidler, F. and C. Hopf. 1998. Measurement results of the electric fields in cloud-to-ground lightning in nearby Munich, Germany. IEEE Trans. Electromagn. Compat. 40: 436-43.

[127] Heidler, F., W. Zischank, and J. Wiesinger. 2000. Statistics of lightning current parameters and related nearby magnetic fields measured at the Peissenberg tower, Proc. 25th Int. Conf. on Lightning Protection, Rhodes, Greece, University of Patras, 78–83.

[128] Hermant, A. 2000.Traqueur d'Orages, Nathan/HER, Paris, France.

[129] Hileman, A.R. 1999. Insulation coordination for power systems, 767 p., New York: Marcel Dekker.

[130] Hubert, P., and G. Mouget. 1981. Return stroke velocity measurements in two triggered lightning flashes. J. Geophys. Res. 86: 5253-61.

[131] Hussein, A. M., W. Janischewskyj, J. -S. Chang, V. Shostak, W. A. Chisholm, P. Dzurevych, and Z. -I. Kawasaki. 1995. Simultaneous measurement of lightning parameters for strokes to the Toronto Canadian National Tower. J. Geophys. Res. 100: 8853-61.

[132] Idone, V. P. and R. E. Orville. 1982. Lightning return stroke velocities in the Thunderstorm Research International Program (TRIP). J. Geophys. Res. 87: 4903-15.

[133] Idone, V. P., R. E. Orville, P. Hubert, L. Barret, and A. Eybert-Berard. 1984. Correlated observations of three triggered lightning flashes. J. Geophys. Res. 89: 1385-94.

[134] Idone, V. P., R. E. Orville, D. M. Mach, and W. D. Rust. 1987. The propagation speed of a positive lightning return stroke. Geophys. Res. Lett. 14: 1150-3.

[135] IEC Standard 62305-1. 2010. Protection against lightning - Part 1: General principles, Edition 2.0.

[136] IEC Standard 62305-2. 2010 Protection against lightning - Part 2: Risk management, Edition 2.0.

[137] IEC Standard 62305-3. 2010. Protection against lightning - Part 3: Physical damage to structures and life hazard, Edition 2.0.

[138] IEC Standard 62305-4. 2010. Protection against lightning - Part 4: Electrical and electronic systems within structures, Edition 2.0.

[139] IEEE Standard 998-1996. 1996. IEEE Guide for Direct Lightning Stroke Shielding of Substations.

[140] IEEE Standard 1243-1997. 1997. IEEE Guide for Improving the Lightning Performance of Transmission Lines.

[141] IEEE Standard 1410-2010. 2010. IEEE Guide for Improving the Lightning Performance of Electric Power Overhead Distribution Lines.

[142] IEEE Working Group on Estimating the Lightning Performance of Transmission Lines. 1985. A Simplified Method for Estimating Lightning Performance of Transmission Lines. IEEE Trans. Power App. Syst. PAS-104: 918–32.

[143] IEEE Working Group on Estimating the Lightning Performance of Transmission Lines. 1993. Estimating lightning performance of transmission lines. II. Updates to analytical models. IEEE Trans. Power Del. 8:1254–67.

[144] Ishii, M., F. Fujii, M. Matsui, K. Shinjo, M. Saito, J. -I. Hojo, and N. Itamoto. 2005. LEMP from lightning discharges observed by JLDN. IEEJ Trans. PE 125: 765-70.

[145] Ishii, M. and D. Natsuno. 2011. Statistics of recent lightning current observations at wind turbines in Japan – preliminary report. CIGRE WG C4.407 meeting, June 17, 2011, Sapporo, Japan.

[146] Ishii, M., M. Saito, F. Fujii, M. Matsui, and D.Natsuno. 2011. Frequency of upward lightning from tall structures in winter in Japan. In Proc. 7th Asia-Pacific International Conference on Lightning. pp. 933-936, doi: 10.1109/APL.2011.6111049.

[147] Ishii, M., K. Shimizu, J. Hojo, and K. Shinjo. 1998. Termination of multiple-stroke flashes observed by electromagnetic field. Proc. 24th Int. Conf. on Lightning Protection, Birmingham, U. K., Staffordshire University, pp. 11–16.

[148] Janischewskyj, W., A. M. Hussein, V. Shostak, I. Rusan, J. -X. Li, and J. -S. Chang. 1997. Statistics of lightning strikes to the Toronto Canadian National Tower (1978-1995). IEEE Trans. Power Del. 12: 1210-21.

[149] Javor, V. and P. D. Rancic. 2011. A channel-base current function for lightning return-stroke modeling. IEEE Trans. Electromagn. Compat. 53: 245–49, doi: 10.1109/TEMC.2010.2066281.

[150] Jayakumar, V., V. A. Rakov, M. Miki, M. A. Uman, G. H. Schnetzer, and K. J. Rambo. 2006. Estimation of input energy in rocket-triggered lightning. Geophys. Res. Lett. 33: L05702, doi:10.1029/2005GL025141.

[151] Jerauld, J., V. A. Rakov, M. A. Uman, K. J. Rambo, D. M. Jordan, K. L. Cummins, and J. A. Cramer. 2005. An evaluation of the performance of the U.S. National Lightning Detection Network in Florida using rocket-triggered lightning. J. Geophys. Res. 110: D19106.

[152] Jerauld, J. E., M. A. Uman, V. A. Rakov, K. J. Rambo, D. M. Jordan, and G. H. Schnetzer. 2009. Measured electric and magnetic fields from an unusual cloud-to-ground lightning flash containing two positive strokes followed by four negative strokes, J. Geophys. Res. 114: D19115, doi:10.1029/2008JD011660.

[153] Jones, A. R. 1954. Evaluation of the Integration Method for Analysis of Nonstandard Surge Voltages. Trans. Am. Inst. Electr. Eng., Part 3. 73: 984–90.

[154] Kind, D. 1958. Die Aufbauflache bei Stossspannungsbeanspruchung technischer Elektrodenanordnungen in Luft. ETZ-A 79: 65–9.

[155] Kitagawa, N., M. Brook, and E. J. Workman. 1962. Continuing current in cloud-to-ground lightning discharges. J. Geophys. Res. 67: 637–47.

[156] Kitterman, C. G. 1980. Characteristics of lightning from frontal system thunderstorms. J. Geophys. Res. 85: 5503–5.

[157] Kong, X., X. Qie, and Y. Zhao. 2008. Characteristics of downward leader in a positive cloud-to-ground lightning flash observed by high-speed video camera and electric field changes. Geophys. Res. Lett. 35: L05816, doi:10.1029/2007GL032764.

[158] Kong, X. Z., X. S. Qie, Y. Zhao, and T. Zhang. 2009. Characteristics of negative lightning flashes presenting multiple-ground terminations on a millisecond-scale. Atmos. Res. 91: 381-6.

[159] Krider, E. P., C. J. Biagi, K. L. Cummins, S. Fleenor, and K.E. Kehoe. 2007. Measurements of Lightning Parameters Using Video and NLDN Data. 13th Intl. Conf. on Atmospheric Electricity, Beijing, China.

[160] Krider, E. P. and G. J. Radda. 1975. Radiation field wave forms produced by lightning stepped leaders. J. Geophys. Res. 80: 2,635–57, doi:10.1029/JC080i018p02653.

[161] Lacerda, M., O. Pinto, I. R. C. A. Pinto, J. H. Diniz, and A. M. Carvalho. 1999. Analysis of negative downward lightning current curves from 1985 to 1994 at Morro do Cachimbo research station (Brazil). In Proc. 11th Int. Conf. on Atmospheric Electricity, Guntersville, Alabama, pp. 42-45.

[162] Leteinturier, C., J. H. Hamelin, and A. Eybert-Berard. 1991. Submicrosecond characteristics of lightning return-stroke currents. IEEE Trans. Electromagn. Compat. 33: 351-7.

[163] Livingston, J. M. and E. P. Krider. 1978. Electric fields produced by Florida thunderstorms. J. Geophys. Res. 83: 385-401.

[164] Lopez, R. E., R. L. Holle, R. Ortiz, and A. I. Watson. 1992. Detection efficiency losses of networks of direction finders due to flash signal attenuation with range. In Proc. 15th Int. Aerospace and Ground Conf. on Lightning and Static Electricity, Atlantic City, New Jersey, pp. 75/1-18.

[165] Lundholm, R. 1957. Induced overvoltage-surges on transmission lines and their bearing on the lightning performance at medium voltage networks. Trans. Chalmers Univ. Technol. No. 120, 117 p.

[166] MacGorman, D. R., M. W. Maier, and W. D Rust. 1984. Lightning strike density for the contiguous United States from thunderstorm duration records, NUREG/CR-3759, Office of Nuclear Regulatory Research, U.S. Nuclear Regulatory Commission, Washington, D.C., 44 p.

[167] Mach, D. M. and W. D. Rust. 1993. Two-dimensional velocity, optical risetime, and peak current estimates for natural positive lightning return strokes. J. Geophys. Res. 98: 2635-8.

[168] Mach, D. M. and W. D. Rust. 1989. Photoelectric return-stroke velocity and peak current estimates in natural and triggered lightning. J. Geophys. Res. 94: 13,237-47.

[169] Mallick, S., V.A. Rakov, J.D. Hill, W.R. Gamerota, M.A. Uman, S. Heckman, C.D. Sloop, and C. Liu. 2013a. Calibration of the WTLN against rocket-triggered lightning data. SIPDA 2013, Belo Horizonte, Brazil.

[170] Mallick, S., V.A. Rakov, D. Tsalikis, A. Nag, C. Biagi, D. Hill, D.M. Jordan, M.A. Uman, and J.A. Cramer. 2013b. On Remote Measurements of Lightning Peak Currents, Atmos. Res., in press, http://dx.doi.org/10.1016/j.atmosres.2012.08.008.

[171] Martinez, J. A. and F. Castro-Aranda. 2005. Lightning Performance Analysis of Overhead Transmission Lines Using the EMTP. IEEE Trans. Power Del. 20: 2200–10.

[172] Mata C. T. and A. G. Mata. 2012. Summary of 2011 Direct and Nearby Lightning Strikes to Launch Complex 39B, Kennedy Space Center, Florida. ICLP 2012, Vienna, Austria, 9 p.

[173] Mata C. T., A. G. Mata, V. A. Rakov, A. Nag, and J. Saul. 2012. Evaluation of the Performance Characteristics of CGLSS II and U.S. NLDN Using Ground-Truth Data From Launch Complex 39B, Kennedy Space Center, Florida. ICLP 2012, Vienna, Austria, 10 p.

[174] Mata, C. T. and V. A. Rakov. 2008. Evaluation of Lightning Incidence to Elements of a Complex Structure: A Monte Carlo Approach. In Proc. of the 3rd International Conference on Lightning Physics and Effects (LPE) and GROUND' 2008, Florianopolis, Brazil, November 16-20, 2008, pp. 351-354.

[175] Matsubara, I. and S. Sekioka. 2009. Analytical Formulas for Induced Surges on a Long Overhead Line Caused by Lightning with an Arbitrary Channel Inclination. IEEE Trans. Electromagn. Compat. 51: 733–40.

[176] Matsumoto Y., 0. Sakuma, K. Shinjo, M. Saiki, T. Wakai, T. Sakai, H. Nagasaka, H. Motoyama, and M. Ishii. 1996. Measurement of Lightning Surges on Test Transmission Line Equipped with Arresters Struck by Natural and Triggered Lightning. IEEE Trans. Power Del. 11: 996–1002.

[177] Meliopoulos, A. P. S., W. Adams, and R. Casey. 1997. An integrated backflashover model for insulation coordination of overhead transmission lines. Int. J. Electr. Power Energy Syst. 19: 229–34.

[178] McCann, D.G. 1944. The measurement of lightning currents in direct strokes. Trans. AIEE 63: 1157-64.

[179] McEachron, K. B. 1939. Lightning to the Empire State Building. J. Franklin Inst. 227: 149–217.

[180] McEachron, K. B. 1941. Lightning to the Empire State Building. American Institute of Electrical Engineers, Transactions of the, 60: 885-90, doi: 10.1109/T-AIEE.1941.5058410.

[181] Medeiros, C. and M. M. F. Saba. 2012. Presence of continuing currents in negative cloud-to-ground flashes. International Conf. on Lightning Detection, Denver, Colorado.

[182] Melander, B. G. 1984. Effects of tower characteristics on lightning arc measurements. In Proc. 1984 Int. Conf. on Lightning and Static Electricity, Orlando, FL, 1984, pp. 34/1–34/12.

[183] Michishita, K. and Y. Hongo. 2012. Flashover Rate of 6.6-kV Distribution Line Due to Direct Negative Lightning Return Strokes. IEEE Trans. Power Del. 27: 2203–10.

[184] Miki, M. 2006. Observation of current and leader development characteristics of winter lightning, paper presented at 28th International Conference on Lightning Protection, Inst. of Electr. Installation Eng. of Jpn., Kanazawa, Japan.

[185] Miki, M., T. Miki, A. Wada, A. Asakawa, Y. Asuka, N. Honjo. 2010. Observation of lightning flashes to wind turbines. In proceedings of 30th International Conference on Lightning Protection (ICLP), Cagliari, Italy.

[186] Miki, M., T. Miki, A. Wada, A. Asakawa, T. Shindo, S. Yokoyama. 2011. Characteristics of upward leaders of winter lightning in the coastal area of the Sea of Japan, paper presented at 3rd International Symposium on

Winter Lightning, Univ. of Tokyo, Sapporo, Japan.

[187] Miki, M., V. A. Rakov, T. Shindo, G. Diendorfer, M. Mair, F. Heidler, W. Zischank, M. A. Uman, R. Thottappillil, and D. Wang. 2005. Initial stage in lightning initiated from tall objects and in rocket-triggered lightning. J. Geophys. Res. 110: D02109, doi:10.1029/2003JD004474.

[188] Miki, M., A. Wada, and A. Asakawa. 2004. Observation of upward lightning in winter at the coast of Japan sea with a high-speed video camera. Proc. 27th Int. Conf. on Lightning Protection, Avignon, France, 63-67.

[189] Mikropoulos, P. N. and T. E. Tsovilis. 2010. Lightning attachment models and maximum shielding failure current of overhead transmission lines: implications in insulation coordination of substations. IET Gener. Transm. Dis. 4: 1299-1313.

[190] Military Standard. 1983. Lightning qualification test techniques for aerospace vehicles and hardware. MIL-STD-1757A.

[191] Miyake, K., T. Suzuki, and K. Shinjou. 1992. Characteristics of winter lightning current on Japan Sea coast. IEEE Trans. Power Del. 7: 1450-6.

[192] Moini, R., B. Kordi, G. Z. Rafi, and V. A. Rakov. 2000. A new lightning return stroke model based on antenna theory. J. Geophys. Res. 105: 29,693-702.

[193] Montandon, E. 1992. Lightning positioning and lightning parameter determination experiences and results of the Swiss PTT research project. In Proc. 21st Int. Conf. on Lightning Protection, Berlin, Germany, pp. 307-312.

[194] Montandon, E. 1995. Messung und Ortung Von Blitzeinschlagen und Ihren Auswirkungen am Fernmeldeturm "St. Chrischona" Bei Basel der Schweizerischen Telecom PTT. Elektrotechnik und Informationstechnik 112: 283-9.

[195] Motoyama, H. 1996. Experimental study and analysis of breakdown characteristics of long air gaps with short tail lightning impulse. IEEE Trans. Power Del. 11: 972-9.

[196] Motoyama, H. and H. Matsubara. 2000. Analytical and experimental study on surge response of transmission tower. IEEE Trans. Power Del. 15: 812-9.

[197] Motoyama, H., K. Shinjo, Y. Matsumoto, and N. Itamoto. 1998. Observation and analysis of multiphase back flashover on the Okushishiku test transmission line caused by winter lightning. IEEE Trans. Power Del. 13: 1391-8.

[198] Mousa, A. M. and K. D. Srivastava. 1989.The implications of the electrogeometric model regarding effect of height of structure on the median amplitude of collected lightning strokes. IEEE Trans. Power Del. 4: 1450-60.

[199] Nag, A., S. Mallick, V. A. Rakov, J. S. Howard, C. J. Biagi, J. D. Hill, M. A. Uman, D. M. Jordan, K. J. Rambo, J. E. Jerauld, B. A. DeCarlo, K. L. Cummins, and J. A. Cramer. 2011. Evaluation of NLDN Performance Characteristics Using Rocket-Triggered Lightning Data Acquired in 2004–2009, J. Geophys. Res. 116: D02123, doi:10.1029/2010JD014929.

[200] Nag, A. and V. A. Rakov. 2012. Positive Lightning: An Overview, New Observations, and Inferences. J. Geophys. Res. 117: D08109, doi:10.1029/2012JD017545.

[201] Nag, A., V. A. Rakov, W. Schulz, M. M. F. Saba, R. Thottappillil, C. J. Biagi, A. O. Filho, A. Kafri, N. Theethayi, and T. Gotschl. 2008. First versus subsequent return-stroke current and field peaks in engative cloud-to-ground lightning discharges. J. Geophys. Res. 113: D19112.

[202] Nakada, K., T. Yokota, S. Yokoyama, A. Asakawa, M. Nakamura, H. Taniguchi, and A. Hashimoto. 1997. Energy absorption of surge arresters on power distribution lines due to direct lightning strokes-effects of an

overhead ground wire and installation position of surge arresters. IEEE Trans. Power Del. 12: 1779-85.

[203] Nakano, M., M. Nagatani, H. Nakada, T. Takeuti, and Z. Kawasaki. 1987. Measurements of the velocity change of a lightning return stroke with height. Res. Lett. Atmos. Electr. 7: 25-8.

[204] Nakano, M., M. Nagatani, H. Nakada, T. Takeuti, and Z Kawasaki. 1988. Measurements of the velocity change of a lightning return stroke with height. In Proc. 1988 Int. Aerospace and Ground Conf. on Lightning and Static Electricity, Oklahoma City, Oklahoma, pp. 84-86.

[205] Narita, T., T. Yamada, A. Mochizuki, E. Zaima, and M. Ishii. 2000. Observation of current waveshapes of lightning strokes on transmission towers. IEEE Trans. Power Del. 15: 429-35.

[206] NFPA 780 (National Fire Protection Association). 2011. Standard for the installation of lightning protection systems. Available from NFPA, 1 Batterymarch Park, PO Box 9101, Quincy, Massachusetts 02169-7471, USA.

[207] Nucci, C. A. 1995a. Lightning-induced voltages on overhead power lines. Part I: Return-stroke current models with specified channel-base current for the evaluation of the return-stroke electromagnetic fields. Electra 161: 74-102.

[208] Nucci, C. A. 1995b. Lightning-induced voltages on overhead power lines. Part II: Coupling models for the evaluation of the induced voltages. Electra 162: 121-45.

[209] Nucci, C. A. 2009. A survey on CIGRÉ and IEEE procedures for the estimation of the lightning performance of overhead transmission and distribution lines. In X International Symposium on Lightning Protection, pp. 151–165.

[210] Nucci, C. A., G. Diendorfer, M. A. Uman, F. Rachidi, M. Ianoz, and C. Mazzetti. 1990. Lightning return stroke current models with specified channel-base current: a review and comparison. J. Geophys. Res. 95: 20,395-408.

[211] Nucci, C. A. and F. Rachidi. 2003. Interaction of electromagnetic fields with electrical networks generated by lightning. In The Lightning Flash: Physical and Engineering Aspects, V. Cooray, Ed. IEE - Power and Energy Series 34, pp. 425–478.

[212] Nucci, C. A., F. Rachidi, M. Ianoz, C. Mazzetti. 1993. Lightning-Induced Voltages on Overhead Lines. IEEE Trans. Electromagn. Compat. 35: 75-86.

[213] Okabe, S. and J. Takami. 2011. Occurrence probability of lightning failure rates at substations in consideration of lightning stroke current waveforms. IEEE Trans. Dielectr. Electr. Insul. 18: 221-31.

[214] Oliveira Filho, A., W. Schulz, M. M. F. Saba, O. Pinto Jr. and M. G. Ballarotti. 2007. The relationship between first and subsequent stroke electric field peak in negative cloud-to-ground lightning. 13th Intl. Conf. on Atmospheric Electricity, Beijing, China.

[215] Olsen, R. C., D. M. Jordan, V. A. Rakov, M. A. Uman, and N. Grimes. 2004. Observed two-dimensional return stroke propagation speeds in the bottom 170 m of a rocket-triggered lightning channel. Geophys. Res. Lett. 31: L16107, doi: 10.1029/2004GL020187.

[216] Orville, R. E., G. R. Huffines, W. R. Burrows, and K. L. Cummins. 2011. The North American Lightning Detection Network (NALDN) – Analysis of flash data: 2001-2009. Mon. Wea. Rev. 139: 1305-22.

[217] Orville, R. E., G. R. Huffines, W. R. Burrows, R. L. Holle, and K. L. Cummins. 2002. The North American Lightning Detection Network (NALDN) - First Results: 1998-2000. Mon. Wea. Rev. 130: 2098–109.

[218] Paolone, M., C. A. Nucci, E. Petrache, and F. Rachidi. 2004. Mitigation of Lightning-Induced Overvoltages in Medium Voltage Distribution Lines by Means of Periodical Grounding of Shielding Wires and of Surge Arresters: Modeling and Experimental Validation. IEEE Trans. Power Del. 19: 423-31.

[219] Pettersson, P. 1991. A unified probabilistic theory of the incidence of direct and indirect lightning strikes. IEEE Trans. Power Del. 6: 1301-10.

[220] Piantini, A. 2008. Lightning protection of overhead power distribution lines. In Proc. of 29th Int. Conf. on Lightning Protection (ICLP), Uppsala, Sweden, 29 p.

[221] Piantini, A. and J. M. Janiszewski. 1996. The influence of the upward leader on lightning induced voltages. In Proc. 23rd Int. Conf. Lightning Protection (ICLP), Florence, Italy.

[222] Piantini, A. and J. M. Janiszewski. 2003. The Extended Rusck Model for calculating lightning induced voltages on overhead lines. In Proc. VII Int. Symp. Lightning Protection (SIPDA), Curitiba, Brazil.

[223] Piantini, A. and J. M. Janiszewski. 2009. Lightning-Induced Voltages on Overhead Lines - Application of the Extended Rusck Model. IEEE Trans. on Electromagn. Compat. 51: 548-558.

[224] Piantini A. and J. M. Janiszewski. 2013. The use of shield wires for reducing induced voltages from lightning electromagnetic fields. Electr. Power Syst. Res. 94: 46-53.

[225] Pierce, E. T. 1971. Triggered Lightning and Some Unsuspected Lightning Hazards. Stanford Research Institute, Menlo Park, CA, pp. 20.

[226] Pigini, A., G. Rizzi, E. Garbagnati, A. Porrino, G. Baldo, and G. Pesavento. 1989. Performance of large air gaps under lightning overvoltages: experimental study and analysis of accuracy predetermination methods. IEEE Trans. Power Del. 4: 1379-92.

[227] Pinto Jr., O., K. P. Naccarato, I. R. C. A. Pinto, W. A. Fernandes, and O. Pinto Neto. 2006. Monthly distribution of cloud-to-ground lightning flashes as observed by lightning location systems, Geophys. Res. Lett. 33: L09811, doi:10.1029/2006GL026081.

[228] Pinto Jr., O., I. R. C. A. Pinto, M. Lacerda, A. M. Carvalho, J. H. Diniz, and L. C. L. Cherchiglia. 1997. Are equatorial negative lightning flashes more intense than those at higher latitudes? J. Atmos. Solar-Terr. Phys. 59: 1881-3.

[229] Pinto Jr., O., I. R. C. A. Pinto, and K. P. Naccarato. 2007. Maximum cloud-to-ground lightning flash densities observed by lightning location systems in the tropical region: A review. Atmos. Res. 84: 189-200, doi:10.1016/j.atmosres.2006.11.007.

[230] Popolansky, F. 1972. Frequency distribution of amplitudes of lightning currents. Electra 22: 139-47.

[231] Popolansky, F. 1990. Lightning current measurement on high objects in Czechoslovakia. In Proc. of 20th Int. Conf. on Lightning Protection, Interlaken, Switzerland, paper 1.3, 7 p.

[232] Qie X. S., J. Yang, R. B. Jiang. 2013. Characteristics of current pulses in rocket-triggered lightning, Atmos. Res. dx.doi.org/10.1016/j.atmosres.2012.11.012.

[233] Qie, X., Y. Yu, D. Wang, H. Wang, and R. Chu. 2002. Characteristics of Cloud-to-Ground Lightning in Chinese Inland Plateau. J. Meteorol. Soc. Jpn. 80: 745-54.

[234] Qie, X. S., Q. L. Zhang, Y. J. Zhou, G. L. Feng, T. L. Zhang, J. Yang, X. Z. Kong, Q. F. Xiao, and S. J. Wu. 2007. Artificially triggered lightning and its characteristic discharge parameters in two severe thunderstorms. Sci. China, Ser. D: Earth Sci. 50: 1241-50, doi:10.1007/s11430-007-0064-2.

[235] Rachidi, F., C. A. Nucci, M. Ianoz, and C. Mazzetti. 1996. Influence of a lossy ground on lightning-induced voltages on overhead lines. IEEE Trans. Electromagn. Compat. 38: 250-64.

[236] Rachidi, F., V. A. Rakov, C. A. Nucci, and J. L. Bermudez. 2002. Effect of vertically extended strike object on the distribution of current along the lightning channel. J. Geophys. Res. 107: 4699, doi:10.1029/2002JD002119.

[237] Rakov, V. A. 1985. On estimating the lightning peak current distribution parameters taking account of the measurement threshold level (in Russian). Elektrichestvo, No. 2, 57-59.

[238] Rakov, V. A. 1998. Some inferences on the propagation mechanisms of dart leaders and return strokes. J. Geophys. Res. 103: 1879-87.

[239] Rakov, V. A. 2001. Transient response of a tall object to lightning. IEEE Trans. Electromagn. Compat. 43: 654–66.

[240] Rakov, V. A. 2003a. A Review of the interaction of lightning with tall objects. Recent Res. Devel. Geophysics, 5, pp. 57-71, Research Signpost, India.

[241] Rakov, V. A. 2003b. A review of positive and bipolar lightning discharges. Bull. Amer. Meteor. Soc. 84: 767–76.

[242] Rakov, V. A. 2005. Lightning flashes transporting both negative and positive charges to ground. In Recent Progress in Lightning Physics, edited by C. Pontikis, pp. 9-21, Research Signpost, Kerala, India.

[243] Rakov, V. A. 2007. Lightning Return Stroke Speed. J. Lightning Research 1: 80-9.

[244] Rakov, V. A. 2009. Triggered Lightning, in "Lightning: Principles, Instruments and Applications", eds. H.D. Betz, U. Schumann, and P. Laroche, Springer, 691 p., ISBN 978-1-4020-9078-3, pp. 23-56.

[245] Rakov, V. A. 2011. Upward lightning discharges: An update. In proceedings of 7th Asia-Pacific International Conference on Lightning (APL), pp.304-307, doi: 10.1109/APL.2011.6110131.

[246] Rakov, V.A., D.E. Crawford, K.J. Rambo, G.H. Schnetzer, M.A. Uman, and R. Thottappillil. 2001. M-Component Mode of Charge Transfer to Ground in Lightning Discharges. J. Geophys. Res. 106: 22,817-31.

[247] Rakov, V. A. and A. A. Dulzon. 1986. Study of some features of frontal and convective thunderstorms, Meteor. Hidrol. 9: 59-63.

[248] Rakov, V. A. and A. A. Dulzon. 1987. Calculated electromagnetic fields of lightning return stroke. Tekh. Elektrodinam. 1: 87-9.

[249] Rakov, V. A. and A. A. Dulzon. 1991. A modified transmission line model for lightning return stroke field calculations. In Proc. 9th Int. Zurich. Symp. on Electromagnetic Compatibility, Zurich, Switzerland, pp. 229-235.

[250] Rakov, V. A. and G. R. Huffines. 2003. Return-Stroke Multiplicity of Negative Cloud-to-Ground Lightning Flashes. J. Applied Meteor. 42: 1,455-62.

[251] Rakov, V. A., R. Thottappillil, and M. A. Uman. 1992. On the empirical formula of Willett et al. relating lightning return-stroke peak current and peak electric field. J. Geophys. Res. 97: 11527-33.

[252] Rakov, V. A. and M. A. Uman. 1990a. Long continuing current in negative lightning ground flashes. J. Geophys. Res. 95: 5455-70.

[253] Rakov, V.A. and M. A. Uman. 1990b. Some properties of negative cloud-to-ground lightning flashes versus stroke order. J. Geophys. Res. 95: 5447-53.

[254] Rakov, V.A., and M. A. Uman. 1994. Origin of lightning electric field signatures showing two return-stroke waveforms separated in time by a millisecond or less. J. Geophys. Res. 99: 8157-65.

[255] Rakov, V.A., and M. A. Uman. 1998. Review and evaluation of lightning return stroke models including some aspects of their application. IEEE Trans. on Electromagn. Compat. 40: 403-26.

[256] Rakov, V.A. and M. A. Uman. 2003. Lightning: Physics and Effects, Cambridge University Press, 687 p., HB ISBN 0521583276, PB ISBN 0521035414.

[257] Rakov, V. A., M. A. Uman, D. M. Jordan and C. A. Priore III. 1990. Ratio of leader to return-stroke electric field change for first and subsequent lightning strokes. J. Geophys. Res. 95: 16,579-87.

[258] Rakov, V. A., M. A. Uman, K. J. Rambo, M. I. Fernandez, R. J. Fisher, G. H. Schnetzer, R. Thottappillil, A. Eybert-Berard, J. P. Berlandis, P. Lalande, A. Bonamy, P. Laroche, and A. Bondiou-Clergerie. 1998. New insights into lightning processes gained from triggered-lightning experiments in Florida and Alabama. J. Geophys. Res. 103: 14117-30.

[259] Rakov, V.A., M. A. Uman, and R. Thottappillil. 1994. Review of lightning properties from electric field and TV observation, J. Geophys. Res. 99: 10,745-50.

[260] Rizk, F. A. M. 1990. Modeling of Transmission Line Exposure to Lightning Strokes. IEEE Trans. Power Del. 5: 1983-97.

[261] Rizk, F. A. M. 1994a. Modeling of lightning incidence to tall structures. I. Theory. IEEE Trans. Power Del. 9: 162-71.

[262] Rizk, F. A. M. 1994b. Modeling of lightning incidence to tall structures. II. Application. IEEE Trans. Power Del. 9: 172-93.

[263] Romero, C., M. Paolone, M. Rubinstein, F. Rachidi, A. Rubinstein, G. Diendorfer, W. Schulz, B. Daout, A. Kälin, and P. Zweiacker. 2012a. A system for the measurements of lightning currents at the Säntis Tower. Electr. Power Syst. Res. 82: 34-43.

[264] Romero, C., F. Rachidi, M. Paolone, and M. Rubinstein. 2013a. Statistical distributions of lightning current parameters based on the data collected at the Säntis tower in 2010 and 2011. IEEE Trans. Power Del., in press.

[265] Romero, C., F. Rachidi, M. Rubinstein, and M. Paolone. 2012c. Instrumentation of the Säntis Tower in Switzerland and obtained results after 18 months of operation. 2012 CIGRE Colloquium, Hakodate, Japan.

[266] Romero, C., F. Rachidi, M. Rubinstein, M. Paolone, V.A. Rakov, D. Pavanello. 2013b. Positive lightning flashes recorded on the Säntis tower in 2010 and 2011. J. Geophys. Res. submitted 2013.

[267] Romero, C., M. Rubinstein, M. Paolone, F. Rachidi, V. A. Rakov, and D. Pavanello. 2012b. Some characteristics of positive and bipolar lightning flashes recorded on the Säntis Tower in 2010 and 2011. In Proc. 31st Int. Conf. on Lightning Protection, Vienna, Austria.

[268] Ross M., S. A. Cummer, T. K. Nielsen, and Y. Zhang. 2008. Simultaneous remote electric and magnetic field measurements of lightning continuing currents. J. Geophys. Res. 113: D20125, doi:10.1029/2008JD010294.

[269] Rusck, S. 1958a. Effect of non-standard surge voltage on insulation. CIGRE.

[270] Rusck, S. 1958b. Induced lightning overvoltages on power transmission lines with special reference to the overvoltage protection of low voltage networks. Trans. R. Inst. Technol. vol. 120.

[271] Rust, W. D. 1986. Positive cloud-to-ground lightning. In The Earth's Electrical Environment, pp. 41-45, National Academy Press, Washington, D.C.

[272] Rust, W. D., D. R. MacGorman, and R. T. Arnold. 1981. Positive cloud to ground lightning flashes in severe storms. Geophys. Res. Lett. 8: 791-794.

[273] Rust, W. D., D. R. MacGorman, and W. L. Taylor. 1985. Photographic verification of continuing current in positive cloud-to-ground flashes. J. Geophys. Res. 90: 6144-6.

[274] Saba, M. M. F., M. G. Ballarotti, and O. Pinto Jr. 2006a. Negative cloud-to-ground lightning properties from high-speed video observations. J. Geophys. Res. 111: D03101, doi:10.1029/2005JD006415.

[275] Saba, M. M. F., O. Pinto Jr., and M. G. Ballarotti. 2006b. Relation between lightning return stroke peak current and following continuing current. Geophys. Res. Lett. 33: L23807, doi:10.1029/2006GL027455.

[276] Saba, M. M. F., W. Schulz, T. A. Warner, L. Z. S. Campos, C. Schumann, E. P. Krider, K. L. Cummins, and R. E. Orville. 2010. High-speed video observations of positive lightning flashes to ground. J. Geophys. Res. 115: D24201, doi:10.1029/2010JD014330.

[277] Saba, M. M. F., C. Schumann, T. A. Warner, J. H. Helsdon, W. Schulz, and R. E. Orville. 2013. Bipolar cloud-to-ground lightning flash observations. J. Geophys. Res. 115: D24201, submitted.

[278] Sabot, A. 1995. An engineering review on lightning, transient overvoltages and the associated elements of electrogeometric compatibility. 9th Int. Symposium on High Voltage Engineering.

[279] Saraiva, A. C. V. 2011. On relationships between the multiplicity and duration of negative cloud to ground lightning flashes and the horizontal extent of the inferred negative charge region, Ph.D. Thesis, Brazilian Institute of Space Research.

[280] Saraiva, A. C. V., M. M. F. Saba, O. Pinto Jr., K. L. Cummins, E. P. Krider, and L. Z. S. Campos. 2010. A comparative study of negative cloud-to-ground lightning characteristics in São Paulo (Brazil) and Arizona (United States) based on high-speed video observations. J. Geophys. Res. 115: D11102, doi:10.1029/2009JD012604.

[281] Sarajcev, P. and R. Goic. 2012. Assessment of the backflashover occurrence rate on HV transmission line towers. Eur. Trans. Electr. Power 22: 152-69.

[282] Sargent, M. A. 1972. The frequency distribution of current magnitudes of lightning strokes to tall structures. IEEE Trans. Pow. Appar. Syst. 91: 2224-9.

[283] Savic, M. S. 2005. Estimation of the Surge Arrester Outage Rate Caused by Lightning Overvoltages. IEEE Trans. Power Del. 20: 116-22.

[284] Schoene, J., M. A. Uman, and V. A. Rakov. 2010. Return stroke peak current versus charge transfer in rocket-triggered lightning. J. Geophys. Res. 115: D12107, doi:10.1029/2009JD013066.

[285] Schoene, J., M. A. Uman, V. A. Rakov, V. Kodali, K. J. Rambo, and G. H. Schnetzer. 2003. Statistical characteristics of the electric and magnetic fields and their time derivatives 15 m and 30 m from triggered lightning. J. Geophys. Res. 108: 4192, doi: 10.1029/2002JD002698.

[286] Schoene, J., M. A. Uman, V. A. Rakov, K. J. Rambo, J. Jerauld, C. T. Mata, A. G. Mata, D. M. Jordan, and G. H. Schnetzer. 2009. Characterization of return-stroke currents in rocket-triggered lightning. J. Geophys. Res. 114: D03106, doi:10.1029/2008JD009873.

[287] Schonland, B.F.J. 1956. The lightning discharge. In Handbuch der Physik 22: 576-628, Berlin, Springer-Verlag.

[288] Schonland, B. F. J., D. J. Malan, and H. Collens. 1935. Progressive Lightning II. Proc. Roy. Soc. (London) A152: 595-625.

[289] Schroeder, M. A. O., A. Soares, S. Visacro, L. C. L. Cherchiglia, and V. J. de Souza. 2002. Lightning current statistical analysis: Measurements of Morro do Cachimbo station - Brazil. In Proc. 26th Int. Conf. on Lightning Protection, Cracow, Poland, pp. 20-23.

[290] Schulz, W., K. Cummins, G. Diendorfer, and M. Dorninger. 2005. Cloud-to-ground lightning in Austria: A 10-year study using data from a lightning location system. J. Geophys. Res. 110: D09101.

[291] Schulz, W. and G. Diendorfer. 2006. Flash multiplicity and interstroke intervals in Austria. In Proc. of 28th Intl. Conf. on Lightning Protection, Kanazawa, Japan, paper II-4, pp. 402-404.

[292] Schulz, W., S. Sindelar, A. Kafri, T. Gotschl, N. Theethayi, and R. Thottappillil. 2008. The ratio between first and subsequent lightning return stroke electric field peaks in Sweden. Paper presented at 29th International Conference on Lightning Protection, Dep. of Eng. Sci., Uppsala Univ., Uppsala, Sweden.

[293] Schumann, C. and M. M. F. Saba. 2012. Continuing current intensity in positive ground flashes, International Conf. on Lightning Protection, Vienna, Austria.

[294] Schumann, C., M. M. F. Saba, R. B. G. da Silva, and W. Schulz. 2013. Electric fields changes produced by positives cloud-to-ground lightning flashes. J. Atoms. Terr. Physics 92: 37–42, doi: 10.1016/j.jastp.2012.09.008.

[295] Scott-Meyer, W. 1982. EMTP Rule Book. Bonneville Power Admin., Portland, Oreg.

[296] Sekioka, S., T. Sonoda, and A. Ametani. 2005. Experimental Study of Current-Dependent Grounding Resistance of Rod Electrode. IEEE Trans. Power Del. 20: 1569-76.

[297] Shindo, T., and M. A. Uman. 1989. Continuing current in negative cloud-to-ground lightning. J. Geophys. Res. 94: 5189-98.

[298] Silveira, F. H., A. De Conti, and S. Visacro. 2010. Lightning overvoltage due to first strokes considering a realistic current representation. IEEE Trans. Electromagn. Compat. 52: 929-35, doi:10.1109/TEMC2010.2044042.

[299] Silveira, F. H., A. De Conti, and S. Visacro. 2011. Voltages Induced in Single-Phase Overhead Lines by First and Subsequent Negative Lightning Strokes: Influence of the Periodically Grounded Neutral Conductor and the Ground Resistivity. IEEE Trans. Electromagn. Compat. 53: 414-20.

[300] Silveira, F. H. and S. Visacro. 2008. The Influence of Attachment Height on Lightning-Induced Voltages. IEEE Trans. Electromagn. Compat. 50: 1-5.

[301] Silveira, F. H. and S. Visacro. 2009. On the Lightning-Induced Voltage Amplitude: First Versus Subsequent Negative Strokes. IEEE Trans. Electromagn. Compat. 51: 741-7.

[302] Silveira, F. H., S. Visacro, and A. R. Conti. 2013. Lightning Performance of 138-kV Transmission Lines: The Relevance of Subsequent Strokes. IEEE Trans. Electromagn. Compat. Accepted for publication, pp. 1-6.

[303] Silveira, F. H., S. Visacro, A. R. Conti, and C. R. Mesquita. 2012. Backflashovers of Transmission Lines Due to Subsequent Lightning Strokes. IEEE Trans. Electromagn. Compat. 54: 316-22.

[304] Silveira, F. H., S. Visacro, J. Herrera, and H. Torres. 2009. Evaluation of Lightning-Induced Voltages Over a Lossy Ground by the Hybrid Electromagnetic Model. IEEE Trans. Electromagn. Compat. 51: 156-60.

[305] Smorgonskiy, A., F. Rachidi, M. Rubinstein, G. Diendorfer, W. Schulz, and N. Korovkin. 2011. A new method for the estimation of the number of upward flashes from tall structures. In Proceeding XI International Symposium on Lightning Protection (SIPDA), Fortaleza, Brazil. doi: 10.1109/SIPDA.2011.6088466.

[306] Soares, A. J., M. A. Schroeder, and S. Visacro. 2005. Transient Voltages in Transmission Lines Caused by Direct Lightning Strikes. IEEE Trans. Power Del. 20: 1447-52.

[307] Srivastava, K. M. L. 1966. Return stroke velocity of a lightning discharge. J. Geophys. Res. 71: 1283-6.

[308] Stall, C.A., K.L. Cummins, E.P. Krider, and J.A. Cramer. 2009. Detecting Multiple Ground Contacts in Cloud-to-Ground Lightning Flashes. J. Atmos. Ocean. Tech. 26: 2392-402.

[309] Stekolnikov, I.S. 1941. The parameters of the lightning discharge and the calculation of the current waveform. Elektrichestvo 3: 63-8.

[310] Stenstrom, L. and J. Lundquist. 1999. Energy stress on transmission line arresters considering the total

lightning charge distribution. IEEE Trans. Power Del. 14: 148-51.

[311] Suzuki, T. and K. Miyake. 1977. Experimental study of breakdown voltage-time characteristics of large air gaps with lightning impulses. IEEE Trans. Power App. Syst. 96: 227-33.

[312] Takami, J. and S. Okabe. 2007. Observational results of lightning current on transmission towers. IEEE Trans. Power Del. 22: 547-56.

[313] Thottappillil, R., J. D. Goldberg, V. A. Rakov, and M. A. Uman. 1995. Properties of M components from currents measured at triggered lightning channel base. J. Geophys. Res. 100: 25, 711-20.

[314] Thottappillil, R., V. A. Rakov, M. A. Uman. 1997. Distribution of charge along the lightning channel: Relation to remote electric and magnetic fields and to return-stroke models. J. Geophys. Res. 102: 6987-7006.

[315] Thottappillil, R., V. A. Rakov, M. A. Uman, W. H. Beasley, M. J. Master and D. V. Shelukhin. 1992. Lightning subsequent stroke electric field peak greater than the first stroke peak and multiple ground terminations. J. Geophys. Res. 97: 7503-9.

[316] Thottappillil, R. and N. Theethayi. 2006. Realistic sources for modeling lightning attachment to towers. In Proc. Int. Conf. On Grounding and Earthing & 2nd Int. Conf. on Lightning Physics and Effects, Maceo, Brazil, 6 p.

[317] Uman, M. A. 1987. The Lightning Discharge, 377 p., San Diego: Academic Press.

[318] Uman, M. A. 2001. The Lightning Discharge, 377 p., Mineola, New York: Dover.

[319] Uman, M. A. and D. K. McLain. 1969. Magnetic field of lightning return stroke. J. Geophys. Res. 74: 6899-910.

[320] Uman, M. A., V. A. Rakov, K. J. Rambo, T. W. Vaught, M. I. Fernandez, D. J. Cordier, R. M. Chandler, R. Bernstein, and C. Golden. 1997. Triggered-lightning experiments at Camp Blanding, Florida (1993-1995). Trans. of IEE Japan, Special Issue on Artificial Rocket Triggered Lightning 117-B: 446-52.

[321] Uman M. A., V. A. Rakov, G. H. Schnetzer, K. J. Rambo, D. E. Crawford, and R. J. Fisher. 2000. Time derivative of the electric field 10, 14 and 30m from triggered lightning strokes. J. Geophys. Res. 105: 15,577-95.

[322] Valine, W.C. and E.P. Krider. 2002. Statistics and characteristics of cloud-to-ground lightning with multiple ground contacts. J. Geophys. Res. 107: AAC 8-1-11.

[323] Visacro, S. 2004. A Representative Curve for Lightning Current Waveshape of First Negative. Geophys. Res. Lett. 31: L07112 / 1- 3.

[324] Visacro, S. 2007. A Comprehensive Approach to the Grounding Response to Lightning Currents. IEEE Trans. Power Del. 22: 381-6.

[325] Visacro, S. 2012a. Reflections on parameters for application in lightning protection, in Proc. of 8th Int. Conf. on Grounding and Earthing & Lightning Physics and Effects GROUND & LPE, pp. 100-103, Bonito, Brazil.

[326] Visacro, S. and R. Alipio. 2012b. Frequency Dependence of Soil Parameters: Experimental Results, Predicting Formula and Influence on the Lightning Response of Grounding Electrodes. IEEE Trans. Power Del. 27: 927-35.

[327] Visacro, S., C. R. de Mesquita, R. N. Dias, F. H. Silveira, and A. De Conti. 2012e. A Class of Hazardous Subsequent Lightning Strokes in Terms of Insulation Stress. IEEE Trans. Electromagn. Compat. 54: 1028-33.

[328] Visacro, S., R. N. Dias, C. R. Mesquita. 2005c. Novel Approach for Determining Spots of Critical Lightning Performance along Transmission Lines. IEEE Trans. Power Del. 20: 1459-64.

[329] Visacro, S., B. Hermoso, M. T. Almeida, H. Torres, M. Loboda, S. Sekioka, A. Geri, and W. Chisholm. 2009. The response of grounding electrodes to lightning currents. CIGRE Report WG C4.406.

[330] Visacro, S., C. R. Mesquita, M. P. P. Batista, L. S. Araújo, and A. M. N. Teixeira. 2010. Updating the statistics of lightning currents measured at Morro do Cachimbo Station. Proceedings of the 30th International Conference on Lightning Protection - ICLP 2010, Cagliari, Italy.

[331] Visacro, S., C. R. Mesquita, A. De Conti, F. H. Silveira. 2012. Updated statistics of lightning currents measured at Morro do Cachimbo station. Atmos. Res. 117: 55-63.

[332] Visacro, S. and F. H. Silveira. 2005. Lightning current waves measured at short instrumented towers: The influence of sensor position. Geophys. Res. Lett. 32: L18804-1-5, doi: 10.1029/2005GL023255.

[333] Visacro, S., F. H. Silveira, and A. R. Conti. 2012c. The use of underbuilt wires to improve the lightning performance of transmission lines. IEEE Trans. Power Del. 27: 205-13.

[334] Visacro, S., F. H. Silveira, S. Xavier, and H. B. Ferreira. 2012d. Frequency Dependence of Soil Parameters: The Influence on the Lightning Performance of Transmission Lines. In Proc. 31st International Conference on Lightning Protection (ICLP), pp. 1-4, Vienna, Austria.

[335] Visacro, S. and A. Soares Jr.. 2005b. HEM: A Model for Simulation of Lightning Related Engineering Problems. IEEE Trans. Power Del. 20: 1206-8.

[336] Visacro, S., A. Soares Jr., M. A. O. Schroeder, L. C. L. Cherchiglia, and V. J. de Sousa. 2004. Statistical analysis of lightning current parameters: Measurements at Morro do Cachimbo Station. J. Geophys. Res. 109: D01105, doi:10.1029/2003JD003662.

[337] Visacro, S., M. H. M. Vale, G. M. Correa and A. M. Teixeira. 2010. The early phase of lightning currents measured in a short tower associated with direct and nearby lightning strikes. J. Geophys. Res. 15: D16104.

[338] Wagner, C.F. 1963. Relation between stroke current and velocity of the return stroke. AIEE Trans. Power Appar. Syst. 82: 609-17.

[339] Wagner, C.F. and A. R. Hileman. 1961. Surge impedance and its application to the lightning stroke. AIEE Trans. on PAS 80: 1011-20.

[340] Wagner, C. F. and G. D. McCann. 1942. Induced voltages on Transmission Lines. Trans. Am. Inst. Electr. Eng. 61: 916-30.

[341] Wang, D., V. A. Rakov, M. A. Uman, M. I. Fernandez, K. J. Rambo, G. H. Schnetzer, and R. J. Fisher. 1999. Characterization of the initial stage of negative rocket-triggered lightning. J. Geophys. Res. 104: 4213-22.

[342] Wang, D. and N. Takagi. 2008b. Characteristics of Upward Bipolar Lightning Derived from Simultaneous Recording of Electric Current and Electric Field Change, Proceedings of the XXIX General Assembly of the International Union of Radio Science, Chicago ,USA.

[343] Wang, D. and N.Takagi. 2011. Characteristics of Winter Lightning that Occurred on a Windmill and its Lightning Protection Tower in Japan, paper presented at 3rd International Symposium on Winter Lightning, University of Tokyo, Sapporo, Japan.

[344] Wang, D. and N. Takagi. 2012. Characteristics of Winter Lightning that Occurred on a Windmill and its Lightning Protection Tower in Japan. IEEJ Transactions on Power and Energy 132: 568-72.

[345] Wang, D., N. Takagi, T. Watanabe, V. A. Rakov, and M. A. Uman. 1999c. Observed leader and return-stroke propagation characteristics in the bottom 400 m of the rocket triggered lightning channel. J. Geophys. Res. 104: 14,369-76.

[346] Wang, D., N. Takagi, T. Watanabe, H. Sakurano, and M. Hashimoto. 2008a. Observed characteristics of

upward leaders that are initiated from a windmill and its lightning protection tower. Geophys. Res. Lett. 35: L02803, doi:10.1029/2007GL032136.

[347] Warner, T. A., K. L. Cummins, and R. E. Orville. 2011. Comparison of upward lightning observations from towers in Rapid City, South Dakota with National Lightning Detection Network data - preliminary findings. Paper presented at 3rd International Symposium on Winter Lightning, University of Tokyo, Sapporo, Japan.

[348] Weidman, C.D. 1998. Lightning return stroke velocities near channel base. In Proc. 1998 Int. Lightning Detection Conf., GAI, Tucson, Arizona, 25 p.

[349] Willett, J.C., J. C. Bailey, V. P. Idone, A. Eybert-Berard, and L. Barret. 1989. Submicrosecond intercomparison of radiation fields and currents in triggered lightning return strokes based on the transmission-line model. J. Geophys. Res. 94: 13,275-86.

[350] Willett, J.C., V. P. Idone, R. E. Orville, C. Leteinturier, A. Eybert-Berard, L. Barret, and E. P. Krider. 1988. An experimental test of the "transmission-line model" of electromagnetic radiation from triggered lightning return strokes. J. Geophys. Res. 93: 3867-78.

[351] Witzke, R. L. and T. J. Bliss. 1950a. Co-ordination of Lightning Arrester Location with Transformer Insulation Level. Trans. Am. Inst. Electr. Eng. 69: 964-75.

[352] Witzke, R. L. and T. J. Bliss. 1950b. Surge Protection of Cable-Connected Equipment. Trans. Am. Inst. Electr. Eng. 69: 527-42.

[353] Yang, J., X. Qie, G. Zhang, Q. Zhang, G. Feng, Y. Zhao, and R. Jiang. 2010. Characteristics of channel base currents and close magnetic fields in triggered flashes in SHATLE. J. Geophys. Res. 115: D23102, doi:10.1029/2010JD014420.

[354] Yokoyama, S., K. Yamamoto, and H. Kinoshita. 1985. Analogue simulation of lightning induced voltages and its application for analysis of overhead-ground-wire effects. IEE Proc. C Generat. Transm. Distrib. 132: 208-16.

[355] Zhou, H., G. Diendorfer, R. Thottappillil, H. Pichler and M. Mair. 2011a. Characteristics of upward bipolar lightning flashes observed at the Gaisberg Tower. J. Geophys. Res. 116: D13106, doi:10.1029/2011JD015634.

[356] Zhou, H., G. Diendorfer, R. Thottappillil, H. Pichler and M. Mair. 2011b. Mixed mode of charge transfer to ground for initial continuous current pulses in upward lightning, Paper presented at 2011 7th Asia-Pacific International Conference on Lightning, Tsinghua University, Chengdu, China.

[357] Zhou, H., G. Diendorfer, R. Thottappillil, H. Pichler and M. Mair. 2012. Characteristics of upward positive lightning flashes initiated from the Gaisberg Tower. J. Geophys. Res., 117, D06110, doi:10.1029/2011JD016903.

[358] Zhou, H., N. Theethayi, G. Diendorfer, R. Thottappillil, and V.A. Rakov. 2010. On Estimation of the Effective Height of Towers on Mountaintops in Lightning Incidence Studies. J. Electrost. 68: 415-8.

Appendix 1. List of Acronyms

AM	Arithmetic Mean
BFR	Backflashover Rate
CB	Camp Blanding
CC	Continuing Current
CFO	Critical Impulse Flashover
CG	Cloud-to-Ground
EGLA	Externally Gapped Line Arrester
EGM	Electrogeometrical Model
EUCLID	European Cooperation for Lightning Detection
GBT	Gaisberg Tower
GIS	Gas Insulated Substation
GLD360	Global Lightning Dataset 360
GM	Geometric Mean
HEM	Hybrid Electromagnetic
IC	Intracloud
ICC	Initial Continuous Current
IEC	International Electrotechnical Commission
IEEE	Institute of Electrical and Electronics Engineers
IS	Initial Stage
JLDN	Japanese Lightning Detection Network
KSC	Kennedy Space Center
LASA	Los Alamos Sferic Array
LC39B	Launch Complex 39B
LFC	Lightning Flash Counter
LINET	LIghtning detection NETwork
LLS	Lightning Locating System
LPM	Leader Progression Model
LPS	Lightning Protective System
LSA	Line Surge Arrester
MCS	Mesoscale Convective System
NGLA	Non-Gapped Line Arrester
NLDN	U.S. National Lightning Detection Network
OHGW	Overhead Ground Wire
OPGW	Optical Fiber Ground Wire
RINDAT	Rede Integrada de Detecção de Descargas Atmosféricas (Integrated Network of Atmospheric Discharges) - Lightning Locating System in Brazil
RS	Return Stroke
SFFOR	Shielding Failure Flashover Rate
SPD	Surge Protective (or Protection) Device
TL	Transmission Line
TOV	Temporary Overvoltage
USPLN	United States Precision Lightning Network
WTLN	WeatherBug Total Lightning Network
WWLLN	World Wide Lightning Location Network

Appendix 2. Term of Reference (TOR) for CIGRE WG C4.407, Lightning Parameters for Engineering Applications

Study Committee C4

Proposal for the formation of a new Working Group

WG No. : WG C4-407	**Name of Convener :** Vladimir Rakov (US)
Title of the Group: Lightning Parameters for Engineering Applications	

Scope, deliverables and proposed time schedule:

Background: Traditional lightning parameters needed in engineering applications include lightning peak current, maximum current derivative (di/dt), average current rate of rise, current risetime, current duration, charge transfer, and action integral, all derivable from direct current measurements. Distributions of these parameters presently adopted by CIGRE are based on measurements by K. Berger and co-workers in Switzerland. There also exist more recent direct current measurements obtained using instrumented towers in Austria, Germany, Russia, Canada, and Brazil, as well as those obtained using rocket-triggered lightning. Further, modern lightning locating systems report peak currents estimated from measured magnetic field peaks. There is urgent need to evaluate these new experimental data to determine the limits of their applicability to various engineering calculations. Evaluation should include both instrumental and methodological aspects. Possible geographical, seasonal and other variations in lightning parameters, as well as the need to extend the list of traditional parameters to include, for example, characteristics of continuing currents and M-components should be examined. Additional lightning parameters to be analysed in view of availability of new data include number of strokes per flash, interstroke interval, number of channels per flash, relative intensity of strokes within a flash, return-stroke speed, and equivalent impedance of the lightning channel. More detailed information about less frequent, but potentially more destructive positive and bipolar lightning flashes is needed.

Scope: The scope of the working group includes the following:

- Evaluation of current measurements on instrumented towers
- Evaluation of current measurements for rocket-triggered lightning
- Evaluation of the procedures used to estimate lightning currents from measured fields, with emphasis on those implemented in lightning locating systems
- Inclusion of additional lightning parameters (e.g., characteristics of continuing currents, return-stroke propagation speed, equivalent lightning channel impedance, etc.) that are presently not on the CIGRE list, but needed in engineering applications
- Further characterization of positive and bipolar lightning discharges
- Characterization of upward lightning discharges
- Search for any geographical, seasonal and other variations in lightning parameters
- Preparation of a reference document “Lightning Parameters for Engineering Applications” based on the current understanding of lightning processes and taking into account limitations of various measuring techniques

Deliverables: Report, a summary of which may be published in the Electra. **Time schedule:** Initiation of the WG: April 2008; Final deliverables: March 2011.
Other SCs concerned by the work. A3, B2, B3.

Approval by TC Chairman : Klaus FRÖHLICH Date : 09-04-2008